NON-IONIC MICROEMULSION

MECHANISM AND THEORY OF FORMATION

By

NABIL NAOULI

A dissertation submitted to the Graduate Faculty in Chemistry in partial fulfillment of the requirements for the degree of Doctor of Philosophy, The City University of New York.

2005

UMI Number: 3187476

ProQuest Information and Learning Company
300 North Zeeb Road
P.O. Box 1346
Ann Arbor, MI 48106-1346

This manuscript has been read and accepted for the Graduate Faculty in Chemistry in satisfaction of the dissertation requirement for the degree of Doctor in Philosophy.

_____	_____
Date	Professor Henri. L. Rosano
	_____
	Professor Charles Maldarelli
	Chairs of Examining Committee
_____	_____
Date	Professor Gerald Koeppl
	Executive Officer

_____

Professor John Lombardi

_____

Professor David Locke

Supervisory Committee

THE City University of New York

Abstract

NON-IONIC MICROEMULSION

MECHANISM AND THEORY OF FORMATION

By

Nabil Naouli

Adviser: Professor Henri Louis Rosano

An investigation of the mechanism of formation of non-ionic microemulsions began with the preparation, using the titration method, of a series of microemulsions, both W/O and O/W, based on non-ionic surfactants of the form ($NP(EO)_n$). Mixing a constant weight of surfactant with a constant volume of the dispersed phase and an initial volume of continuous phase produces an emulsion, which is titrated to clarity with another surfactant (cosurfactant). Plotting (a) the volume of cosurfactant necessary to transform an emulsion into a microemulsion containing a fixed volume of dispersed phase and a constant weight of surfactant versus (b) different initial continuous-phase volumes yields a straight line. Extrapolating from experimentally determined values for the cosurfactant volume to the value corresponding to a zero-volume continuous phase allows the determination of the surfactant molar composition and the average number of ethylene oxides (EO) per nonylphenol adsorbed at the interface. Using a surfactant with the same number of ethylene oxides yields a single-surfactant microemulsion. Measurement of surfactant(s) transmittance in the oil and water phases demonstrates that

microemulsification occurs when the surfactant interfacial film is equally soluble in the two phases. Surface pressure and potential measurements reveal that oil penetration impedes formation of O/W microemulsions with n-tetradecane or n-hexadecane as dispersed phase.

These experimental results afford strong support for a previously proposed mathematical model of the formation of a microemulsion system. W/O microemulsions with various straight chain hydrocarbons as the continuous phase and nonylphenol ethylene oxide ($NP(EO)_n$) condensates as surfactants were prepared using the titration method. The free energies of the system were determined using the Gibbs equation. Next, the free energy of formation of a single microemulsion droplet was calculated. The free energy value obtained from the titration method showed a high degree of agreement with the free energy predicted by the mathematical model when experimental values for the interfacial tensions at the water/oil interface and bare interface, free energy of formation of the interfacial sheath, natural radius of the microemulsion, rigidity constant of the interfacial sheath, and maximum and minimum radii of the microemulsion were inserted in the appropriate equation.

Acknowledgements

I would like to express my high gratitude to Professor Henri L. Rosano, my mentor and friend, who provided me with confidence, knowledge, and a good research topic. I am very lucky to have Professor Henri Rosano as a mentor. Dr. Rosano, as I heard once from his former students is an encyclopedia of surface chemistry. If you have a question for him, his answer always starts with a history of the subject and in this recounting of this history, you find your answer.

I would like to thank Professor Mouhcine Kanouni, who advised me to apply to the PhD Program in Chemistry, helped me to get an internship in Ciba Specialty Chemicals, and a lot more. His help will not be forgotten. I would like to thank my friend Yehya El-sayed for his friendship.

At this point, I would like to thank my father Naouli Mahjoub, my mother El Hamraoui Fatna, and my brother Hassan Naouli.

I would like to express my loving gratitude to my wife Samah, my daughter Salma and my son Hamza, whom are a never-ending source of love, pride and inspiration to me.

I would like to thank the members of the City University of New York for their guidance, financial support: Professor Gerald Koeppl (Excutive Officer of the Doctoral Program in Chemistry), Professor Charles Maldarelli (Co-mentor), Professor John Lombardi, and Professor David Locke (members of my thesis Committee), who always were available and provided time for me.

Table of Contents

List of Tables

.

List of Figures

CHAPTER 1

HISTORICAL OVERVIEW: MICROEMULSIONS

1.1 INTRODUCTION

1.1.1 EMULSIONS

It is impossible to overestimate the importance of emulsions to the study of colloids and surfaces, both from the viewpoint of basic theory and due to their multifarious applications. It is not an exaggeration to say that our understanding of emulsions constitutes the greater part of the foundations of the discipline as a whole. With respect to the applications of emulsions, a previously clearcut distinction between naturally occurring systems and man-made ones is becoming increasingly blurred. Examples of naturally occurring emulsions are those connected with mammalian physiological processes—for example, lactation and digestion of food—while primitive man-made emulsions used as foods, paints, cosmetics, etc., date back many centuries. The first surviving mention of what is undoubtedly a man-made emulsion dates to the second century A.D., when the Greek physician Galen described a sort of cold cream (I am indebted to Bourrel et al. [1] for their helpful historical account). Recent medical applications of emulsions in such areas as drug delivery systems make this distinction less meaningful, however. The word "emulsion" did not enter the English language until the 17th century; it is derived from the Latin *mulgere*, 'to milk,' reflecting the milky appearance of many emulsions.

An emulsion is the system that results from the mixing of two immiscible (or partially miscible) liquids, the "phases," and one or more suitable surfactants (surface

active agents) in the proper ratio, so that one phase becomes dispersed in the other—the "continuous" phase—in the form of globules. Usually, one of the phases is aqueous—the so-called "water" phase—and the other an "oil" in the wide sense, i.e., a hydrophobic substance such as an aliphatic or aromatic hydrocarbon (e.g., n-decane, toluene) or a vegetable oil (soybean oil, canola oil). Emulsion nomenclature places the dispersed phase first: when the dispersed phase is water and the continuous phase oil, the emulsion is called a water-in-oil (W/O) emulsion; when the dispersed phase is oil and the continuous phase water, it is called an oil-in-water (O/W) emulsion. The visual appearance of an emulsion results from the scattering of light by the droplets of the dispersed phase and is dependent on the droplet diameter. As droplet diameter decreases, emulsions range in appearance from a milky-white-opaque solution or "macroemulsion" (in which the droplets, with diameter larger than 0.3 μm, scatter the entire spectrum of incident visible light) through a gray translucent solution or "miniemulsion" (with diameters between 0.1 μm and 0.3 μm, the droplets are too small to scatter the entire spectrum of incident visible light) and finally to a transparent solution or "microemulsion" (with droplet diameter less than approximately ¼ the wavelength of the incident visible light, i.e., less than 0.1 μm). Microemulsions are particularly interesting from the practical viewpoint, since emulsion applications are typically accompanied by stability problems, creaming and flocculation in particular. These problems are obviated if the particle size is sufficiently small.

1.1.2 MICROEMULSIONS

Despite their structural similarities, microemulsions and macroemulsions (henceforth, "emulsions") differ substantially in their physical and thermodynamic properties.

In the case of emulsions, the diameter of the droplets grows continuously with time, so that phase separation eventually occurs under gravitational forces; i.e., they are kinetically stable and their formation requires input of work. In the case of microemulsions, once the right conditions are satisfied, microemulsification occurs spontaneously; they are thermodynamically stable and isotropic [2-7].

Interest in microemulsions surged in the late 1970s, when their potential applications in improved oil recovery were recognized; at a time of volatile oil prices, so-called tertiary oil recovery techniques became increasingly important.

From the point of view of fundamental research, a great deal of progress has been made in the last 30 years in understanding microemulsion properties. The rest of this chapter presents a historical overview of the field and some of its most noteworthy investigators.

1. 2 THE SCHULMAN MICROEMULSION

1. 2.1 EARLY WORK ON MICROEMULSIONS

Microemulsions were not known until the pioneering work of Hoar and Schulman. In a 1943 publication [8], they observed that certain mixtures of oil, alkali-metal soap (or cationic soap such as cetyl trimethyl ammonium bromide), a short chain alcohol, and water would yield a transparent, electrically non-conducting dispersion with oil as the continuous phase. (Hoar and Schulman subsequently referred to such W/O dispersions as oleopathic hydro-micelles and to the analogous O/W dispersions as hydrophilic swollen micelles.) For the microstructure of these transparent systems, they visualized a spherical microdroplet core of W/O or O/W surrounded by a monolayer

sheath of amphipathic molecule. The theoretical droplet size of these systems was calculated to be 200 Å in diameter, in agreement with their optical properties. The essential conditions for their formation were: (1) a high soap-to-water ratio, and (2) the presence of a non-ionized amphipathic substance (e.g., alcohol, fatty acid, amine) in a concentration approximately equal to that of the soap. Dilution of these oil continuous phases with excess water inverted them to O/W emulsion. Hoar and Schulman's idea was that the undissociated soap molecules (surfactant) were oriented at the water/oil interface with the non-ionized amphipathic substance (cosurfactant) between them, and formed a complex with the alcohol to produce a net attraction among the molecules at the interface.

In 1946, Schulman and McRoberts [9] studied the role of the alcohol in forming these transparent systems, using potassium oleate as the soap and straight chain and cyclic alcohols of varying chain lengths as the cosurfactants. They found that as the chain length of the alcohol was increased from C_2 to C_{10}, there was a sudden transition (inversion) from water continuous phase to oil continuous phase. These results suggested to them that phase continuity was dependent on the wettability of the mixed interfacial monolayer: the phase with the smaller contact angle against the interfacial monolayer would be the continuous phase. They also discovered that the formation of these transparent systems was dependent on the oil-alcohol combination used. On this basis, they believed that the soap existed as a lamellar film, which had to be penetrated by an amphipathic molecule to enable spherical micelles to form.

In 1951, Schulman, Matalon, and Cohen [10] developed evidence to support the existence of lamellar, cylindrical, and spherical micelles in their systems. Solutions of

long chain non-ionics (polyethylene oxide alcohol) dissolved in petroleum ether were titrated with water and the structure of the systems was studied with x-ray, optical, and rheological means. In the absence of water, the systems exhibited no structure. Upon addition of water and depending on the number of different species of non-ionic surfactants, lamellar, cylindrical, and spherical aggregates were observed by means of x-rays. Transparent systems were obtained only when the hydrophobic and hydrophilic portions of the surfactants were of different lengths. If only one type of polyethylene oxide was used, gel structures resulted. Proposing that as the disorder among the surfactants increased, the lamellae changed into cylinders and then into spheres, they concluded that some kind of disorder had to be introduced into the interfacial film to enable the surfactant film to swell and form spherical micelles containing the oil or water.

In a 1955 review article (delivered as a lecture by Schulman) entitled "Emulsion, Control of the Droplet Size and Phase Continuity in Transparent Oil-Water Dispersion Stabilized by the Addition of Soap and Alcohol," Bowcott and Schulman [11] made an important contribution to the theory of microemulsion formation. They attributed the formation of these emulsions to the molecular interactions taking place at the interface. The mixed monolayer was regarded as a third phase, in equilibrium with the oil and water phases. Therefore, the alcohol (which would now be termed a cosurfactant) was distributed among the three phases and all of the potassium oleate (the surfactant) was at the interface. This assumption was not valid when there was insufficient water present to provide an interfacial area large enough for the oleate soap to be at the interface. They considered a liquid condensed film to be essential for the interfacial flexibility that would allow a tension gradient across the interface to produce curvature.

In later work by Schulman et al., electron micrographs [12], obtained by staining the double bonds of the unsaturated aliphatic oil with osmium tetroxide, revealed discrete spherical droplets for O/W emulsion stabilized with potassium oleate. The staining of the double bonds with osmium tetroxide caused the oil and surfactant to polymerize, producing solid spheres that could be separated and washed. These aggregates were then imbedded in a polymethacrylate matrix and photographed. Observing a discrete phase, Schulman et al. called these transparent systems "microemulsions." They also concluded that an association between the oil and surfactant molecules was critical in the formation of these systems. The coinage "microemulsion," which has become standard, is an unfortunate word reflecting a hasty choice of a name for an incompletely understood phenomenon; it continues to generate confusion.

1. 2.2 THE CONCEPT OF NEGATIVE INTERFACIAL TENSION

The concept of a transient negative interfacial tension as the factor responsible for the formation of microemulsions came next. In 1960, Stoeckenius, Schulman, and Prince [13] proposed a mechanism to explain microemulsion formation, suggesting that during the preparation of these transparent systems, surfactant and cosurfactant would form a mixed film at the oil/water interface that would reduce the interfacial tension γ_i below zero, resulting in a metastable negative value of γ_i. This effect would produce the free energy required to increase the interfacial area resulting in spontaneous microemulsification. This was inferred from the relationship between interfacial tension and surface pressure. Stoeckenius et al. proposed Equation 1.1.

$$\gamma_i = \gamma_{o/w} - \pi_i \tag{1.1}$$

where $\gamma_{o/w}$ is the interfacial tension at the oil/water interface, and π_i is the two-dimensional spreading pressure of the surfactant present at the interface. According to this equation, if $\pi_i > \gamma_{o/w}$ due to the oil penetration into the interfacial film, emulsification would occur spontaneously, since a negative free energy variation $-\gamma_i$ dA (dA: the change in the interfacial area) would be available to subdivide the macrodroplets until their diameter became less than ¼ the wavelength of the incident visible light. This was considered to be the condition for the formation of the microemulsion. In this scenario the temporary existence of a film pressure higher than $\gamma_{o/w}$ would be the driving force that reduced droplet size in the dispersed phase. Equilibrium would be achieved when the negative interfacial tension rose to zero value by virtue of crowding of molecules and loss of pressure in the interface. Therefore, the dispersions were thermodynamically stable. This account assumes the use of a surfactant with a large ionic polar group or the presence of large-sized counterions; the interfacial tension was assumed to become negative when the asymmetric alcohol used as cosurfactant penetrated the surfactant mixed film. In the remaining case, with $\gamma_{o/w} > \pi_i$, a macroemulsion would form and the system would achieve equilibrium by separating into two phases.

In 1961, Schulman and Montagne [14] used monolayer expansion to show that oil molecules are capable of penetrating a monolayer of AMP (2-amino-2-methyl-1-propanol) stearate at pH 10.4 at a hexadecane/water interface. In the duplex film method, a solution of the two oils and the surfactant is spread over the water, forming a monolayer, and the two interfaces formed—oil/water and oil/air—behave independently from each other, each maintaining its own characteristic tension. The uniqueness of the duplex method is that it allows the direct measurement of the force-area per molecule at

the liquid/liquid interface, and the study of the interaction of the oil molecules and the monolayer.

Direct measurement of the metastable negative interfacial tension at the oil/water interface is impossible, since the interface would immediately break up and spontaneously emulsify. On the other hand, if a countertension is placed on an interfacial measuring device (Wilhelmy plate) to support the interface and prevent surface breakup, π_i can be directly calculated using Equation 1.2.

$$\gamma_i = \gamma_{o/w} - \pi_i = \gamma_{a/w} - \gamma_{o/a} - \pi_d \quad (1.2)$$

where

$\gamma_{a/w}$ is the surface tension at the air/water interface;

$\gamma_{o/a}$ is the oil/air surface tension;

π_d is the surface pressure of the duplex film; and

π_i is the interfacial pressure due to the presence of the surfactant film. For the interfacial γ_i to be negative, the surface pressure π_i would have to be approximately 50 mN/m or higher when hexadecane was used as the oil phase ($\gamma_{o/w} = 50$ mN/m, and $\gamma_{o/a} = 29$ mN/m). The measured pressure π_d would only have to be 43 mN/m. The authors reported values higher than 43 mN/m if stearic acid and n-hexadecane were spread on an aqueous phase containing 2-amino-2-methyl-1-propanol at pH 10.4. The film became more expanded when hexadecanol was injected into the monolayer but collapsed at a lower pressure.

Although the authors claim that these results support the concept of negative interfacial tension in forming microemulsions, none of the previously reported work on

which they based their conception was done under the same conditions. Also, since pressures > 50 mN/m were attained using AMP stearate at pH 10.4, it should have been possible to form microemulsions with n-hexadecane using AMP stearate at this pH; but this was not the case.

Prince [15] agreed with the concept of negative interfacial tension suggested by Schulman. On the other hand, he pointed out that the interfacial tension $\gamma_{o/w}$ was quite high for aliphatic hydrocarbons (~50 mN/m) and benzene (~35 mN/m). High surface pressures were required to achieve negative interfacial tension necessary for spontaneous microemulsification. Prince realized that in Equation 1.2 the interfacial tension $\gamma_{o/w}$ could be replaced by $(\gamma_{o/w})_a$, the reduced interfacial tension resulting from the solubility of a fraction of alcohol in the oil continuous phase. Therefore, Equation 1.2 became:

$$\gamma_i = (\gamma_{o/w})_a - \pi_i \qquad (1.3)$$

As a consequence of this insight, it became obvious that in any given system, negative interfacial tension may occur only at an intermediate concentration of alcohol and surfactant.

Schulman's explanation of microemulsion formation—as he left it—was that a microemulsion would form when the interfacial tension at the water/oil interface was reduced below zero; when the interfacial tension rose back to zero, the system would reach equilibrium, with no subsequent separation. But Schulman's interpretation was not valid, since $\gamma_i = 0$ by itself is not sufficient to ensure that the dispersed phase is distributed in spherical droplets, as is found in microemulsion systems. The type of molecular interaction involved at the interface serves to distinguish microemulsions from liquid crystalline phases (cylindrical and lamellar micelles), which are known to exist in

equilibrium state. Schulman never made a distinction between microemulsions and micellar solution based on his mechanism of formation. He differentiated between the two systems only on the basis of size.

1. 2.3 PRESSURE GRADIENT AND PRINCE'S MIXED FILM THEORY

Prince [15-17], studying O/W microemulsions with oleate as surfactant and an alcohol as cosurfactant, assumed that the pressure required to create a negative interfacial tension arose from the alcohol's penetration into the surfactant monolayer and the subsequent formation of a hydrogen bond complex between the alcohol and the surfactant. In this scenario, the alcohol penetrates the oleate monolayer, shielding the charged carboxyl groups, allowing the oleate monolayer to contract and bond with the alcohol. This in turn causes closer adlineation of the hydrocarbon tails, increasing the attraction among them. Curvature of the previously flat interface occurs as a pressure gradient develops across it due to the interaction among the hydrophilic and hydrophobic portions of the oleate molecule.

Prince characterized the film/oil surface and the film/water surface of an O/W emulsion by their own hypothetical ($\pi - A$) curves. Under these circumstances, $(\pi_w)'$ and $(\pi_o)'$ are the pressures at the water and oil sides, respectively, of the flat duplex film, and π_w and π_o are the corresponding pressures at the sides of the curved film. The initial pressure gradient, π_G, across the flat film derives from the magnitude of $(\pi_w)'$ and $(\pi_o)'$.

$\gamma_{Ø}$ --the "total potential minimum interfacial tension" corresponding to $(\pi_G)'$ --is the interfacial tension before curvature; the interfacial tension before curvature should reach

a minimum value, since curvature is assumed to develop to relieve the excess pressure. The interfacial tension after curvature, γ_i, corresponds to lower film pressure π. Equation 1.3 was rewritten to give Equation 1.4.

$$\gamma_{\varnothing} = (\gamma_{o/w})_a - \pi_G \tag{1.4}$$

Purely hypothetical curves of π_G and $(\gamma_{o/w})_a$ versus concentration of alcohol were constructed. π_G was pictured as a parabola (concave down), reaching a maximum at some alcohol concentration. The interfacial tension $(\gamma_{o/w})_a$ was shown as a monotonically decreasing function of alcohol concentration. If there was an interaction of the two curves, a microemulsion formed.

The essential characteristic of Prince's mixed film theory is its description of the interfacial film as a liquid, two-dimensional third phase in equilibrium with both oil and water. This film could be presented as a duplex film, as was suggested by Bowcott and Schulman [11]. Developing a theory similar to Prince's [15-17], they proposed that, at the interface, different surface pressures, π_w and π_o, may exist on the two sides of the film. To eliminate the built-up surface pressure, curvature of the film would occur in the direction of the smaller value of π, until the pressure is equal on both sides. In the case of $\pi_o > \pi_w$, the curvature of the interfacial film would curve towards π_w, producing a W/O microemulsion. In the case of $\pi_w > \pi_o$, an O/W microemulsion would result. The driving force for this behavior is the pressure gradient (π_G) across the interface.

The mixed film theory predicts that surface pressure at the interface depends on the interaction between the hydrophilic and hydrophobic portions of a surfactant molecule. As an example, if the hydrophobic portion of the surfactant is bulky compared

to the hydrophilic group, the interaction among the hydrophobic portion will dominate, resulting in a higher surface pressure at the oil side of the film. In this case bending occurs to expand the oil side, forming a W/O microemulsion. In the case of a surfactant with relatively bulky hydrophilic group, hydrophilic interaction will dominate, producing a curvature towards the oil side of the film, leading to the formation of an O/W microemulsion. A central aspect of mixed film theory is its identification of asymmetries in the interactions across the interface as determining whether a microemulsion will form, and which form—W/O or O/W—such a microemulsion will take.

1. 3 THERMODYNAMICS OF MICROEMULSIONS

Although the models presented before give sufficient qualitative description of the forces occurring at the interface, they omit any expressions that take into account the effects of entropy or the structure of the interface.

From the point of view of traditional thermodynamics, a microemulsion is a multicomponent mixture formed of oil, water, surfactant, cosurfactant, and electrolyte. There are major differences between a solution and a microemulsion, however. In the former case, the components are mixed on a molecular scale, while in the latter, oil or water is dispersed within the opposite phase as globules on the order of 10-50 nm in diameter. The surfactant and cosurfactant are mainly located at the interface but are also distributed at equilibrium between the two media. In usual mixtures, the sizes of the component species are fixed. In microemulsions, the sizes of the globules are not given but are determined by the condition of thermodynamic equilibrium.

In 1982 at the Lund meeting on surfactant in solution, Ruckenstein et al. [18-19] presented a thermodynamic treatment of microemulsion formation, in which they proposed a drop model for microemulsion and derived an expression for its free energy that contains terms for the interfacial free energy of the droplets, for the entropy of dispersion of the globules in the continuous phase and the double layer, and for van der Waals interactions between globules. A lattice model was used to derive an approximate expression for the entropy of dispersion, in which the size difference between globules and the molecules of the continuous phase was taken into account. Varying the free energy with the radius of the globule, Ruckenstein's model allowed various states to be distinguished, and demonstrated a transition from kinetically stable to thermodynamically stable microemulsions depending on the droplet radius. Ruckenstein showed that thermodynamically stable microemulsions could form when the negative free energy changes due to the entropy of dispersion of the globules in the continuous phase combined with the dilution effect to overcome the positive product of the low interfacial tension and the large interfacial area produced.

The entropy effect generated by a very flexible, fluctuating interface has been considered by Talmon and Prager [20]. They suggested that for microemulsion systems, the interface is very soft and highly bendable. Their work demonstrated that, in the absence of other interaction effects, this entropy term might impose a certain phase transition; when the amount of surfactant is decreased, they predicted that the microemulsion separates into two phases (oil-rich and water-rich). Talmon and Prager developed a statistical thermodynamic model of microemulsion using a one-parameter free energy function. The behavior predicted by Talmon and Prager's model for their

idealized systems—transition from two-phase to three-phase and back to two-phase equilibrium—bears a strong resemblance to the phase behavior described by Shinoda and Friberg in their experimental microemulsion studies [21-23]. For Shinoda and Friberg, a continuous change from a two-phase to three-phase to two-phase system occurs with a change in the HLB.

Similar attempts had previously been made by Likhtman et al. [24], using the ideal mixture expression for the entropy, and by Reiss [25], using nucleation theory. Both Likhtman and Reiss also added an expression for the interfacial free energy contribution, but neither proposal provides a radius corresponding to the minimum free energy.

1. 4 ISOLATED MICROEMULSION

Rosano et al. [26] made use of a procedure—developed earlier by Schulman (described in Bowcott and Schulman [11])—in which a coarse emulsion of surfactant, water, and oil as the continuous phase is titrated with an alcohol to induce clarity, i.e., a water-in-oil microemulsion. In the Rosano study, after the first clearing point was obtained, more oil was added—breaking the microemulsion and re-forming a macroemulsion—and the system was then titrated back to clarity with the alcohol. This procedure was repeated several times to give several points of transparency at different volumes of the continuous phase. Rosano et al. showed that this so-called point method gave the distribution of alcohol in the microemulsion. The explanation was based on the reasonable assumption that the alcohol was distributed among three phases in the microemulsion: the dispersed phase, the continuous phase, and the interface.

Using the point method, Gerbacia and Rosano [27] studied the influence on W/O microemulsions of varying the chain length and the type of cation of the surfactant as well as the nature of the surfactant. Hexadecane and benzene were used as oil phase. Based on the distribution of pentanol between the dispersed phase and the interface, they determined the free energy accompanying the adsorption of cosurfactant at the interface, finding small negative values. Gerbacia and Rosano carried out various measurements of the water/oil interfacial tension as a function of time, observing the evolution of the interfacial tension after pentanol had been injected above and below the interface. Measurements were made both with and without SDS (sodium dodecyl sulfate) at a concentration below the CMC (critical micelle concentration), to avoid any interference from the micelles in the bulk of the aqueous phase. It was found that the interfacial tension of the system dropped to zero for a certain period of time due to the redistribution of amphipathic molecules, while at equilibrium the interfacial tension remained positive.

Later work on the theory of microemulsion formation has shown that neither the entropy effect nor interfacial tension is sufficient by itself to explain microemulsion formation. A more complete description should include a term describing the interfacial curvature and the bending energy.

1. 5 RIGIDITY AND STRUCTURE OF THE INTERFACIAL FILM

Film rigidity is an important parameter associated with the interfacial curvature. The concept of film bending energy was first introduced by Helfrich [28] and is now considered essential for an understanding of the properties of microemulsions and

vesicles. It can be described by two elastic moduli [29] that measure the energy required to deform the interfacial film from a preferred mean curvature:

- The mean bending elasticity (or rigidity), K, is associated with the mean curvature, which represents the energy required to bend a unit area of surface by a unit amount.
- The factor $\overline{K}$ is associated with the Gaussian curvature, and thus accounts for the film topology.

Theoretically, it is expected that the bending moduli should depend on (a) surfactant chain length, (b) area per surfactant molecule in the film, and (c) electrostatic head group interaction. A number of techniques have been used to determine K and $\overline{K}$ separately: in particular, ellipsometry, X-ray reflectivity, and small angle x-ray scattering (SAXS) techniques [30-32].

Helfrich's flexible surface model affords a very powerful tool for establishing the relation between geometrical description and thermodynamics. The local energy is given by the local curvature, and the total curvature free energy is obtained by integrating over the surface. The curvature of the film is defined by the parameter 1/R, the radius of curvature, and the rigidity of the film is defined by the parameter K. For curvature 1/R we expect an energy contribution per unit area of the film:

$$F = \gamma - \frac{K}{R_o R} + \frac{K}{2R^2} \qquad (1.5)$$

In this equation, the rigidity of the interface has the dimension of energy; $1/R_o$ is defined as the spontaneous curvature of the interface and can be of either sign (i.e., we consider R_o to be positive for direct micelles and negative for inverse micelles).

Considering the conditions under which microemulsions could form, De Gennes and Taupin [5] noted that the phase diagram of an oil, water, and surfactant system is usually dominated by a variety of regularly organized phases; in some cases, however, these systems form isotropic microemulsions where no periodicity occurs. They also noted that, in contrast to the high viscosity of the regularly organized phases, microemulsions are transparent fluids of low viscosity. After demonstrating that the interfacial film undulates due to the flexibility of the interface and that the amplitude of the undulation is related to the interaction between adjacent lamellae, they invoked this interfacial flexibility to explain the role of the curvature of the interface on the formation of microemulsions. Their suggestion—based on speculation rather than experimentation—was that an oil, water, and surfactant system can form a microemulsion when two conditions are satisfied:

- The surfactant is able to saturate the oil/water interface, rather than form separate aggregates (cylinders, micelles) inside the continuous phase; and
- The oil/water interface, saturated with surfactants, is very flexible and long-range interactions are weak enough so that the macrocrystal (lamellae or rods structure) must melt.

De Gennes and Taupin also developed a model for the special case of bicontinuous microemulsion systems, determining free energy expressions that include van der Waals attraction and repulsive interaction terms.

Cavallo and Rosano [33] proposed a theory of the formation of microemulsion systems that predicted the behavior of these systems only up to a certain critical dispersed phase volume, the so-called percolation threshold. For dispersed phase volumes below

the percolation threshold, the model found a single total free energy minimum corresponding to a stable system; above the percolation threshold, Cavallo and Rosano predicted instability with no free energy minimum for microemulsion systems. This model proposed that G_T, the free energy change per unit volume for the formation of microdroplets in these transparent systems, should consist of three different free energy terms. Equation 1.6 was formulated.

$$G_T = G_{SH} + G_A + G_B \tag{1.6}$$

where

G_{SH} is the free energy of formation of the interfacial sheath structure (J);

G_A is the work required to expand the interface (J); and

G_B is the interfacial bending energy (J).

Expanding these different terms of the free energy, they obtained Equation 1.7:

$$G_T = -\frac{4}{3}\pi R^3 G_S + 4\pi R^2 \left[\gamma_i + \frac{K_R}{2}\left(\frac{1}{R} - \frac{1}{R_0} \right)^2 \right] \tag{1.7}$$

where

γ_i = interfacial tension;

K_R = rigidity constant of the interface;

R = radius of the microemulsion droplet;

G_S = energy of solvation between the dispersed phase oil and the hydrocarbon tail of the surfactant molecules; and

R_o = natural radius of the curvature.

In a subsequent publication Chan and Rosano [34] discussed the mechanism of microemulsion formation using a theoretical model that considers four different free energy terms. The free energy term in this paper is identical to the expression used by Cavallo and Rosano except that it also includes G_I, a free energy term for microdroplet interactions.

$$G_I = 16\pi^2 K_R \left(\frac{R - R_{min}}{R_{min}} \right)^2 \left(\frac{R - R_{max}}{R_{max}} \right)^2 \quad (1.8)$$

where R_{min} and R_{max} are the radii of the smallest and the largest droplets that can be found in a stable microemulsion, for a given value of the rigidity constant K_R.

Since the probability of interaction between droplets, which depends on the Laplace pressure, is responsible for the stability of the microemulsion, Oleksiak and Rosano [35] introduced another factor ($\frac{\gamma_i}{\gamma_{io}}$ ratio of Laplace pressure) into the energy of interaction G_I. They formulated Equation 1.9.

$$\Delta G_T = -\varepsilon \frac{4}{3}\pi R^3 \Delta G_F + 4\pi R^2 \left[\gamma_i + \frac{K_R}{2} \left(\frac{1}{R} - \frac{1}{R_0} \right)^2 \right] + 16\pi^2 K_R \frac{\gamma_i}{\gamma_{io}} \left(\frac{R - R_{min}}{R_{min}} \right)^2 \left(\frac{R - R_{max}}{R_{max}} \right)^2 \quad (1.9)$$

This final version of the theoretical model elaborated by Rosano and various coworkers to explain the mechanism of microemulsion formation agrees with De Gennes and Taupin that the interfacial sheath rigidity is high for monodispersed systems. As the rigidity of the interface decreases, the diameter of the droplet increases and the system becomes polydispersed due to the interaction between droplets.

1. 6 STRUCTURE DETERMINATION: NMR METHOD

Lindman, Stilbs, et al., working in various groupings [36-40], studied the microstructure of "isotropic surfactant solutions" containing oil and water (microemulsions). Some years before the publication of the first of these papers in 1980, it had become evident that basic structural information on these isotropic surfactant solutions was reflected by the long-range (lateral) mobility of the individual molecules and that, therefore, molecular self-diffusion studies should offer a convenient route to investigate microemulsion structure. With the advent of the Fourier transform (FT) version of the pulsed-gradient spin-echo (PGSE) NMR techniques [39-41], it became feasible to measure rapidly and simultaneously the self-diffusion coefficients of several constituents in a complex mixture with high precision and over a broad range of molecular mobilities and compositions. They undertook an ambitious program of research into the structure of the microemulsion phases appearing in different surfactant systems based on these techniques [40].

In order to determine the self-diffusion coefficient by the FT PGSE NMR techniques, a spin-echo is Fourier-transformed to resolve individual contributions of the echo in the frequency domain. From the variation of the signal amplitudes over the time during which diffusion is monitored, the self-diffusion coefficient of a large number of components can generally be determined simultaneously. The signal amplitudes of the different constituents decay proportionally to their decay rate; a rapid decay rate thus corresponds to a rapid diffusion.

The use of self-diffusion coefficients [as in 41-43] for extracting information on solution structure is based on the relation between diffusivity and the size of the diffusing

objects. This relation is defined by the Stokes-Einstein equation; in the particular case of a spherical object, there is an inverse proportionality between the self-diffusion coefficient and the radius. A molecule that is part of a big aggregate and has a long lifetime in the aggregate will diffuse slowly over macroscopic distances, as its translational mobility is governed by the entire aggregate. Conversely, the molecule may move rapidly within the aggregate and have a high, short time-diffusion coefficient, but this is not monitored by the present type of experiments. If there is a certain probability for the studied molecule to exist in a non-aggregate state in the interaggregation solution, the self-diffusion coefficient will become higher than if it is confined entirely to the aggregate. In fact, the effective observable self-diffusion is the weighted average over the different environments of the molecule samples as a function of time.

Based on such simple reasoning, molecular self-diffusion over macroscopic distances is very sensitive to confinement into closed domains. Thus, multicomponent self-diffusion studies, as obtained most conveniently in the Fourier transform spin-echo NMR work, can easily distinguish among different structural models in many cases. These models include a water-in-oil, an oil-in-water, and a bicontinuous structural model.

- Water-in-oil structure: since water is confined to closed domains for a water-in-oil structure, water diffusion will be slow for this type of structure. If surfactant molecules occur only at the interface, their diffusion will be the same as that of the droplets themselves. Oil diffusion will be high, since oil forms the continuous domains, and will be retarded with respect to the neat oil only by an obstruction effect due to the droplets and by penetration between surfactant alkyl chains. Therefore, a water-in-oil structure predicts that

$$D_{oil} >> D_{water} \approx D_{surfactant} \approx D_{droplet}$$

- Oil-in-water structure: in this case water diffusion occurs in a continuous medium and is retarded compared to neat water only by surfactant solvation and obstruction. Therefore, an oil-in-water structure predicts that

$$D_{water} >> D_{oil} \approx D_{surfactant} \approx D_{droplet}$$

- Bicontinuous structure: There are many possible structures in which both water and oil form domains that are continuous over macroscopic distances and where surfactant molecules are located at the interfaces between these domains. Examples include layered or channel-type structures. D_{water} and D_{oil} will both be high for continuous microemulsions, lowered by the value of the neat liquids only by obstruction and solvation/penetration effects. Diffusion of surfactant will be hindered by its location at the interfacial film.

1. 7 THE R-RATIO

The R-ratio was first proposed by Winsor [44] as a way to account for the influence of "amphiphiles" (surfactants) and solvents on interfacial curvature. Winsor's initial insight identified the amphiphile layer's preferential tendency to disperse—into the oil region, or into the water region—as determining the curvature of the interfacial region. If one phase is favored, the interfacial region tends to take on a definite curvature. There are three possibilities for this R-ratio, defined as the ratio of the sum of cohesive energies stemming from interaction of the interfacial layer with oil to the sum of the energies resulting from the interface's interaction with water: (I) if R>1, the interface tends to increase its area of contact with oil while decreasing its area of contact with

water, and oil will tend to become the bulk or continuous phase; (II) if R<1, the interface tends to increase its area of contact with water, and water will tend to become the bulk phase; finally, (III) R=1 corresponds to a balanced interfacial layer.

1. 8 PACKING PARAMETER

Changes in film curvature and microemulsion type can be addressed quantitatively in terms of geometric requirements. This concept was introduced by Israelachvili et al. [45] and is widely used to relate surfactant molecular structure to interfacial topology. The authors pointed out that the nature of the aggregation formed depends on the packing ratio given by $V/a_o l_c$, where V is the partial molecular volume, a_o the head group area of the surfactant molecule, and l_c the maximum chain length. Adsorption of a cosurfactant into the surfactant aggregates produces a "wedge effect" that increases the volume per surfactant molecule without affecting l_c or a_o. Accordingly, $V/a_o l_c$ should increase with the addition of cosurfactant. In practice, however, the packing parameter is affected by many factors, including the ionic strength of the solution, temperature, pH, and hydrophilic head group of the surfactant. The preferred curvature is governed by the relative areas of the head group, a_o, and the tail group, V/l_c. In terms of microemulsion types,

- If $a_o > V/l_c$, an oil-in-water microemulsion forms;
- If $a_o < V/l_c$, a water-in-oil microemulsion forms;
- If $a_o \approx V/l_c$, a "middle-phase microemulsion" is the preferred structure.

1.9 PHASE BEHAVIOR AND RULE

Solubilization and interfacial properties of microemulsions depend on pressure and temperature as well as on the nature and concentration of the components. It is thus of prime importance to establish phase stability diagrams (or phase maps), and to locate the different structures formed within these water (salt)-oil-surfactant-alcohol systems, in terms of these variables. Several types of phase diagrams can be identified depending on the number of variables involved. Using an adequate mode of representation, it is possible not only to describe the limits of existence of the single and multiphase regions, but also to characterize equilibria between phases (tie-lines, tie-triangles, critical points, etc.).

The phase rule (discussed at length in Rock [46]) makes it possible to relate the number of variables (or degrees of freedom) in a system to its composition and conditions. The rule is generally written as:

$$F = C - P + 2$$

where F is the number of possible independent changes of state or degrees of freedom, C is the number of independent chemical constituents, and P is the number of phases present in the system. A system is called invariant, monovariant, bivariant, and so on, according to whether F is zero, 1, 2, and so on. In general, microemulsions contain at least three components: oil (O), water (W), and surfactant (S), and, as we have seen, a cosurfactant (alcohol) is usually added to tune the system stability. Even with the addition of a cosurfactant, however, these systems can be considered (at least to a first approximation) as simple O-W-S systems: whenever a cosurfactant is used, the oil:alcohol ratio is kept constant, and it is assumed that the alcohol does not interact with

any other component. Reducing the number of variables by keeping one term constant and/or by combining two or more variables makes it possible to produce ternary and binary phase.

An example of the diagrams made possible by such simplification can be seen in a review paper by Rosano [7]. His ternary phase equilibria diagram for a system of 0.3M aqueous potassium oleate, n-hexadecane, and 1-hexanol (reproduced here as Figure 1.1) shows two microemulsion systems, O/W and W/O, separated by a clear birefringent gel system.

1.10 NON-IONIC SURFACTANT SYSTEMS

Microemulsion systems stabilized by non-ionic surfactants differ significantly from those using ionic surfactants. The latter have been characterized by their response to surfactant/cosurfactant ratio, for W/O microemulsions, and by the corresponding behavior depending on the water/surfactant ratio, for O/W systems. Temperature effects and the nature of the hydrocarbon have little significance for the formation of these systems. In contrast, both the nature of the hydrocarbon and the temperature play key roles in microemulsion formation for non-ionic surfactant-based systems. Shinoda [47] provides a good example of this profound dual dependence, which is described in greater detail by Shinoda and coworkers [48, 49].

When a solution of a non-ionic surfactant in water is heated, the solution becomes visibly turbid at a temperature known as the cloud point. At this temperature the solution separates into a surfactant-rich phase and a water-rich phase [50-53].

The important feature of non-ionic surfactants—from an applications-based, cost-effectiveness viewpoint—is the notable increase in the solubility of oil in an aqueous non-ionic surfactant solution at the cloud point (and in the solubility of water in a non-aqueous solution at the analogous haze point) [47]. The solubilization curve of the oil in an aqueous non-ionic solution as a function of temperature is observed at a relatively low temperature: solubilization of the oil increases as the temperature is raised and increases markedly close to the cloud point. This pattern is mirrored by that displayed by the solubility curve of water in a non-aqueous surfactant solution: starting at a relatively high temperature, the solubility of water increases as the temperature decreases, most dramatically near the haze point.

A key determinant of microemulsion phenomena in systems based on a non-ionic surfactant is the PIT (for "phase inversion temperature") point, the temperature range over which such a surfactant causes the phase reversal of an O/W micellar solution to a W/O solution (also referred to as the HLB, or "hydrophilic/lipophilic balance" temperature). From Shinoda's empirical studies [47-53], the requirements for increased solubilization using a lesser amount of solubilizer may be summarized as follows:

- Optimum Temperature for a Given Non-ionic Surfactant

  The solubilization of water in a non-aqueous, or oil in an aqueous, solution of non-ionic surfactant exhibits a maximum at an optimum temperature. Thus, for a given non-ionic surfactant, solubilization efficiency—microemulsification with least solubilizer—will occur at temperatures close to its PIT.

- Optimum Ratio of Surfactant

In order to increase solubilization, the HLB (or PIT) of a surfactant mixture must be matched to the given oils.

- Solubilization Range

  The solubilization of oil (or water) is greater when the non-ionic surfactant is monodispersed than when the distribution of hydrophobic chain lengths is broad or when the difference in the PITs is large.

- Solubilization Power

  If the size of the hydrophile and lipophile groups of the solubilizer increases, the CMC (critical micelle concentration) will decrease, the aggregation number will increase, and the solubilization power will be enhanced. This mechanism can be exploited by appropriate replacement of a given solubilizer's hydrophilic or head group; for example, where the head group is a polyoxyethylene chain—not strongly lipophobic—replacing it with a suitable mixture of sucrose monoester and sorbitan monoester in the oil phase will decrease the CMC and increase the solubilization of water.

- Temperature Range Stability

  Non-ionic surfactants are good solubilizers, but only over a limited temperature range. In contrast, ionic surfactants are stable over wide temperature ranges but must be used in higher concentrations. A mixture of non-ionic surfactant and ionic surfactant seems ideal.

Although the first microemulsion systems studied by Hoar and Schulman [8] involved four components, the greater simplicity of the three-component systems based

on non-ionic surfactants has led to their use both in the experimental work of establishing phase behavior and in theoretical modeling. Shinoda in particular has made great progress in simplifying our understanding of the phase behavior of non-ionic microemulsion; working independently of Shinoda, Kahlweit has also contributed to this area. Working in separate teams, both Lindman and Friberg have made successful use of the so-called "Shinoda cut"; in this technique, developed by Shinoda and Friberg, the surfactant concentration is kept constant while both the temperature and the volume of solvents are varied, in order to illustrate microemulsion structure applicable to surfactant systems [53].

Figure 1.2, from Kumar and Mittal [54], presents a generic picture for a non-ionic surfactant-water-oil ternary system: pressure and surfactant concentration are kept constant, leaving two variables, temperature and water-to-oil ratio. This diagram shows the various surfactant phases obtained as a function of temperature and water-to-oil ratio. At markedly positive curvature we have oil-swollen micelles or oil droplets; at significant negative spontaneous curvature there are discrete water reversed micelles or water droplets. In this model, as the volume of the dispersed phase increases, droplets increase in size, eventually becoming connected, and the bicontinuous structure is disrupted into discrete particles.

1.11 HYDROTROPE FUNCTION

During the last fifteen years or so, a large number of review articles and monographs on microemulsions have been published. In contrast, as Friberg et al. point out [60], the related phenomenon of hydrotropic solutions has not received a lot of

attention, and the number of review articles is limited [55-58]. Hydrotropes, typically used in high concentrations, are used as solubilizing agents, and lead to a very high degree of solubilization. The presence of a hydrotrope—Friberg used sodium xylenesulfonate (SXS) in the experimental work reported in this study—destabilizes the lyotropic liquid crystalline phase, and prevents phase separation in aqueous solubilized systems. The hydrotrope is understood to act as a compound, joining formerly separate oil-in-water areas into one region by connecting oil-soluble and water-soluble compounds.

By comparing two-phase diagrams with and without the presence of the hydrotrope (reproduced here as Figures 1.3 and 1.4), Friberg showed that with the addition of a hydrotrope, O/W and W/O isotropic liquid regions in a phase diagram could be united into a single region, while the lyotropic liquid crystalline phase vanished.

1.12 VALIDITY OF THE TITRATION METHOD

The validity of the dilution method or "point method" developed by Rosano et al. on the basis of earlier work by Schulman (see Section 1.4 above) was checked by Taupin et al. [60] using neutron scattering techniques. The variable-contrast images possible with neutron scattering reveal information on the internal structure of the objects studied. In the case of the microemulsion systems examined by Taupin, where interactions are not too strong the composition and structure of the micelles are not modified until dispersed-phase volume fractions of about 30% are reached.

In 2004, Giustini et al. [61] published an important paper entitled "Does the Schulman's Titration of Microemulsion Really Provide Meaningful Parameters?" in

which they demonstrated, based on results from pulsed gradient spin-echo NMR, that Schulman's titration method quantitatively describes the cosurfactant partition and that the titration path corresponds to a dilution path for reverse micelles dispersed in a continuous bulk. They concluded that analysis of the data obtained from the classic Schulman titration effectively describes the microemulsion behavior along a path where the self-assembled aggregates are separated by increasing inter-aggregate distances with the composition of both the aggregates and the continuous phase remaining unchanged.

1.13 CONCLUDING REMARKS

With general agreement on important issues regarding thermodynamic stability and microstructure, the microemulsion field has become a well integrated part of research into colloids and surfaces. This prevailing agreement does not imply unanimity on all aspects of microemulsion formation, however. Although many theories have been proposed to explain the mechanism and theory of microemulsion formation, negative interfacial tension—as proposed by Schulman et al. in 1960 [13]—continues to be the most widely accepted hypothesis. Currently, although many scientists have been trying to modify the Schulman concept, they still accept the idea of negative interfacial tension during emulsification. Some of them also retain the notion of zero interfacial tension at the equilibrium. As early as 1973, Rosano went even further in modifying the original Schulman model, suggesting that a positive interfacial tension at equilibrium would be an appropriate assumption for the formation of droplets, since the interfacial tension for a droplet is always positive [27].

The experimental work presented in the rest of this dissertation supports Rosano's insight, and demonstrates that a positive interfacial tension at equilibrium is required. More important, it shows that these microemulsion systems form when the surfactant interfacial film has equal solubility in the two phases ("borderline solubility").

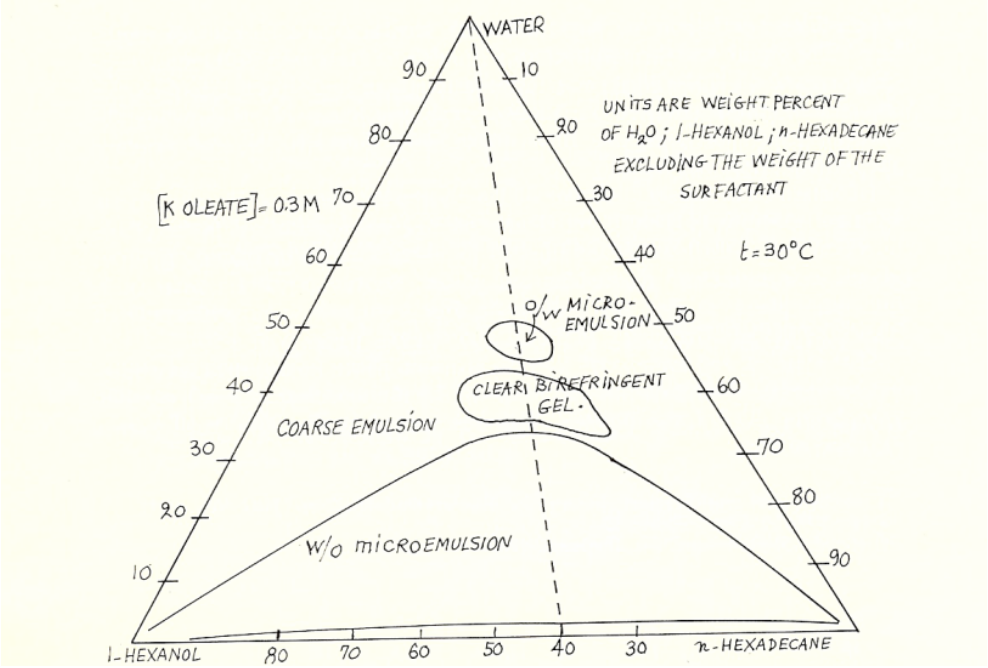

Figure 1.1 Ternary phase equilibria diagram for a system of 0.3M aqueous potassium oleate, n-hexadecane, and 1-hexanol

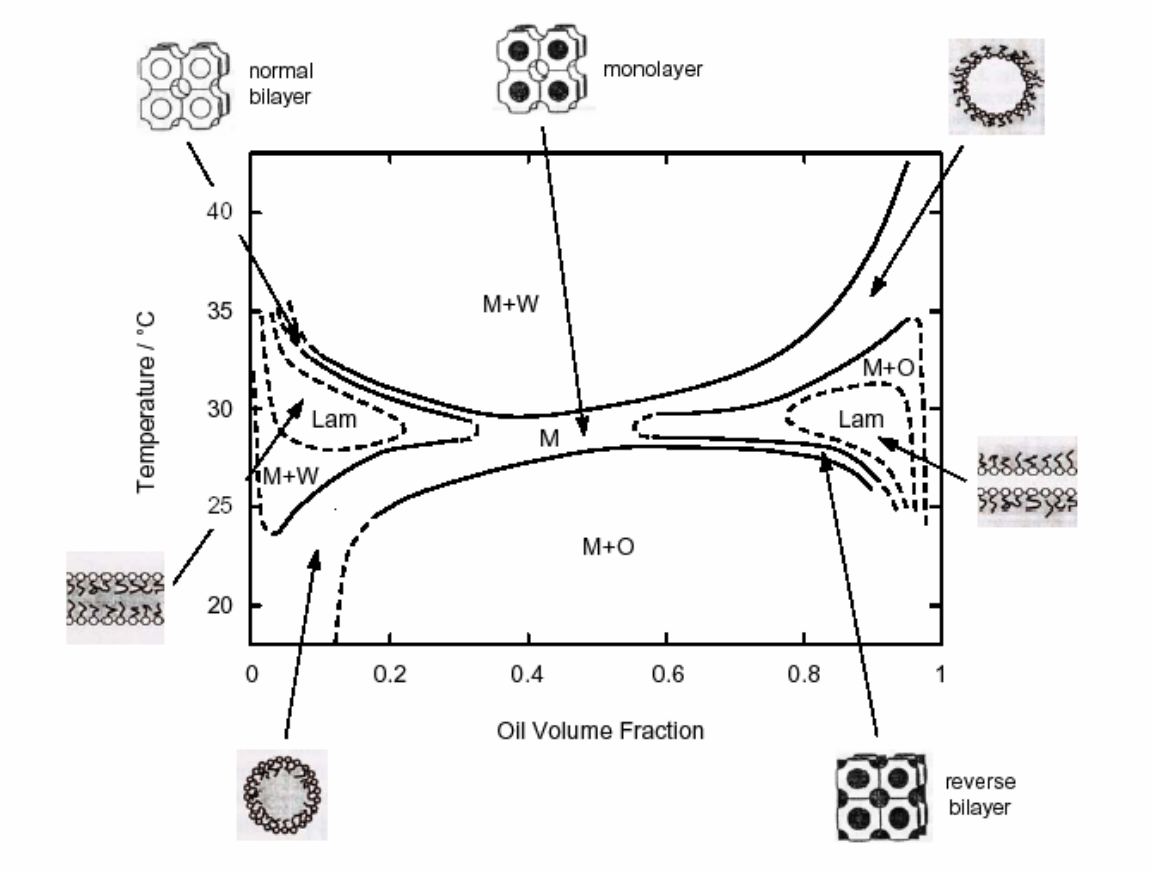

Figure 1.2 A generic picture for a non-ionic surfactant-water-oil ternary system

Pressure and surfactant concentration are kept constant

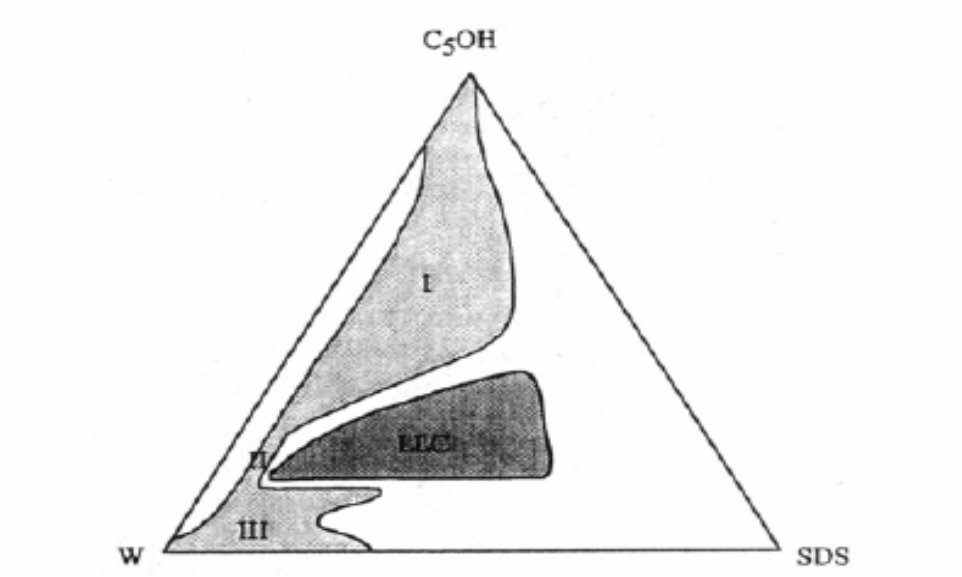

Figure 1.3 Phase diagram of water, surfactant (SDS), pentanol (C_5OH), and water without the presence of a hydrotrope

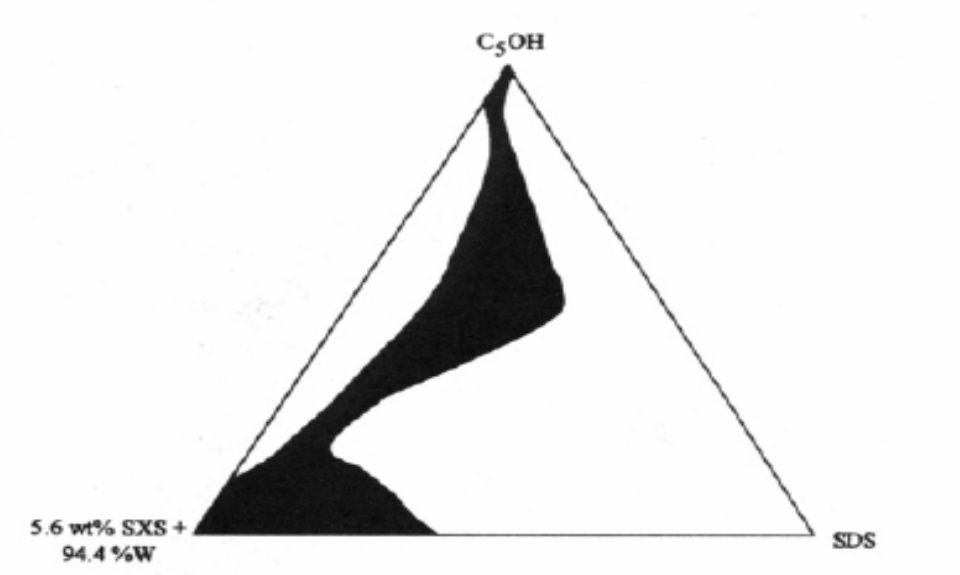

Figure 1.4 Phase diagram of water, surfactant (SDS), pentanol (C_5OH), and water with the presence of a hydrotrope (SXS)

CHAPTER 2

MECHANISM OF FORMATION AND PERCOLATION IN NON-IONIC MICROEMULSION SYSTEMS USING ($NP(EO)_n$) SURFACTANTS

2.1 INTRODUCTION

A microemulsion is defined as an isotropic, thermodynamically stable dispersion of two immiscible liquids—generally, "oil" and "water," one being the dispersed phase, the other the continuous phase—in which the individual droplets of the dispersed phase have an average diameter in the range of 6-50 nm. In practice, microemulsions are stabilized by the presence of surfactants [1-6]. My intent, in the investigation that was the basis for this dissertation, was to consider the formation and characteristics of a class of microemulsions containing such non-ionic surfactants as nonylphenolethylene oxide ($NP(EO)_n$): these are surfactants with a hydrophilic part consisting of a varying number of ethylene oxides and a hydrophobic part consisting of a nonylphenol.

Along with "microemulsion" [7], such other terms as "swollen micellar solution" [8], "hydrophilic lipomicelles" [9], "micellar solution" [10], "middle phase" [11], "unstable microemulsion" [12], and "spontaneous transparent emulsion" [9]—transparency is a consequence of the small diameter of the dispersed-phase droplets—have been used to describe these systems. Microemulsions differ fundamentally from macroemulsions in that the former are thermodynamically stable whereas the latter are kinetically stable. Furthermore, microemulsions form relatively spontaneously due to

specific interactions among the constituent molecules at the oil/water interface. Early work by Rosano et al., studying the sedimentation rate of microemulsion systems using ultracentrifugation [13], yielded important insights into the molecular configuration at the interface: it was found that a fixed amount (by weight) of surfactant will cover only a constant total interfacial area, and within this constraint, a change in dispersed-phase volume will cause the droplets to swell, shrink, or change in number. Rosano et al. concluded that the surfactant maintains a configuration at the interface capable of producing these finely dispersed systems. Later experiments using titration and differential scanning calorimetry (DSC) techniques [14] indicated that the amount and the composition of the interfacial layer surrounding the dispersed phase of a microdroplet system remain constant, while the volume of the dispersed phase can vary within limits.

My investigation, which used the "point method" of microemulsion preparation described by Rosano et al. [14, 15], included measurements of transmittance, interfacial and surface tension, surface pressure and potential, and electrical conductance, as well as particle size determination for a class of microemulsions formed with surfactants of the form ($NP(EO)_n$) and hydrocarbons from C_7 to C_{16}. Both W/O systems—Water/O and Saline/O—and O/W systems—O/Saline only—were studied. Table 2.1 summarizes the composition—hydrocarbon, surfactant, and cosurfactant—of the 18 microemulsions studied.

2.2 MATERIALS, EQUIPMENT, AND METHOD

2.2.1 MATERIALS

All chemicals were used as received from their suppliers: n-heptane, n-octane, n-decane, n-dodecane, n-tetradecane, and n-hexadecane, all 99+% (Aldrich Chemical Co., Milwaukee, WI); sodium chloride and nitric acid (J. T. Baker, Phillipsburg, NJ); nonylphenolethylene oxide compounds, or $NP(EO)_n$ (Igepals), all 100 % active (Rhodia HPCII, Cranbury, NJ); ferric nitrate (Spectrum, New Brunswick, NJ); and potassium thiocyanate (Mallinckrodt, St. Louis, MO).

Freshly distilled water was used in all preparations, and all glassware was first cleaned with a fresh sulfuric acid/potassium dichromate solution.

2.2.2 EQUIPMENT

Percent transmittance for microemulsions was measured using the Bausch and Lomb Spectronic 20 spectrophotometer (Sci-Bay, Rochester, NY). The isotropic structure of the microemulsions was checked with polarizing discs. Viscosity measurements were performed at room temperature using a Synchro-lectric model LVT Brookfield viscometer (Brookfield Engineering Laboratories, Stoughton, MA). Electrical conductances were measured with a conductivity meter, Model 220A (Denver Instrument Co., Denver, CO). Surface and interfacial tensions were measured using a Rosano surface tensiometer (Biolar Corp., North Grafton, MA), with sand-blasted platinum and sand-blasted Teflon blades, respectively. The force-area (ΔA) and surface potential-area (ΔV-A) characteristics of the $NP(EO)_n$ surfactants at the air/water and oil/water interfaces were investigated. The experimental apparatus for measuring surface pressure and potential was described by Kanouni et al., in a study of which I was a coauthor [16]. All experiments were conducted within a Faraday box. The particle size of the

microemulsion droplets was determined using a 90Plus particle sizer (Brookhaven Instruments Corp., Holtsville, NY).

2.2.3 METHOD OF PREPARATION

CALCULATION OF THE MINIMUM AMOUNT OF PRIMARY SURFACTANT NEEDED

Rosano [15] suggested a way to determine the minimum amount of primary surfactant molecules needed for a particular system. This method is based on geometric considerations; in particular, the assumptions that all the surfactant molecules end up at the interface, and that spherical droplets are formed. The total interfacial area A is given by Equation 2.1.

$$A = n\sigma = 4\pi r^2 \times a \tag{2.1}$$

where

n = number of surfactant molecules;

σ = area per surfactant molecule adsorbed at the interface ($Å^2$/molecule);

r = radius of the dispersed phase droplet (Å); and

a = total number of droplets formed by the dispersed phase.

The total volume of the dispersed phase is given by Equation 2.2.

$$V = \frac{4}{3}\pi r^3 \times a \tag{2.2}$$

Combining Equations 2.1 and 2.2, we have Equation 2.3, which relates the number of surfactant molecules needed to cover the interfacial area to the volume of the dispersed phase.

$$n = \frac{3V}{r\sigma} \tag{2.3}$$

The number of grams of surfactant is then given by Equation 2.4.

$$g = \frac{GMW}{6.02 \times 10^{23} \frac{molecules}{mole}} \times n \tag{2.4}$$

where g = number of grams of surfactant; and

GMW = gram molecular weight of the surfactant.

The value of σ can be obtained either from the plot of surface tension vs. log concentration of the surfactant solution or from monolayer measurements. For microemulsions, the upper limit of r is 1/4 the wavelength of visible light, while the lower limit is set by the surfactant chain length.

This simple calculation provides an approximate value for the minimum amount of surfactant necessary to cover the interface. It takes into account neither the amount of surfactant that is dispersed in both the aqueous and oil phases nor any other aggregates that may form in solution.

TITRATION METHOD

The titration method of microemulsion formation begins by forming an initial emulsion using the estimated minimum amount of primary surfactant calculated as described in the previous section.

To determine if a transparent dispersion is possible, a cosurfactant is gradually added to the coarse emulsion. If the system does not turn clear after the amount of added cosurfactant is equal to the amount of the primary surfactant used, the system can be considered unviable. In this case, one of the components must be replaced to form a

microemulsion. Since the cosurfactant is usually the nonspecific component of the system, it is the first to be altered.

The next option available, once the range of possible cosurfactants is exhausted, is to consider a new primary surfactant. A fresh calculation is made to determine the minimum amount of the new surfactant, and repeat titrations are carried out with the various cosurfactants until a successful result is obtained.

As a last resource, if none of the primary surfactant/cosurfactant pairs can be made to work, the dispersed phase in an O/W system can be altered and the entire procedure repeated. (In the case of a W/O system, no change in the dispersed phase is possible.) In the case of a hydrocarbon dispersed phase, for example, the chain length can be systematically increased or decreased, depending on the requirement of the formulation.

When microemulsions are prepared by the titration method various changes are often noted. Sometimes there are dramatic viscosity increases just before the mixture becomes transparent. Also, mixtures may progress from lactescent to clear, rapidly or slowly, as drops of cosurfactant are added.

Aronson's experimental results [17] show that, above a certain concentration of surfactant molecules, we observe a phenomenon of creamage—due to reversible flocculation by free surfactant—rather than a smooth transition to smaller particle sizes.

APPLYING THE TITRATION METHOD

Each of the 18 systems shown in Table 2.1 started with an identical dispersed-phase volume of 1 ml. Using the Rosano method described in Section 2.2.3.1, an estimated

value of g (minimum number of grams of primary surfactant) was calculated for each case; these values were all close to 1. To facilitate comparisons among the various systems, the amount of primary surfactant was set at 1 g throughout.

All microemulsions were prepared using the titration method (also known as "point method"). The W/O and Saline/O systems used a nonylphenolethylene oxide $NP(EO)_n$ surfactant (HLB greater than 9; see Table 2.2) dispersed in the aqueous phase and a hydrocarbon as the continuous phase, in a 30°C water-jacket beaker. (Since viscosity levels are always quite low with these systems, simple mixing equipment is sufficient.) The emulsions were then titrated to clarity (% transmittance > 95 % at 520 nm), using another $NP(EO)_n$ with an HLB less than 9 as cosurfactant. Continuous stirring was maintained throughout the titration process to ensure homogeneous mixing. (Most of these cosurfactants are liquids and can easily be titrated into the emulsion with gentle mixing.)

One example of the Saline/O microemulsions prepared in this way used 1 ml of saline (1% NaCl), 1 g of NP-6-EO (Igepal CO-530), and 20 ml of n-decane. The emulsion was titrated to clarity with, as cosurfactant, either NP-4-EO (Igepal CO-430) or NP-1.5-EO (Igepal CO-210). (See Table 2.1, Experiments 9 and 12.) In the case of O/Saline systems, the phases are reversed; the surfactant chosen had HLB less than 9, and titration was with NP-9-EO (Table 2.1, Experiments 16-18).

2.3 EXPERIMENTAL

2.3.1 TRANSMITTANCE MEASUREMENTS

Transmittance was measured for each of the nonylphenolethylene oxides $NP(EO)_n$ used. Three drops of each one were added to a separate pair of test tubes, one containing 5 ml of saline (1% NaCl) and the other containing n-decane. After mixing, the percent transmittance at 520 nm was determined. The results are shown in Figure 2.1.

2.3.2 INTERFACIAL AND SURFACE TENSION MEASUREMENTS

To rid the aqueous substrate (saline) of surface impurities, it was cleaned (as described by Christodoulou et al. [18]) by foaming in a 600-ml medium porosity sintered glass funnel, with the foam removed by repeatedly sweeping the surface until unstable bubbles were observed. After this cleansing procedure, the various $NP(EO)_n$ surfactants are dissolved in saline in different concentrations.

The surface tension of these $NP(EO)_n$ solutions was measured, and the CMC (critical micelle concentration) determined for each $NP(EO)_n$ studied. The area per surfactant molecule adsorbed at the water/air interface (σ) was calculated using the Gibbs adsorption equation:

$$\Gamma = -\left(\frac{1}{RT}\right)\frac{d\gamma}{d\ln(c)}, \qquad (2.5)$$

where Γ is the surface excess, R the gas constant, T the temperature, γ the surface tension, and c the concentration of the surfactant; see Table 2.3.

Interfacial tension between n-hexadecane and each $NP(EO)_n$ solution at the CMC determined experimentally was measured (see Section 2.2.2); values are shown in Table 2.4.

2.3.3 SURFACE ISOTHERMS

THEORY

SURFACE PRESSURE

A fluid interface, e.g., an air/water interface, has the advantage of being idealizable as a plane interface, which makes it possible to determine the change in interfacial free energy by a simple measurement of surface pressure. In the Wilhelmy method, the most widely used way to measure the surface pressure of plane fluid interfaces, a thin plate, usually made of platinum, is partially immersed in the liquid phase and is connected to an electromicrobalance. The forces acting on the plate are its weight *P* and surface tension effect downward, and Archimedes buoyancy *A* upward. The net downward force F is given by Equation 2.6:

$$F = P + 2\gamma(W + t)\cos(\theta) - A \tag{2.6}$$

where *W* and t (t<<*W*) are the width and the thickness of the plate, respectively, and θ is the contact angle of the liquid with the solid plate. If the plate is completely wetted (platinum offers the advantage that flaming not only removes contaminants but also renders the plate wettable), the contact angle θ = 0 and cos(θ) = 1; therefore,

$$F = P + 2\,\gamma\,W - A \tag{2.7}$$

When the composition of the interface varies, *P* and *A* (provided the plate in a fixed position), then,

$$\Delta F = 2w\left(\gamma_{\text{solution}} - \gamma_{\text{water}}\right) = -2w\pi \tag{2.8}$$

where π is the surface pressure

and

$$\pi = -\frac{\Delta F}{2w} \tag{2.9}$$

SURFACE POTENTIAL

The tendency of molecules near the liquid surface in a microemulsion to have a specific orientation was noted as long ago as Hoar and Schulman's pioneering work [9] (see Section 1.2.1 above). The orientation of water molecules, which behave as dipoles, produces an asymmetric field near the surface. Spreading a monolayer (surfactant solution) on the clean water surface will produce a change in the orientation of the molecules at the interface and then a change in the nature of the electrical field. The difference, ΔV, in surface potential between the original aqueous phase and the film-covered phase is attributed to the film. ΔV is called the net surface potential or "Volta potential."

Surface potential measurements can be carried out either by the ionizing electrode method or by the vibrating electrode method. The ionizing electrode method, used in my investigation, involves ionization of the air above the film, so that it becomes conducting. The potential difference between two electrodes, a reference electrode (Ag/AgCl, for example) placed in the aqueous subphase and another in the air above the surface, can then be measured directly. The ionization in the air above the film is produced by coating the air electrode with an α-emitter, such as polonium or americium. The gap between the radioactive electrode and the liquid surface (~2 mm) is generally sufficiently conducting that ΔV can be measured by means of a high impedance voltameter.

2.3.4 MEASUREMENTS

Surface pressure for the nonylphenolethylene oxide surfactants at the oil/water interface was measured using the duplex film method. The surfactant solution in n-

hexane-hexadecane-ethanol (90%/9 %/1%, respectively) was deposited onto the aqueous surface with an Alga microsyringe (Burroughs Wellcome, Tuckahoe, NY). The substrate and the film were retained in a fused silica trough (10.7 x 2.5 x 31 cm^3) of 1.3-liter capacity. The surface was cleaned by dusting with calcinated talcum powder, which was removed with the help of a hollow glass tip connected to an aspirator. Surface pressures were then determined from surface tension measurements made by suspending a sandblasted platinum blade from a transducer-amplifier (Model 311A, Sanborn, Waltham, MA). The transducer output was recorded continuously on a recorder (Mocon, type DB/40, Kipp & Zonon, Amsterdam, Holland). The same procedure was repeated to determine the surface pressure of $NP(EO)_n$ surfactants at the air/water interface, except that n-hexadecane was not added to the solution of $NP(EO)_n$ surfactant spread on the surface of water.

To get an idea of the orientation of $NP(EO)_n$ surfactants at the air/water and oil/water interfaces, surface potentials (ΔV) were measured with an air-ionizing electrode (a Radium-226 source, U.S. Radium Corp., Morristown, NJ) placed 1-2 mm above the surface of the liquid substrate and connected to a precision potentiometer (Model 2730, Honeywell, Denver, CO), a high-input resistance electrometer (Model 610B, Keithley Instruments, Cleveland, OH), and a grounded trough electrode (Ag/AgCl or calomel) dipped into the aqueous substrate (saline 1% NaCl). The radioactive electrode was connected to the input terminal of the electrometer with amphenol low noise graphitized shielded cable and connectors. The e.m.f. of the cell composed of the radioactive electrode, the trough electrode, the potentiometer, and the electrometer, all connected in series, was measured immediately after cleaning the surface of the aqueous substrate

(V_o), and compared with the e.m.f. after spreading a film on the surface (V). The difference between the two e.m.f.'s ($V - V_o$) is the surface potential. The surface potential measurements had a precision of ± 0.6 mV. The potentiometer opposed a convenient fraction of the cell e.m.f., and the electrometer output was recorded continuously on a recorder. An automatic barrier drive with variable speed control permitted determination of an optimum compression rate and reproducible ΔA and ΔV-A isotherms. The continuous reduction of the surface area results in a measured surface pressure for stable films, which are considerably above their "equilibrium spreading pressure" but still below their "monolayer stability limit," which is defined as the maximum pressure attainable in the film without collapse. The area per molecule was determined from surface compression isotherms. Figures 2.2, 2.3, and 2.4 represent the surface pressure and potential for NP-4-EO, NP-5-EO, and NP-6-EO, respectively.

2.3.5 CONDUCTANCE MEASUREMENTS

The electrical conductance at 30^{o}C of the non-ionic Saline/O microemulsions studied was measured. Figure 2.5 shows the electrical conductance, and the volume of cosurfactant required to produce a microemulsion, plotted versus the volume of the dispersed phase (1% NaCl). The volume of the continuous phase (25mL n-decane) and the weight of surfactant (1g NP-6-EO) were constant in all formulation of Saline/O microemulsions.

Next, two microemulsions were prepared: the first containing SCN^- (reagent) + HNO_3 + H_2O in the dispersed phase, and the second containing Fe^{3+} (reagent) + H_2O in

the dispersed phase. The two microemulsions were mixed together, and the transmittance measured at 447 nm, where there is maximum absorption for the $[FeSCN]^{2+}$ complex.

2.3.6 PHOTON CORRELATION SPECTROSCOPY

THEORY

In light scattering experiments [19-21], the electric field of the incident light imparts an oscillating polarization on the particles in the sample to be analyzed. Those particles whose polarity differs from the surroundings scatter the incident light. Within the sample, the particles are in constant motion, and it is the movement of particles that causes fluctuations in the detected intensity signal. The duration of fluctuations contains physical information about the particles, including size.

Diffusivity of a particle suspended in a liquid is opposed by the liquid's viscosity, so that the particles spread throughout the liquid more slowly as the thickness of the liquid increases. For slow motion, laminar or steady-state flow is a good assumption. The Stokes-Einstein equation (2.10) for the diffusivity of particles in a liquid defines the diffusion coefficient, D, of the particles as

$$D = \frac{k_B T}{6\pi\eta r} \tag{2.10}$$

where

k_B is Boltzmann's constant;

T is the temperature in Kelvin;

η is the viscosity of the liquid in which the particles are suspended; and

r is the radius of the particles.

Since the fluctuation of the intensity signal is caused by the motion of particles, those particles that diffuse more quickly are characterized by a smaller fluctuation time. The diffusion coefficient is inversely proportional to the size of the particles, and consequently, the smaller the particle, the shorter the fluctuation time.

A correlation equation can be used to determine the correlation or relationship between the measurements of a fluctuating signal. To measure the correlation of an intensity signal, the time average of the signal is taken by the so-called autocorrelation function (see Equation 2.11).

$$g_1(t) = \langle I(t)I(t+\tau)\rangle = \exp(-t\Gamma) \tag{2.11}$$

where

I(t) is the light intensity at time t;

τ is a slight time increment; and

Γ is the linewidth of the spectrum.

For a monodispersed system in Brownian motion, the diffusion of the particles in erratic motion causes the intensity autocorrelation equation to decay exponentially. Γ, the linewidth of the spectrum, is related to the diffusion coefficient by $\Gamma = Dq^2$, and the scattering vector, q, is given by Equation 2.12:

$$q = \frac{4\pi n}{\lambda_o}\sin\left(\frac{\theta}{2}\right) \tag{2.12}$$

where

n is the index of refraction of the liquid medium;

θ is the scattering angle; and

λ_o is the laser wavelength in air.

Geometrically, the scattering vector is defined as the difference between the scattered wave vector and the incident wave vector (see Figure 2.7). Combining Equation 2.10 and the equation for the linewidth, Γ, we obtain the following equation for the radius of the scattering particle:

$$r = \frac{k_B T q^2}{6\pi \eta \Gamma} \tag{2.13}$$

Photon correlation spectroscopy digitally measures the intensity fluctuations of a signal at the level of the photon. Multiple measurements are taken of the number of photons that reach a detector in a sample time. For each sample time, the autocorrelation function is computed by an automated correlator. When the logarithm of the autocorrelation function is graphed versus time, the slope of the resulting line is the linewidth, Γ. Using Equation 2.13, the size of the scattering particles can be determined.

SIZE DETERMINATIONS

The droplet-size analysis of the Saline/O microemulsions was performed at a wavelength of 661 nm and an angle of 90^o. The microemulsion was filtered with a 0.1 micron PTFE syringe to ensure a low, flat baseline. After filtering, the microemulsion was placed inside the 90 plus particle-size analyzer and the size of the droplets determined. Figure 2.8 shows the amount of cosurfactant needed to yield microemulsions of varying dispersed-phase volume, and the droplet diameter and transmittance of the microemulsions produced at constant weight of surfactant (1g NP-6-EO), and constant continuous phase (25 mL n-decane).

2.4 RESULTS AND DISCUSSION

2.4.1 TITRATION

Each microemulsion studied was titrated to clarity (transmission greater than 95% at 520 nm) at 30°C, with constant surfactant concentration and constant volume of the dispersed phase, for various volumes of continuous phase. Figure 2.9 shows the volume of the cosurfactant plotted against the volume of the continuous phase**.** By extrapolating experimentally determined values for the cosurfactant volume to that corresponding to a zero-volume continuous phase, it is possible to determine the composition of the interface—the surfactant/cosurfactant ratio—, assuming that both surfactants are adsorbed at the interface. Also, for a given volume of the continuous phase, the difference between the total amount of surfactant and the amount at the interface represents the amount of cosurfactant at equilibrium in the continuous phase.

Knowing the relative amounts of surfactant and cosurfactant enables us to calculate the average number of ethylene oxide (EO) per nonylphenol adsorbed at the O/W interface.

The following algorithm allows us to use Figure 2.9's interpolated y-intercept (cosurfactant volume at zero volume of continuous phase) to determine the number of ethylene oxides per molecule at the interface. The molar ratio ρ_i of the cosurfactant at the interface can be determined from Equation 2.14:

$$\rho_i = \frac{\text{moles of cosurfactant at the interface}}{\text{moles of primary surfactant at the interface}} = \frac{b \times d_{cosur}}{M_{cosurf}} \times \frac{M_{surf}}{V_{surf} \times d_{surf}} \qquad (2.14)$$

where b is the amount in ml of cosurfactant at the interface;

V_{surf} is the total amount in ml of primary surfactant;

d_{cosurf} and d_{surf} are the densities of the cosurfactant and the primary surfactant, respectively; and

M_{cosurf} and M_{surf} are the molar masses of the cosurfactant and the primary surfactant, respectively. From this molar ratio ρ_i, the average number of ethylene oxides per molecule at the interface (n(EO)) can be calculated using Equation 2.15:

$$n(EO) = \frac{\rho_i EO_{cosurf} + EO_{surf}}{1 + \rho_i} \tag{2.15}$$

where EO_{cosurf} and EO_{surf} are the average number of EO for the cosurfactant and the primary surfactant, respectively.

Table 2.1, listing the 18 microemulsion formulations studied, also shows the extrapolated EO value for each one. Experiments 1-4, all water-in-n-octane W/O microemulsions, yielded an average extrapolated EO value of 5.6. Experiments 5-15, microemulsions of saline in various hydrocarbons, showed average extrapolated EO values of 5.1. Experiments 16, 17, and 18 are, respectively, n-octane-, n-decane-, and n-dodecane-in-saline, with an average extrapolated EO value of 6.

The greater value calculated for EO at the interface in O/Saline microemulsions (Experiments 16-18) as compared to Saline/O microemulsions (Experiments 5-15) is due to the bending of the interface (steric hindrance). In contrast, the lower average EO value for Saline/O microemulsions (Experiments 5-15) as compared with W/O microemulsions (Experiments 1-4) is due to the presence of NaCl, which competes for the water of hydration. Moreover, for W/O microemulsions in general, as the chain length of the hydrocarbon increases, more cosurfactant is needed to clear the system. Note that Table 2.1 does not include O/Saline microemulsion formulations for n-tetradecane or n-hexadecane; attempts to form such microemulsions were unsuccessful, owing to the excess length of the hydrocarbon chain compared to the 12 carbon chain of the nonylphenol. A long hydrocarbon chain (n-tetradecane or n-hexadecane) penetrates to the

surfactant monolayer, with the resultant formation of a structure that is difficult to bend; this in turn impedes the formation of the microemulsion. These results indicate that the structure of the interface plays a significant role in the formation of these systems. The effect of oil penetration or oil uptake in surfactant tail on microemulsion formation has also been demonstrated by Chen et al. [22-23], who found that n-hexadecane does not form microemulsion with didodecyldimethyl ammonium bromide (DDAB) as a surfactant. Chen et al. concluded that curvature of the surfactant film is a major determinant of microemulsion structure.

2.4.2 TRANSMITTANCE

As shown in Figure 2.1**,** the percent transmittance, whether in water or in oil, is somewhat related to the solubility of the $NP(EO)_n$. For EO ranging between 5 and 6 a domain of equal solubility exists, in both the oil phase and the aqueous phase. These results lead me to suggest that when the surfactant interfacial film around the droplets is equally soluble in the two phases, microemulsions will form. Since a surfactant capable of forming W/O or O/W microemulsions will have borderline solubility in each phase, it will stay at the interface. This analysis differs fundamentally from the conclusion reached by Rosano in 1973 [24]; at that time he identified low surface tension as fundamental to spontaneous emulsification, with the surfactant serving merely to stabilize the system against coalescence. With the $NP(EO)_n$ systems considered in the current investigation, the corresponding EO values range from 5.1 for Saline/O, through 5.6 for W/O, to 6.0 EO for O/Saline systems—which is precisely the zone of equal solubility of $NP(EO)_n$ in both

water and oil phases. In short: when the interfacial film is equally soluble in both phases, the system spontaneously forms a microemulsion.

2.4.3 SURFACE AND INTERFACIAL TENSION

Table 2.4 shows that all the values of the interfacial tension at the saline/n-hexadecane interface are positive, and that the interfacial tension is dependent on the number of ethylene oxides in the $NP(EO)_n$ surfactant. These results agree with the findings of Hansen et al. [25] in their investigation of the influence of the oil phase on the adsorption of $NP(EO)_n$: their measurements of interfacial tension at the (n-dodecane or n-octane)/water interface yielded positive values. Therefore, a zero interfacial tension is not necessary for the formation of the microemulsions. The surfactant(s) must reduce the interfacial free energy and facilitate the formation of the interface, but, at equilibrium, the interfacial tension must have a positive value to give rise to the curling of the interface that enables droplet formation.

Table 2.3 indicates that, as the number of ethylene oxides increases, both the area per surfactant molecule at the water/air interface and—as shown by the values of CMC—the solubility of the $NP(EO)_n$ surfactant in water also increase.

2.4.4 SURFACE ISOTHERMS

Analysis of Figures 2.2, 2.3, and 2.4**,** showing surface pressure and potential for various $NP(EO)_n$ surfactants, shows that the $NP(EO)_n$ is an expanded film, and that the area per molecule of $NP(EO)_n$ surfactant at the oil/water interface is higher than the area per molecule at the air/water interface as a result of the oil penetration to the surfactant

monolayer. This hydrocarbon chain length penetration to the surfactant monolayer is responsible for the high extrapolated value of ethylene oxide (EO) at the interface for the O/W microemulsions listed in Table 2.1 (Experiments 16, 17, and 18), which is due to the bending of the interface in the case of O/W microemulsions in general. Moreover, oil penetration to the surfactant monolayer in the case of n-tetradecane and n-hexadecane as the dispersed phase prevents the formation of such O/W microemulsions.

2.4.5 PERCOLATION OF THE MICROEMULSIONS

Figure 2.5 shows the volume of cosurfactant (NP-4-EO) required to produce saline-in-oil microemulsions for different volumes of the dispersed phase (1% NaCl) and the conductance of each microemulsion produced. For this type of microemulsion structure, the oil phase is continuous and all the water is isolated and surrounded by the oil, which is poorly or non-conducting. For dispersed-phase volumes below 1.3 mL, the conductance of the microemulsions is approximately constant and very low. Any further increase in dispersed-phase volume—above 1.3 mL—causes a sharp increase in microemulsion conductance. In contrast to this sharp change in conductance, Figure 2.5 demonstrates that the volume of the cosurfactant needed to produce the microemulsion remains constant.

As shown in Figure 2.8, for dispersed-phase volumes between 0.6 and 1.3 ml, the diameter of the droplets was found to be around 20 nm, approximately constant. Beyond 1.3 mL—threshold volume, or Φ—of the dispersed phase the diameter increases, in agreement with the results noted above and shown in Figure 2.5. For dispersed-phase volumes below 0.5 mL, the microemulsions formed have 87 % transmittance as a result

of insufficient volume of the dispersed phase. Therefore, a minimum volume of the dispersed phase is required to form microemulsions with a given amount of surfactant: in this case, approximately 0.6 mL of dispersed phase for 1 g each of NP-6-EO and NP-4-EO, a total of 2 g of surfactant.

Figure 2.6 reveals that when the volume of the dispersed phase is below the threshold volume Φ, there is no formation of the complex $[FeSCN]^{2+}$and no color change; as the volume of the dispersed phase increases above the threshold volume, the complex is formed, with resulting decrease in transmittance of the two mixed microemulsions, and the mixture remains clear and stable. The reaction between Fe^{3+} and SCN^- that gives rise to the formation of the complex implies that a droplet from the first microemulsion has merged with a droplet from the second microemulsion.

A charge on a water microdroplet can propagate either by "hopping" of surfactant from one microdroplet to another or via transient fusion and mass exchange [3]. The results shown in Figure 2.6 support the scenario involving transient fusion and mass exchange as the mechanism by which a charge propagates from one microdroplet to another.

Figures 2.5, 2.6, and 2.8 demonstrate that when the volume of the dispersed phase (saline 1% NaCl) is low—below the threshold volume Φ—the individual droplets behave like large molecules in solution (isolated microemulsion droplets), with no interdroplet interaction taking place; when the volume of the dispersed phase is higher than the threshold value, a connected set of globules is formed and a dynamic equilibrium is established, with droplets merging and re-forming while the microemulsion remains a single transparent phase (see Figure 2.10). This phenomenon, known as "percolation,"

was previously identified by Safran [26] and Cavallo and Rosano [27] in their vapor-pressure analysis studies of O/W microemulsions.

Despite the fact that the dispersed-phase volume was increased while both the continuous-phase volume (25 mL n-decane) and the amount of surfactant (1 g NP-6-EO) were kept constant, the cosurfactant volume needed to yield a microemulsion remained constant. Therefore, the cosurfactant—NP-4-EO—is insoluble in the dispersed phase, as was assumed in the calculation of the surfactant molar composition at the interface, and the same surfactant/cosurfactant molar ratio prevails in the film surrounding microemulsion droplets for different dispersed-phase volumes.

If the surfactant/cosurfactant composition is the same whether the film is surrounding high or low volumes of the dispersed phase, we may conclude that at low dispersed-phase volumes, the water droplets are strongly bound to the surfactant interfacial film, while for high dispersed-phase volumes, the droplets are weakly bound to the film. The latter conclusion explains the easy merging of droplets observed at high dispersed-phase volumes [28-36].

2.5 CONCLUSION

Taken together, these results suggest that several conditions must be met simultaneously for the formation and stability of a microemulsion based on the non-ionic surfactants under consideration. First, the amount of surfactant(s) used must be sufficient to cover the total interfacial area of the droplets, and the volume of dispersed phase adequate to accommodate the hydrophilic groups of the surfactant. Second, the chain length of the oil must be compatible with the hydrophobic part of the surfactants to

facilitate the formation of O/W microemulsions. Finally, the interfacial mixed film of non-ionic surfactant(s) must be of equal solubility in both the oil and the aqueous phase.

Regarding the dynamic behavior of microemulsion systems, two distinct regions of phase behavior occur, corresponding to low and high volumes of the dispersed phase. At low dispersed-phase volumes—below the threshold volume Φ—the individual droplets behave as isolated entities, with no interdroplet interaction taking place (both electrical conductance and droplet diameter remain constant). When the dispersed-phase volume exceeds Φ, the system changes dramatically, with sharp increases in both electrical conductance and droplet diameter. Individual droplets begin to interact, and a dynamic equilibrium is established, with droplets merging and re-forming while the system as a whole remains a single transparent phase.

Exp.	T (^{o}C)	Continuous Phase	Dispersed Phase	Primary Surfactant	Cosurfactant	Extrapolated n (EO)
1	30	n-octane	Water (1ml)	NP-9-EO (1g)	NP-4-EO	5.7
2	30	n-octane	Water (1ml	NP-9-EO (1g)	NP-1.5-EO	5.5
3	30	n-octane	Water (1ml)	NP-6-EO (1g)	NP-4-EO	5.9
4	30	n-octane	Water (1ml)	NP-6-EO (1g)	NP-1.5-EO	5.4
5	30	n-heptane	Saline (1ml)	NP-6-EO (1g)	NP-4-EO	5.2
6	30	n-octane	Saline (1ml)	NP-9-EO (1g)	NP-4-EO	5.3
7	30	n-decane	Saline (1ml)	NP-9-EO (1g)	NP-4-EO	5.2
8	30	n-decane	Saline (1ml)	NP-7.5-EO (1g)	NP-4-EO	5.4
9	30	n-decane	Saline (1ml)	NP-6-EO (1g)	NP-4-EO	5.3
10	30	n-decane	Saline (1ml)	NP-9-EO (1g)	NP-1.5-EO	5.1
11	30	n-decane	Saline (1ml)	NP-7.5-EO (1g)	NP-1.5-EO	5.2
12	30	n-decane	Saline (1ml)	NP-6-EO (1g)	NP-1.5-EO	5.2
13	30	n-dodecane	Saline (1ml)	NP-9-EO (1g)	NP-4-EO	5.1
14	30	n-tetradecane	Saline (1ml)	NP-6-EO (1g)	NP-4-EO	5.0
15	30	n-hexadecane	Saline (1ml)	NP-6-EO (1g)	NP-4-EO	4.9
16	30	Saline	n-octane (1ml)	NP-5-EO (1g)	NP-9-EO	6.0
17	30	Saline	n-decane (1ml)	NP-5-EO (1g)	NP-9-EO	6.0
18	30	Saline	n-dodecane(1ml)	NP-5-EO (1g)	NP-9-EO	6.0

Table 2.1 W/O and O/W microemulsions prepared with nonylphenol ethylene oxide NP(EO)$_n$ surfactants

Nonylphenol Ethoxylates

Igepal	# of (EO)	HLB
210	1.5	4.6
430	4	8.8
520	5	10
530	6	10.8
610	7-8	12.2
630	9	13

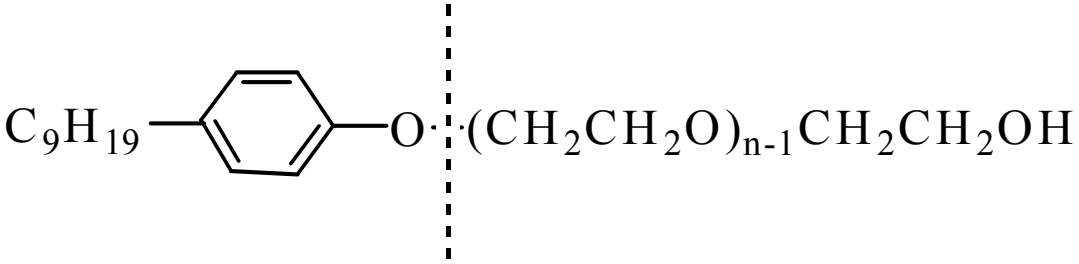

hydrophobic hydrophilic

Table 2.2 Structure and HLB of Nonylphenol ethylene oxide ($NP(EO)_n$) surfactants

$NP(EO)_n$	CMC (mol/l) 10^{-5}	σ (A^2/molecule)
NP-4-EO	3.28	53
NP-5-EO	4.7	55
NP-6-EO	5.17	58
NP-9-EO	7.2	61

Table 2.3 CMC (Critical micelle concentration) and the area per surfactant molecule for $NP(EO)_n$ at the water/air interface at 25°C

.

NP-$(EO)_n$	Interfacial tension (mN/m)
NP-4-EO	12
NP-5-EO	10.3
NP-6-EO	9.2
NP-9-EO	4.3
NP-10-EO	2.2
NP-15-EO	7.2

Table 2.4 Interfacial tension for $NP(EO)_n$ at CMC for saline/n-hexadecane interface at 25 ^oC

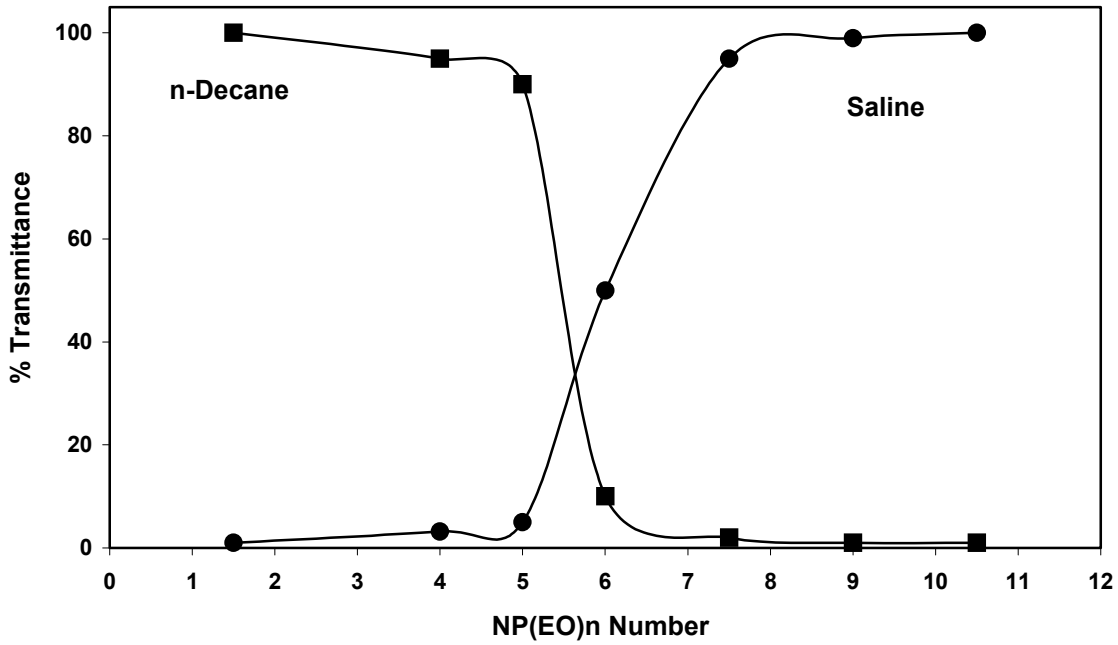

3 drops of NP(EO)n in 5ml of saline (1% Nacl) or n-decane,T= 303 K , Transmittance at 520 nm.

Figure 2.1 Solubility of $NP(EO)_n$ surfactant in n-decane and saline solution

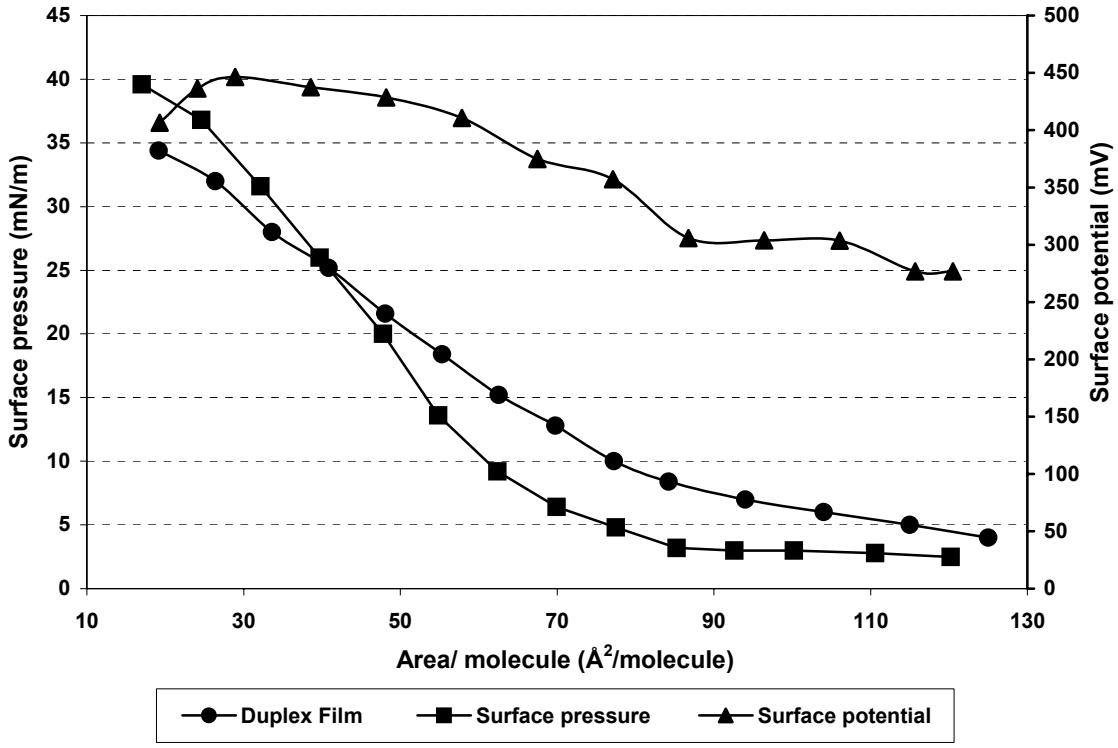

Figure 2.2 Surface pressure and potential for NP-4-EO surfactant

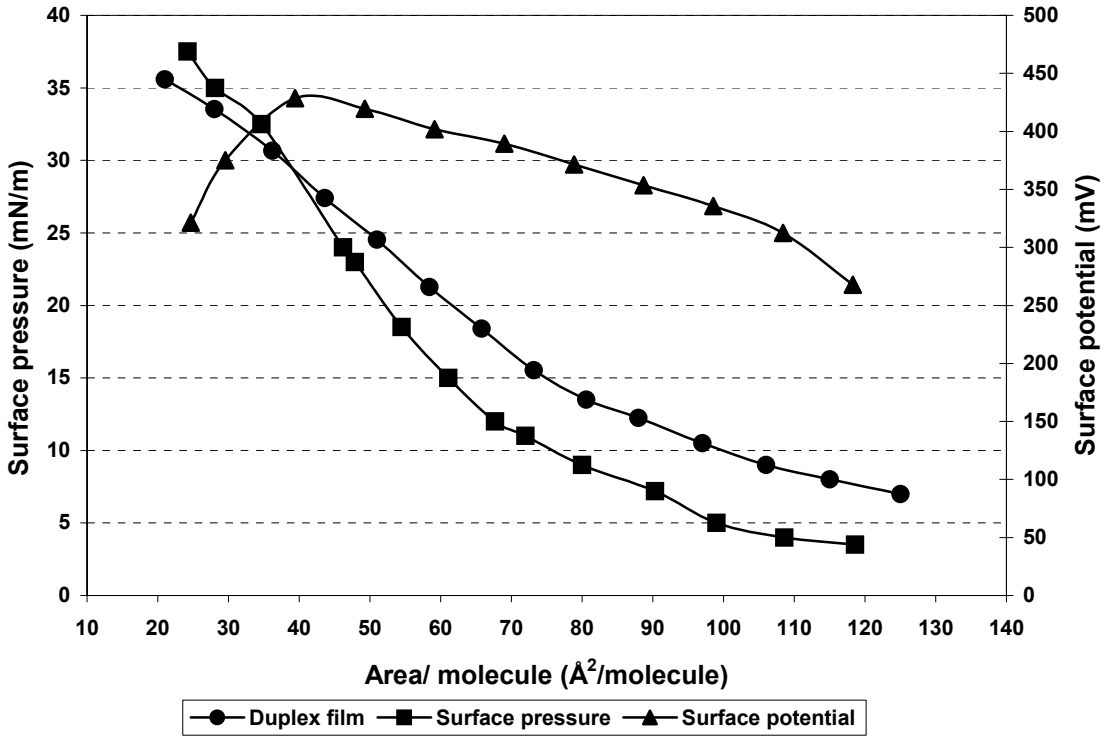

.

Figure 2.3 Surface pressure and potential for NP-5-EO surfactant

.

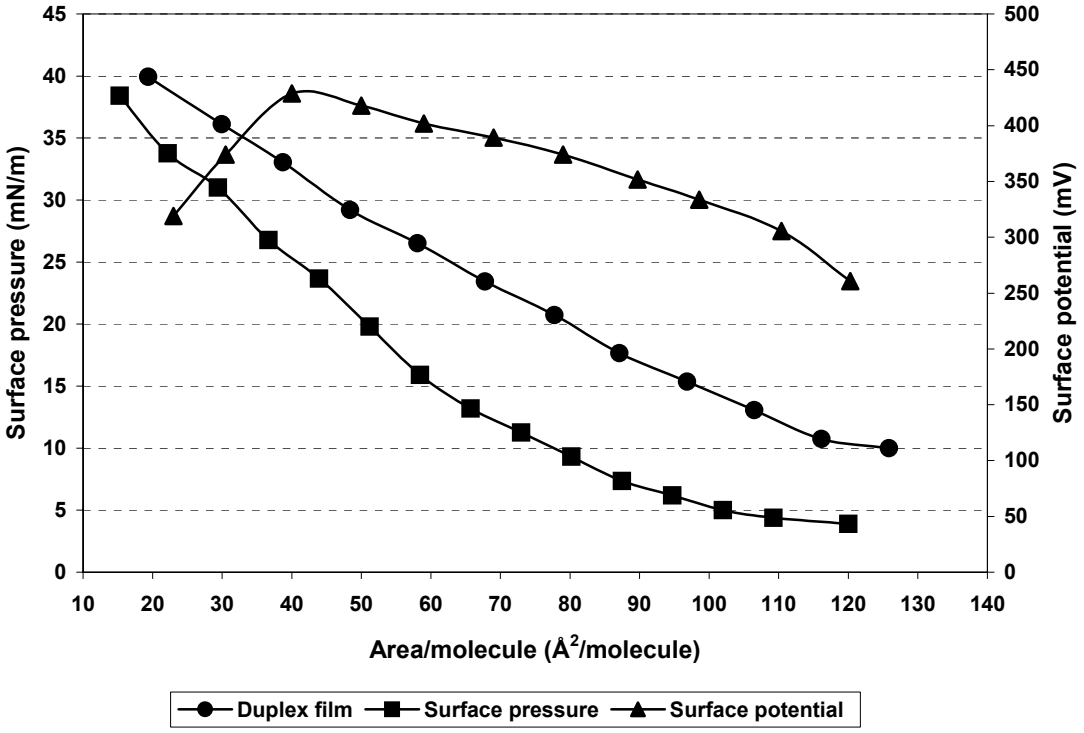

Figure 2.4 Surface pressure and potential for NP-6-EO surfactant

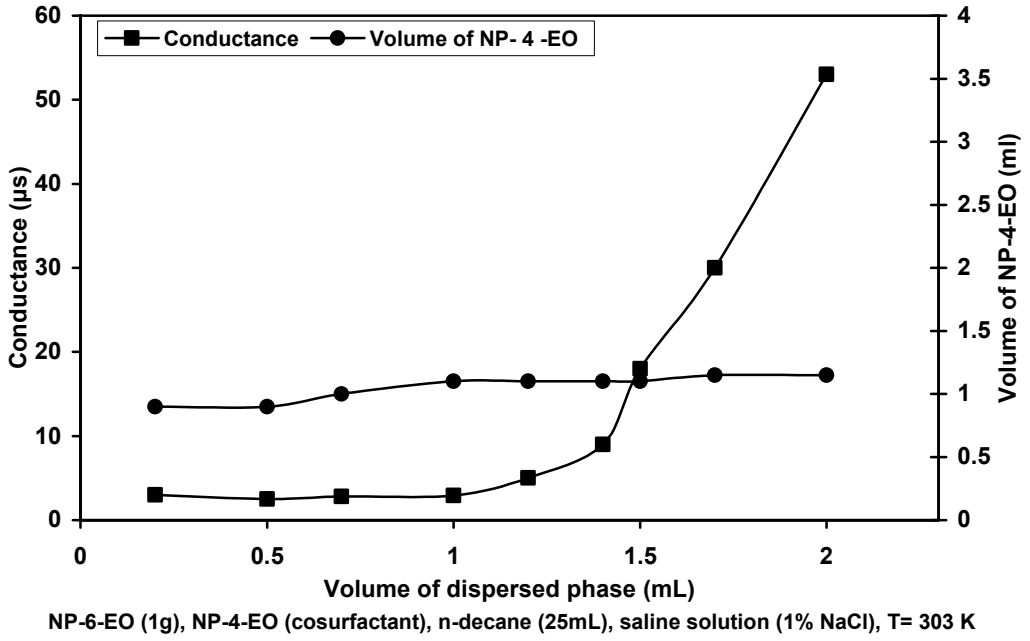

Figure 2.5 Conductance measurements for Saline/O microemulsions

.

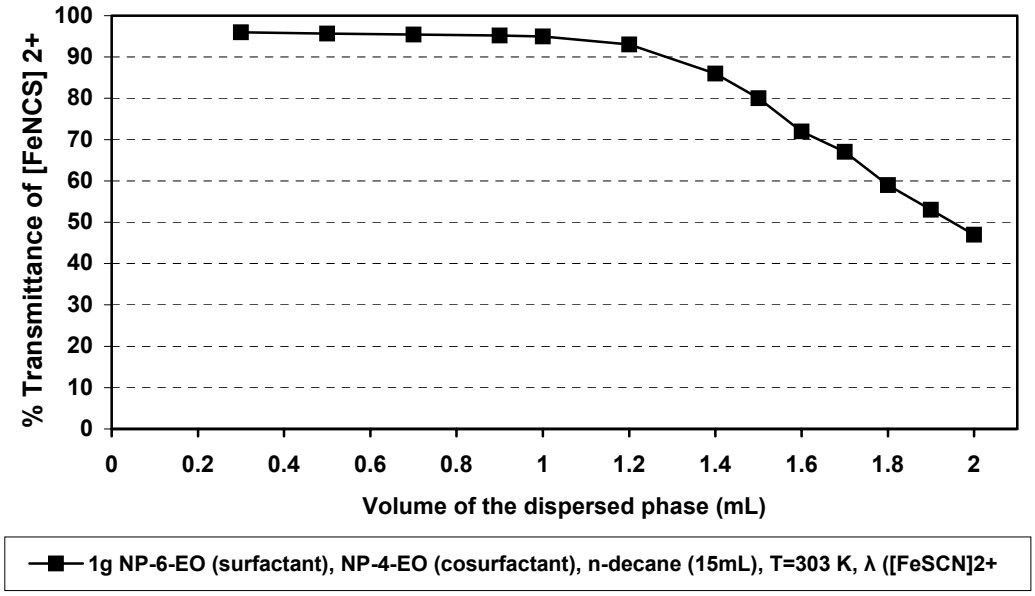

Figure 2.6 Transmittance measurements for two mixed W/O microemulsions

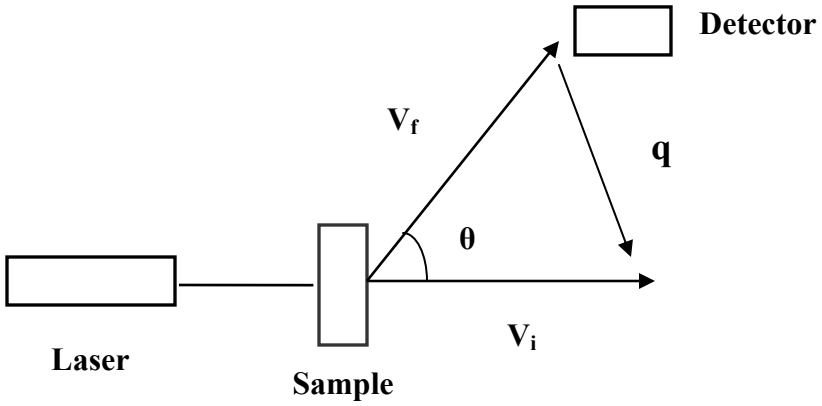

The incident wave vector, V_i, is scattered in all directions upon reaching the scattering sample, but only the light of the wave vector V_f is detected. The geometry of the apparatus defines the scattering vector q; the angle θ is called the scattering angle.

Figure 2.7 Light scattering vectors

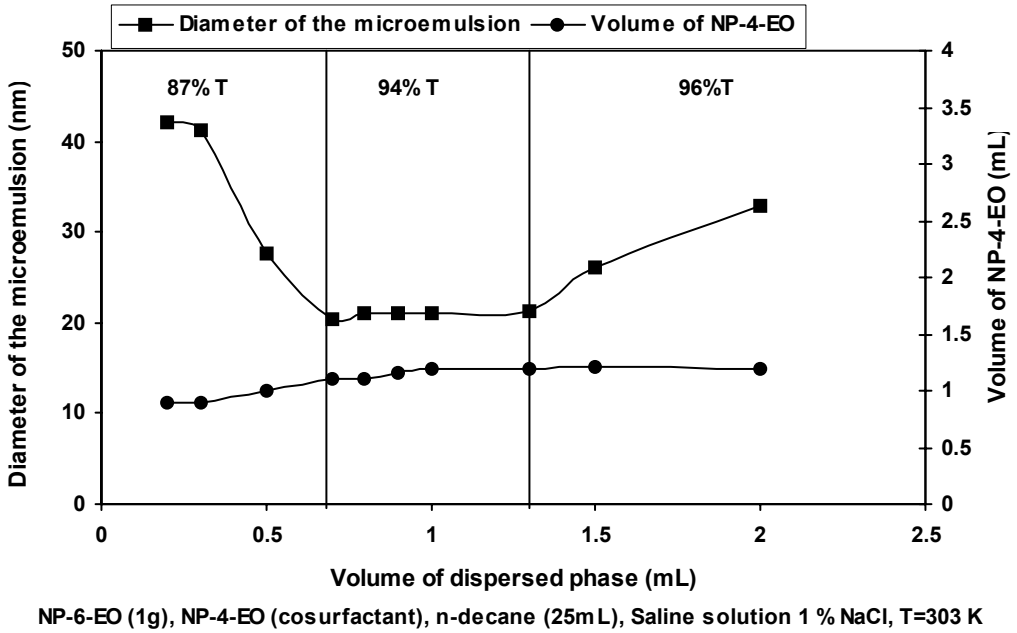

Figure 2.8 Quasi Elastic Light Scattering measurements for W/O microemulsions

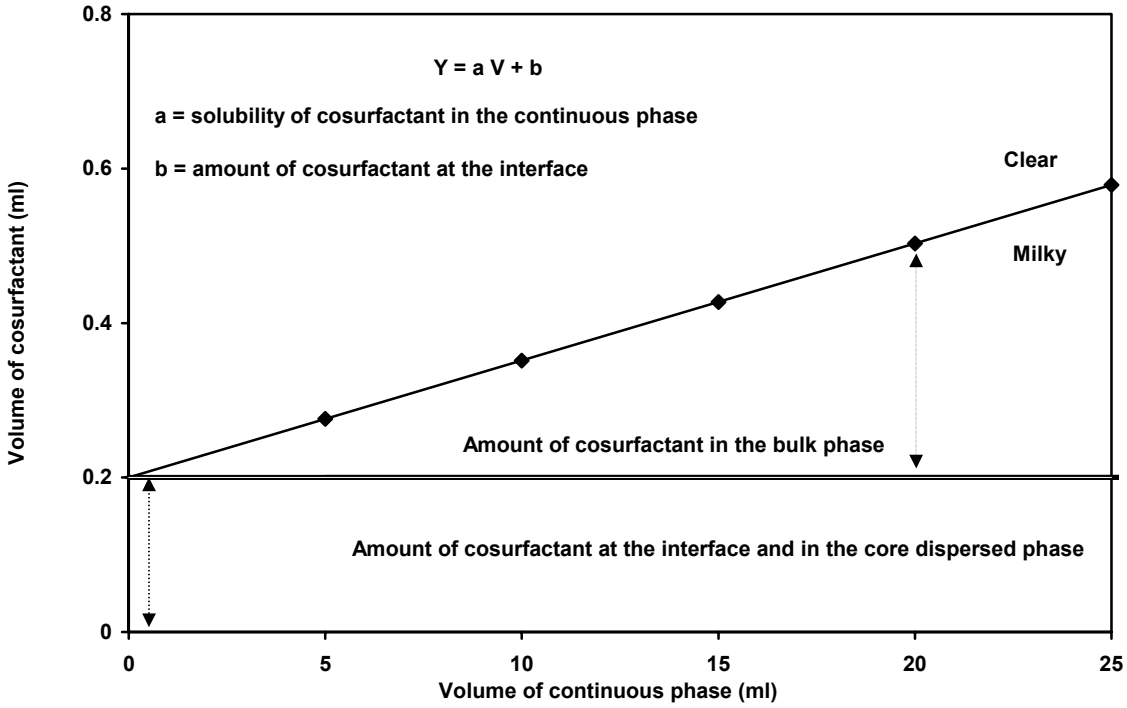

Figure 2.9 Typical graph of microemulsion titration

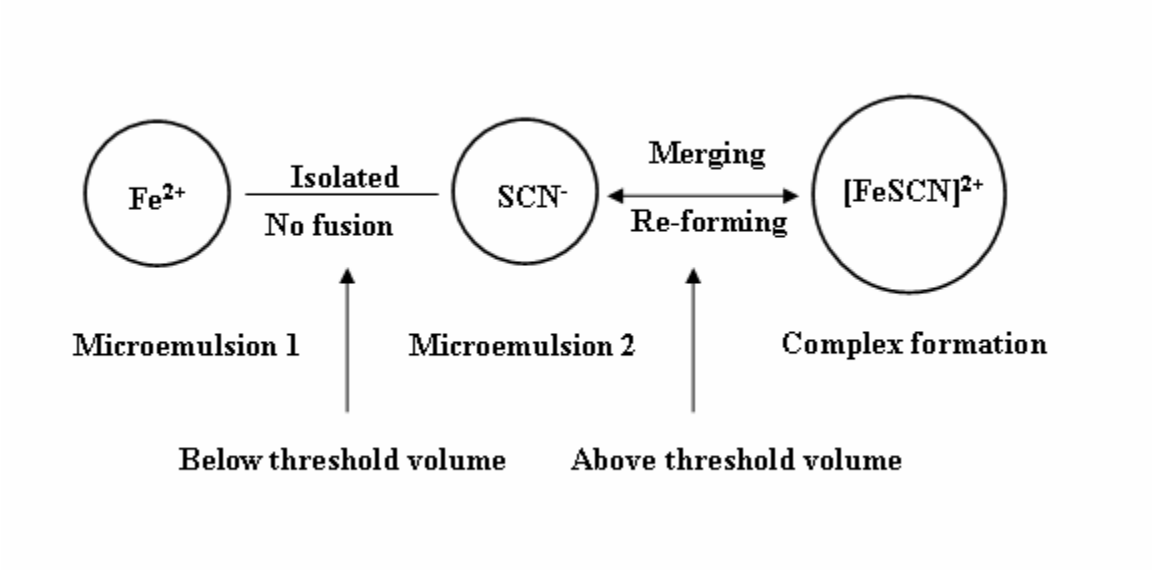

Figure 2.10 Merging and re-forming microemulsion droplets

CHAPTER 3

MICROEMULSION MODEL: EXPERIMENTAL VALIDATION

3.1 INTRODUCTION

As we saw at the beginning of Chapter 1 (Sections 1.1.1 and 1.1.2) a microemulsion is a thermodynamically stable homogeneous mixture of a lipophilic phase ("oil") and an aqueous phase ("water"), stabilized by a surfactant and in some cases by a cosurfactant as well. The diameter of the individual droplets of the dispersed phase is typically in the range of 30-400 Å, or less than 0.1 μm, approximately ¼ the wavelength of incident visible light (hence their transparency). In principle, three structural types have been shown to exist in such systems [1-7].

- oil-in-water (O/W) microemulsions
- water-in-oil (W/O) microemulsions
- bicontinuous structures

All observed O/W and W/O microemulsion systems are characterized by a low relative volume of the inner or dispersed phase, whether this is aqueous or lipophilic. The investigation of the mechanism of microemulsion formation presented above (see Chapter 2) demonstrated that above a threshold volume Φ of the dispersed phase such a system enters a period of dynamic equilibrium, with droplets merging and re-forming—so-called percolation. An increase in dispersed-phase volume beyond that sufficient to cause percolation leads to destabilization, i.e., the breakdown of the microemulsion system or formation of a bicontinuous microemulsion.

3.2 MATHEMATICAL MODELS FOR MICROEMULSION PHENOMENA

Although many articles dealing with microemulsions have been published over the last twenty years or so, there have been very few attempts to propose a mathematical model explaining microemulsion formation and accounting for such commonly observed phenomena as percolation. As noted above (Section 1.5), Helfrich [15] introduced the essential concept of film bending energy. His 1973 paper was the first published model to introduce bending energy and the curvature of the interface to explain the formation and stability of microemulsions. The models developed more recently by Gradzeilski, Safran, and Rosano—discussed below in Sections 3.2.2, 3.2.3, and 3.2.4—all build on Helfrich's initial insight.

3.2.1 DEFINING CURVATURE

Spontaneous (or natural or preferred) curvature C_o is defined as the curvature formed by the surfactant film when a system consists of equal amounts of water and oil. There is no constraint on the film, which is free to adopt the lowest free energy state. If one phase is dominant, the film's curvature will deviate from C_o. In principle, every point on a surface possesses two principal radii of curvature, R_1 and R_2; their associated principal curvatures are $C_1 = \frac{1}{R_1}$ and $C_2 = \frac{1}{R_2}$. Mean and Gaussian curvature are used to define the bending of surfaces. They are defined as follows [12]:

- Mean curvature: $C = \frac{1}{2}\left(\frac{1}{R_1} + \frac{1}{R_2}\right)$
- Gaussian curvature: $k = \frac{1}{R_1} \times \frac{1}{R_2}$

The curvature C_o depends on the composition of the phases it separates and the surfactant structure. It is known from duplex film studies (see above, Chapter 2) that oil can penetrate the surfactant monolayer to some extent. The more extensive the penetration, the more curvature is imposed toward the polar side.

3.2.2 GRADZEILSKI MODEL

Gradzeilski et al. [13] proposed a film rigidity theory based on the interfacial free energy associated with the film curvature. The free energy, F, of a surfactant layer at a liquid interface may be given by the sum of the interfacial energy term, F_i, a bending energy term, F_b, and an entropic term, F_{ent}. For a droplet type structure this is written as:

$$F = F_i + F_b + F_{ent} = \gamma A + \int\left(\frac{K}{2}\left(C_1 + C_2 - 2C_o\right)^2 + \overline{K}C_1C_2\right)dA + nk_BTf(\Phi) \qquad (3.1)$$

where γ is the interfacial tension;

A is the total surface area of the film;

K is the mean elastic bending modulus;

$\overline{K}$ is the Gaussian bending modulus;

C_1 and C_2 are the two principal curvatures and C_o the spontaneous curvature;

n is the number of droplets;

k_B is the Boltzmann constant;

and $f(\Phi)$ is a function accounting for the entropy of mixing of the microemulsion droplets, where Φ is the droplet core volume fraction. For dilute systems, where $\Phi < 0.1$, it could be demonstrated that $f(\Phi) = (\mathrm{Ln}((\Phi) - 1)$.

Since the interfacial tension γ is very low, the term γA can be ignored in an approximation.

Solving Equation 3.1 for spherical droplets, where $R_1 = R_2 = R$, and the interfacial area is $A = n4\pi R^2$, the total free energy for a droplet can be expressed as:

$$\frac{F}{A} = 2K\left(\frac{1}{R} - \frac{1}{R_o}\right)^2 + \frac{\overline{K}}{R^2} + \left[\frac{k_B T}{4\pi R^2} f(\Phi)\right] \tag{3.2}$$

Equation 3.2 shows that the film bending rigidity depends on the main bending elasticity K and the Gaussian curvature $\overline{K}$. These two parameters can be determined using any of several techniques, for example, ellipsometry, x-ray reflectivity, and small-angle neutron scattering (SAXS).

3.2.3 SAFRAN MODEL

Safran [14] also invoked the curvature of the interfacial film in presenting a mathematical model to explain the formation of vesicles, considering systems with a single monolayer at the oil/water interface, and the vesicle radius much larger than the surfactant size. Although the diameter of the vesicles is larger by several orders of magnitude than that of microemulsion droplets, Safran's model is at least partly applicable to microemulsion systems as well. This model assumes that for an oil/water/surfactant system, all the surfactant ends up at the oil/water interface. On this assumption, the system energetics are governed by the energy of this interfacial surfactant layer. In addition, the surfactant film is assumed to be incompressible compared with its resistance to orientational distortion (bending of the surfactant sheath),

while the area per surfactant molecule is kept constant. The total free energy proposed by Safran for such a system is:

$$F_T = n\,F_B - TS_M + F_{AT} \tag{3.3}$$

where $n\,F_B$ is the total bending energy of all the globules of the system;

S_M is the free energy due to the entropy of dispersion;

and F_{AT} is the free energy due to the interaction between globules.

Since for a given amount of surfactant, the total surface area is constant, the surface free energy term corresponding to the creation of this interface can be ignored. The energy of the system is related to the curvature of the interface, and the total bending energy is related to the sum of the bending energies of all the individual droplets of the system. Microemulsion systems with dispersed-phase volumes below Φ can be viewed as collections of non-interacting globules of oil in water; in the absence of inter-globule interaction, the F_{AT} term in Equation 3.3 can be ignored. The bending energy per droplet is given by

$$F_B = \frac{K}{2}\int\left(\frac{1}{R_1}+\frac{1}{R_2}-\frac{2}{\rho_o}\right)^2 ds + \frac{K'}{2}\int\left(\frac{1}{R_1}-\frac{1}{R_2}\right)^2 ds \tag{3.4}$$

where the integral is over the surface of the globule;

R_1 and R_2 are the local radii of curvature;

ρ_o is the spontaneous radius of curvature, which represents the tendency of the interface towards either the water side or the oil side of the interface;

and K and K' are the so-called "elastic" and "saddle-splay" constants related to the rigidity of the interface (see below).

The bending of the surface is determined by the packing parameter (see Section 1.8) and the geometry of the surfactant molecules at the interface. The first term in

Equation 3.4 represents the bending energy of a general interface with spontaneous radius of curvature ρ_o. The second term represents the energy required to distort the surface to a saddle shape. The simplest case of F_B corresponds to structures with equal radii of curvature (spheres and lamellae, rather than cylinders or ellipsoids): the saddle-splay term makes no contribution.

The total curvature energy of the system is then given as the sum of F_B over all globules. It is assumed that for a microemulsion, the curvature energy is minimized by the formation of a monodispersed system.

3.2.4 ROSANO MODEL

Rosano, working with a succession of collaborators, proposed a mathematical model [8-11] in which the total free energy of the formation of the microdroplets is given by Equation 3.5:

$$\Delta G = N \Delta G_T \tag{3.5}$$

where

ΔG_T is the total free energy of the formation of one droplet; and

N is the total number of droplets.

$$\Delta G_T = \Delta G_{SH} + \Delta G_A + \Delta G_B + \Delta G_I \tag{3.6}$$

where

ΔG_{SH} is the free energy of formation of the interfacial sheath structure (J);

ΔG_A is the work required to expand the interface (J);

ΔG_B is the interfacial bending energy (J); and

ΔG_I is the free energy of interaction between droplets (J).

On the basis of these different terms of the free energy, we have Equation 3.7:

$$\Delta G_T = -\varepsilon \frac{4}{3}\pi R^3 \Delta G_F + 4\pi R^2 \left[\gamma_i + \frac{K_R}{2}\left(\frac{1}{R} - \frac{1}{R_o}\right)^2 \right] + 16\pi^2 K_R \frac{\gamma_i}{\gamma_{io}} \left(\frac{R - R_{min}}{R_{min}}\right)^2 \left(\frac{R - R_{max}}{R_{max}}\right)^2 \qquad (3.7)$$

where

ΔG_F is the free energy of formation, in joules per cubic meter (J/m^3), of the interfacial sheath structure, assuming that the interface is an ideal mixture of long chain hydrocarbons (for example, n-octane and n-dodecane (50:50 mole:mole));

ε is a correction factor representing the fractional volume of the interface relative to the total volume of the droplet;

R is the radius of curvature of the microemulsion droplets (m);

γ_i is the interfacial free energy (N/m);

γ_{io} is the interfacial tension at the bare interface (N/m);

K_R is an energy term related to the curvature of the system (O/W or W/O) and the rigidity of the interfacial sheath (J);

R_{min} and R_{max} are the radii of curvature of the smallest and largest droplets found in the microemulsion (m); and

R_o is the spontaneous radius of curvature of the microemulsion droplet (m).

3.2.5 VALIDATION OF THE ROSANO MODEL

What follows is an attempt at validating this mathematical model using insights obtained from the study of O/W and W/O microemulsions prepared with nonylphenolethylene oxide (NP(EO)n) as surfactant described above in Chapter 2 [see also 16]. That study found that microemulsification occurred when surfactant solubility

is equal in the two phases (i.e., when the surfactant has borderline oil and water solubility). The electrical conductance and particle size of a non-ionic saline/oil microemulsion system (saline (1% NaCl)/nonylphenol ethylene oxide + n-decane) were also measured as a function of increasing saline volume in dispersed phase. At low volumes of the dispersed phase (below the threshold volume Φ), the individual droplets behave like large molecules in solution or swollen micelles, with no interdroplet interaction (both electrical conductance and droplet diameter remain constant). When the dispersed-phase volume exceeds Φ, the system changes dramatically, with sharp increases in both electrical conductance and droplet diameter. Individual droplets begin to interact, and a dynamic equilibrium is established, with droplets merging and re-forming while the system as a whole remains a single transparent phase: a classic case of percolation [17-21].

Section 3.4 presents experimentally observed values that make it possible to test the model expressed by Equation 3.7 (henceforth "Rosano's model" or "the model"). As in Chapter 2, the systems under investigation were a family of W/O microemulsions consisting of an oil phase (hydrocarbon), an aqueous phase (water), and nonylphenolethylene oxide surfactants of varying HLB ($NP(EO)_n$). For each system, the interfacial tension at the water/oil interface at the critical micelle concentration (CMC) was measured using Wilhelmy's method; the natural radius of curvature of microemulsion R_o was measured using Quasi Elastic Light Scattering measurement; and the total free energy per mole of surfactant of microemulsion formation was determined using the titration method. Afterward, the free energy of formation of a single microemulsion droplet (ΔG_T) was calculated using the area per molecule of $NP(EO)_n$

surfactant at the oil/water interface. The droplet radii R_{max} and R_{min} were determined from the plot of ΔG_T versus R (radius of the microemulsion) using the first two terms of Equation 3.7, ignoring the last term representing the interaction between droplets (ΔG_I). The same plot (ΔG_T vs. R) was used to determine the rigidity of the interface K_R, for a given set of parameters ($R=R_o=10$ (nm), and γ_i =10 (mN/m)). Finally, for the microemulsion system under study, all the above determined values (R_o, R_{min}, R_{max}, K_R, γ_i) were implemented in Equation 3.7 in order to determine how well the model would agree with the value for the free energy of formation as experimentally determined by the titration method, and thus represent the experimental facts observed.

3.3 EXPERIMENTAL

3.3.1 MATERIALS

All chemicals were used as received from their suppliers: n-hexane, n-octane, n-decane, n-dodecane, n-tetradecane, and n-hexadecane, all 99 %+ (Aldrich Chemical Co., Milwaukee, WI); sodium chloride (J. T. Baker, Phillipsburg, NJ); and nonylphenolethylene oxide compounds, or $NP(EO)_n$ (Igepals), all 100% active (Rhodia HPCII, Cranbury, NJ).

Freshly distilled water was used in all preparations, and all glassware was first cleaned with a fresh sulfuric acid/potassium dichromate solution.

3.3.2 METHOD OF PREPARATION

Microemulsion systems were prepared in water-jacketed beakers maintained at a temperature between 30°C and 40°C, using the titration method. An initial coarse emulsion was prepared from an oil/surfactant mixture added to an aqueous phase. The

system was then titrated to clarity using a cosurfactant delivered from a microburette (% transmittance > 95 % at 520 nm). Continuous stirring was maintained throughout the titration process to ensure homogeneous mixing.

Repeating the titration method at different temperature between 30°C and 40°C, the free energy, the entropy, and the enthalpy accompanying the adsorption of cosurfactant at the interface were determined.

3.3.3 INTERFACIAL TENSION MEASUREMENT

Interfacial tension of various $NP(EO)_n$ solutions at different concentrations was measured at the oil/water interface using a sand-blasted Teflon blade (Wilhelmy's method). Next, the area per molecule for $NP(EO)_n$ surfactants was calculated using the Gibbs adsorption isotherm, Equation 3.8.

$$\Gamma = -\left(\frac{1}{RT}\right)\frac{d\gamma}{d\ln(c)} \tag{3.8}$$

3.3.4 TITRATION AND THERMODYNAMICS OF MICROEMULSION

Using the point method [3, 8] values for free energy accompanying the adsorption of cosurfactant at the interface during the transformation of a primary coarse emulsion into a transparent system were determined using Equation 3.9:

$$\Delta G = -RT\,\mathrm{Ln}\left(\frac{X_i}{X_b}\right) \tag{3.9}$$

where X_i = molar fraction of cosurfactant at the interface; and

X_b = molar fraction of cosurfactant in the continuous phase.

ΔG represents the free energy accompanying the adsorption of cosurfactant at the interface during the transformation of a primary coarse emulsion into a transparent system.

The same procedure was repeated at various temperatures between 30°C and 40°C. Plotting the change in the free energy versus temperature, the entropy change accompanying cosurfactant adsorption was calculated using Equation 3.10:

$$\left(\frac{\partial \Delta G}{\partial T}\right)_P = -\Delta S \tag{3.10}$$

The change in enthalpy corresponding to the transformation from a macroemulsion into microemulsion at 30 °C was calculated using Equation 3.11:

$$\Delta G = \Delta H - T\,\Delta S \tag{3.11}$$

3.4 RESULTS AND DISCUSSION

3.4.1 AREA PER MOLECULE AND THE INTERFACIAL TENSION

Table 3.1 shows the values for the area per molecule of surfactant at the critical micelle concentration (CMC), as calculated using the Gibbs adsorption isotherm, Equation 3.8. These are the values that will be used to calculate ΔG_T, the total free energy required to form a single microemulsion droplet.

As noted above, in the investigation described in Chapter 2, it was found that a W/O microemulsion forms when the surfactant has borderline solubility in both oil and aqueous phases. The surfactant NP-5.5-EO approximates the composition of the surfactant at the oil/water interface for the microemulsions under study, and has a

borderline solubility in both oil and water phases. Therefore, values interpolated from those in Table 3.1 will be used in this calculation: an interfacial tension of 10 (mN/m), and an area per molecule of 65 $Å^2$/molecule.

3.4.2 THERMODYNAMICS OF MICROEMULSIONS

Table 3.2 presents the free energy, entropy, and enthalpy accompanying the adsorption of cosurfactant at the interface at 30°C for the microemulsions studied. The five free energy values corresponding to the adsorption of cosurfactant at the interface are negative numbers, indicating that the process of microemulsion formation is spontaneous. The small positive values of the entropy for these systems indicate that the entropy is due to the rearrangement of the surfactant around the water droplets, and that the formation of microemulsion is entropy-driven. Because the values for the free energy and the entropy accompanying adsorption of cosurfactant at the interface are small, other small effects—such as the interfacial bending energy and the free energy of the interaction between droplets—become important. This is why the model takes into consideration the contribution of the interfacial bending energy (ΔG_B) and the interaction between droplets (ΔG_I).

3.4.3 FREE ENERGY REQUIRED TO FORM A SINGLE DROPLET

The total free energy required to form a single droplet of radius R_o= 10 (nm) for a stable microemulsion system is calculated as follows.

The surface area of a droplet with radius R_o is:

$$4\pi (R_o)^2 = 1.2567\ 10^{-15}\ \ (m^2)$$

The area per molecule σ for the NP(EO)5.5 system is approximately 65 ($Å^2$/molecule), as interpolated from Table 3.1. Accordingly, the number of molecules in one droplet is:

$$\frac{4\pi(R_o)^2}{\sigma} = 1933 \text{ molecules}$$

Hence, the number of moles in one droplet is n = 3.21 10^{-21} (mole). From data in Table 3.2, we see that the free energy/mole for the formation of the microemulsion is around -6000 (J/mole). Therefore, the total free energy for the formation of one droplet is:

$$\Delta G_T = -\ 1.93\ 10^{-17}\ \ \text{(J/droplet)}$$

In order for the mathematical model to be valid, it must have a minimum of the free energy on the order of -1.93 10^{-17} (J/droplet), and it should account for the percolation of the microemulsion for a given value of the rigidity of the interface.

3.4.4 DETERMINATION OF R_{MAX} AND R_{MIN}

$$\Delta G_T = -\varepsilon \frac{4}{3}\pi R^3 \Delta G_F + 4\pi R^2 \left[\gamma_i + \frac{K_R}{2}\left(\frac{1}{R} - \frac{1}{R_0}\right)^2 \right] \qquad (3.12)$$

Using Equation 3.12, and plotting ΔG_T versus R (radius of the microemulsion)—ignoring the term representing the interaction between droplets ΔG_I—we determined R_{max} and R_{min} for the microemulsion.

ΔG_F is the free energy of the formation of the interfacial sheath structure. Assuming the interface is an ideal mixture of octane and dodecane (50:50), ΔG_F is calculated to be $9\ 10^{-9}$ (J/m^3), based on the free energy of mixing between octane and dodecane. ε is calculated to be 0.95, assuming that the thickness of the interface for NP(EO)n surfactant(s) represents 65 % of the volume of the droplet with radius equal to R_o= 10 (nm).

Figure 3.1 plots ΔG_T versus R at various K_R values, for a given set of R_o, ΔG_F, and γ_i. For K_R values greater than $2.4\ 10^{-17}$ (J), we observe a single minimum energy. When K_R is smaller than $2.4\ 10^{-17}$ (J), we observe no minimum energy and the theory predicts instability, i.e., elongated structure and phase separation. At the critical K_R value, $2.4\ 10^{-17}$ (J), called k_R^{Limit}, we find both a minimum and a maximum radius of the microemulsion (R_{max} = 220 (nm), R_{min} = 90 (nm)). Furthermore, the minimum and maximum radii of the microemulsion must be greater than the area per molecule at the water/oil interface observed for NP(EO)n surfactants, and they must fall within the interval of radii found for the system under study. When K_R is equal to $1.2\ 10^{-16}$ (J), called K_R^{Max}, the observed minimum of free energy has a narrow range of possible radius values, in contrast to the polydispersity commonly observed in microemulsion systems.

3.5 INTERFACIAL TENSION AND THE RIGIDITY OF THE INTERFACE

Replacing R_o, R_{max}, R_{min}, and γ_i and ΔG_F (the total free energy of formation) in Equation 3.7 with the values determined for them, we see that the rigidity of the interfacial sheath K_R must be $3.337\ 10^{-17}$ (J) to account for the percolation of the

microemulsion, where the two minima have an equal value of the free energy of formation of a single droplet (see Figure 3.2).

A plot of ΔG_T versus R for Equation 3.7 at various values of the interfacial tension with R_o= 10 (nm), $\gamma_{i/o}$ = 50 (mN/m), R_{max} = 22 (nm), R_{min}= 9 (nm), and K_R = 3.337 10^{-17}(J) is shown in Figure 3.3.

Analyzing Figures 3.2 and 3.3 yields the following conclusions. At high interfacial sheath rigidity K_R, the system is stable and percolation of the microemulsion does not occur. When the interfacial rigidity decreases and is equal to 3.337 10^{-17}(J) , the system exhibits two minima of the same magnitude, which accounts for the observed polydispersity (percolation phenomena). At low K_R values, but above K_R^{limit} , the system is unstable and all the radii belong to the interval corresponding to observed percolation phenomena (Figure 3.2).

At low interfacial free energy (0.1-1mN/m), the total free energy exhibits no minimum. At the equilibrium, low interfacial tensions impede the formation of the microemulsion. At an interfacial free energy of 10mN/m, however, the total free energy exhibits two minima having the same magnitude, the system is stable, and percolation occurs, which accounts for the experimentally observed polydispersity (Figure 3.3).

When the volume of the dispersed phase of the microemulsion increases, with constant mass of the primary surfactant and constant volume of the continuous phase, the radius of the microemulsion increases. Consequently, the vapor pressure difference across the oil/water interface decreases (low Laplace pressure). At that point, we observe that some of the water droplets start to form connected sets of globules, resulting in a large increase of the electrical conductance and droplet size of the system (percolation).

The Rosano model accounts for this scenario. When the volume of the dispersed phase is below the threshold volume, the model predicts a stable and monodispersed system. With a further increase of dispersed-phase volume (above the threshold volume Φ), the radius of the microemulsion increases, and the model predicts another free energy minimum having the same value as the free energy of formation of the microemulsion. The model thus supports the possibility of having two radii of different magnitude. The first minimum in Figure 3.2 represents the monodispersed microemulsion system and the second minimum represents the case in which percolation occurs.

Keeping K_R (rigidity of the interfacial sheath) constant, but varying the interfacial free energy γ_i between values as low as 0.1 (mN/m) and as high as 10 (mN/m) (Figure 3.3), we observe that zero interfacial tension does not give a minimum of free energy; this agrees with the experimentally determined interfacial tension for the system under study.

A zero interfacial tension will result in a very low Laplace pressure ($\Delta P = \frac{2\gamma_i}{R}$), and it is logical to conclude that the microemulsion droplet will lose its spherical geometry and that an elongated structure will form, with resultant instability of the system. A decrease in the Laplace pressure causes the spherical droplets to be flattened and thus increases their surface of contact. Consequently, the merging of pairs of droplets leads to bigger droplets whose Laplace pressure is half as great, since the radius is double during the percolation of the microemulsion. Therefore, the droplets will merge (percolate) rapidly, with a resultant phase separation, or formation of a bicontinuous microemulsion. Very low interfacial free energies have been proven to be unfavorable to the stability of the microemulsion [22-24].

3.6 CONCLUSION

According to the mathematical model, the interfacial tension γ_i and the rigidity of the interfacial sheath K_R between oil and water play a key role towards the formation and stability of the droplet of the microemulsion. This is in agreement with De Gennes and Taupin's emphasis on these same factors in their discussion of microemulsion formation [25].

The Rosano model has two clear points of strength, as compared to those proposed by Gradzeilski [13] and Safran [14]: it is based on physico-chemical properties common to microemulsion, and it successfully accounts for the phenomenon of percolation.

Finally, the value for the free energy of formation of a single droplet of a microemulsion system determined using the titration method is in good agreement with that calculated using Equation 3.7. This finding further supports Rosano's mathematical model.

Nonylphenol ethylene oxide Surfactants	Interfacial tension (mN/m)@ 25°C	Area/molecule ($Å^2$/molecule)
NP-4-EO	12	60
NP-5-EO	10.3	64
NP-6-EO	9.2	66

Table 3.1 Interfacial tension and the area/molecule for $NP(EO)_n$ Surfactant

Experiment	Continuous phase	Dispersed phase	ΔG (KJ/mol)	ΔH (KJ/mol)	ΔS (KJ/K.mol)
1	C_8H_{18}	Water	-10.44	4.33	$4.87\ 10^{-2}$
2	$C_{10}H_{22}$	Water	-6.26	13.40	$6.48\ 10^{-2}$
3	$C_{12}H_{26}$	Water	-7.31	3.32	$3.47\ 10^{-2}$
4	$C_{14}H_{30}$	Water	-6.72	9.36	$5.30\ 10^{-2}$
5	$C_{16}H_{34}$	Water	-6.57	-1.13	$1.79\ 10^{-2}$

Water 1% NaCl (1ml), NP-6-EO Primary Surfactant, NP-4-EO Cosurfactant.

Table 3.2 Thermodynamics of W/O microemulsion

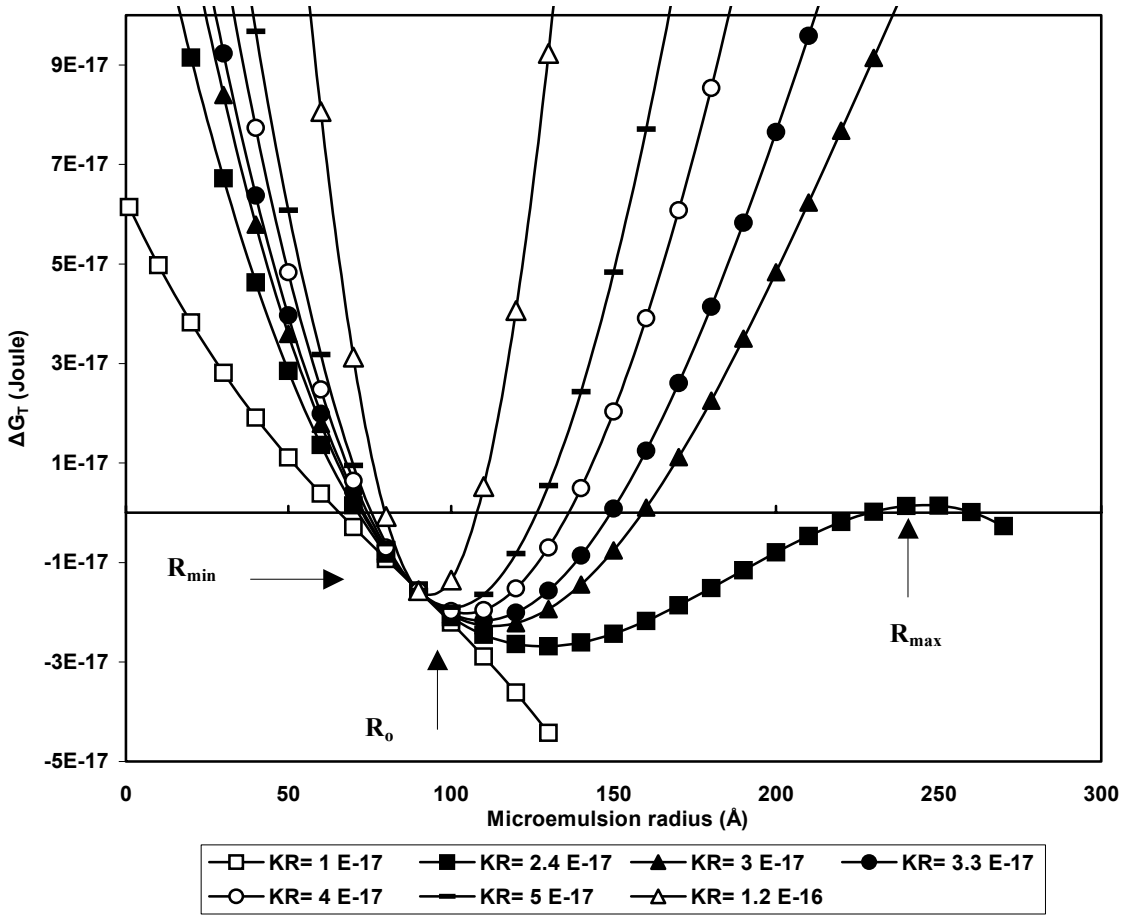

Figure 3.1 Determination of R_{min} and R_{max} for W/O microemulsion

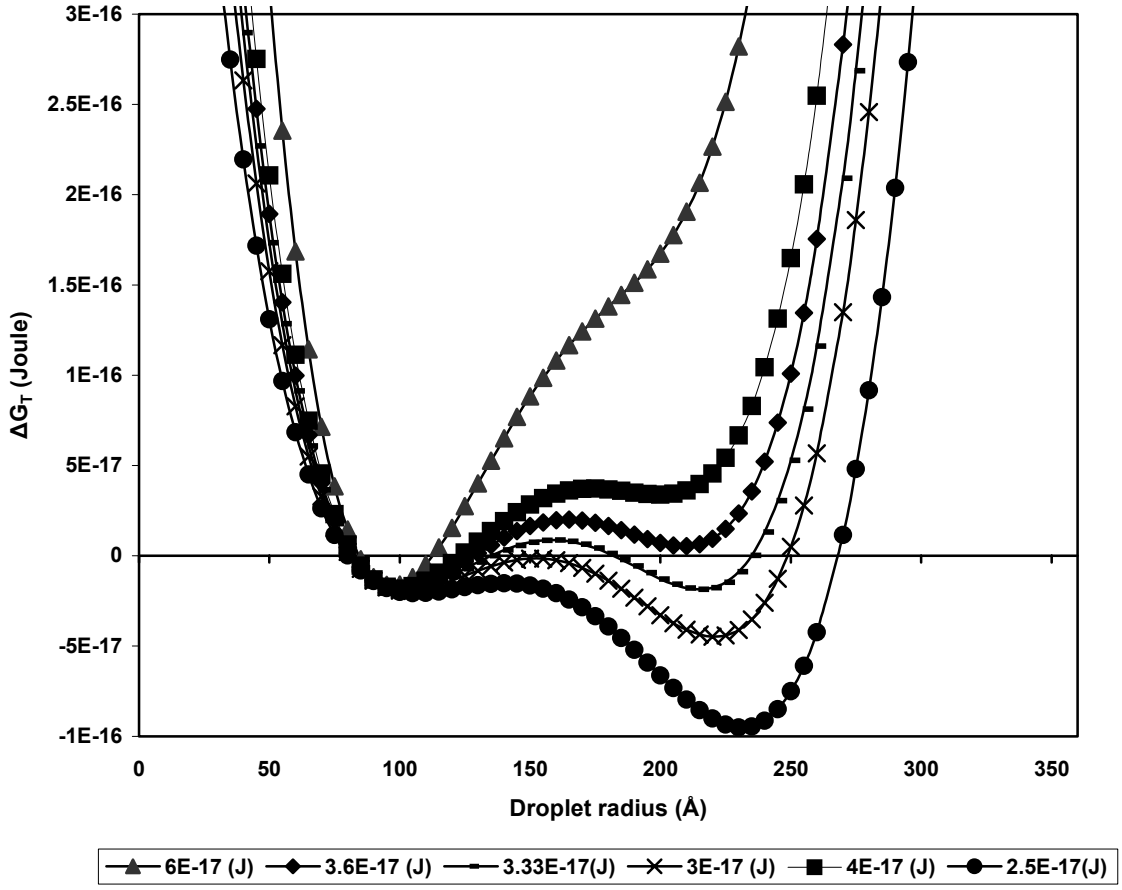

Figure 3.2 Free energy Vs radius of the microemulsion at different K_R values

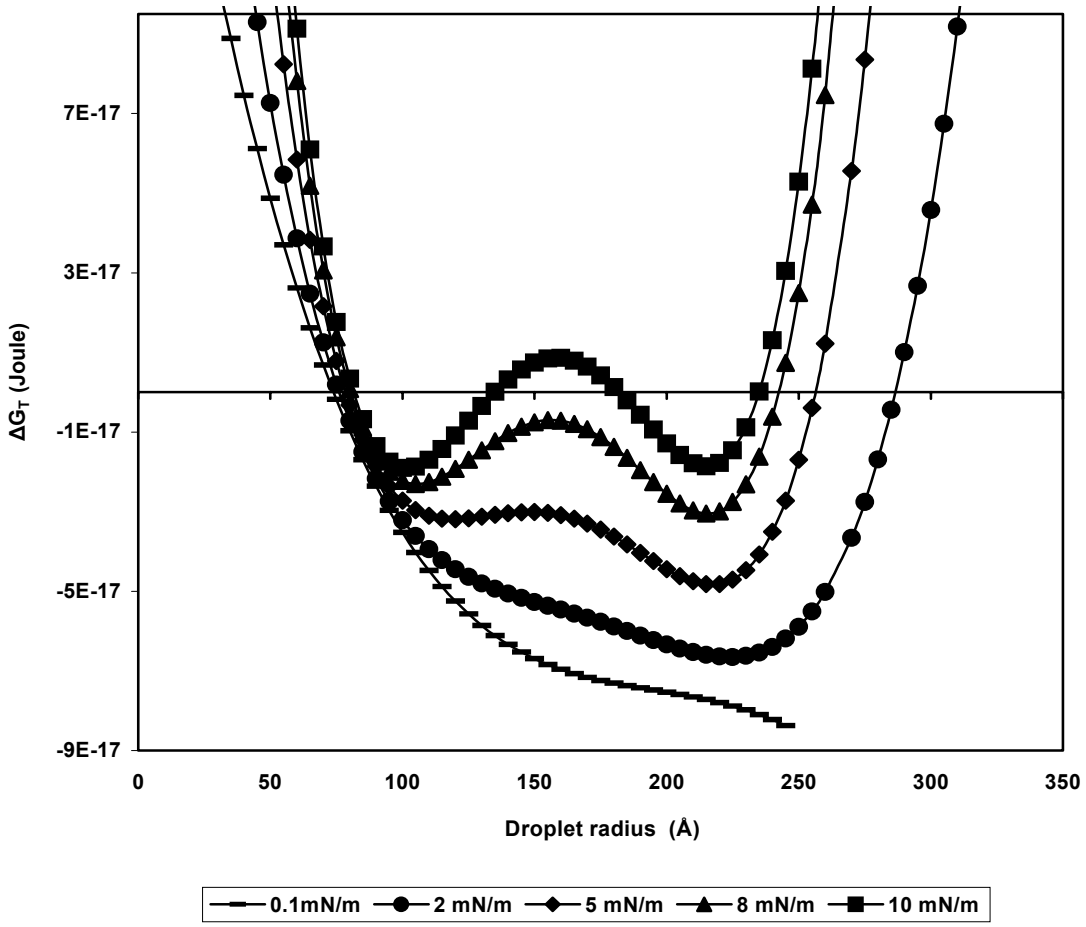

Figure 3.3 Free energy ΔG_T Vs R Radius of the microemulsion for W/O microemulsion

CHAPTER 4

FOOD MICROEMULSIONS

4.1 INTRODUCTION

Although emulsions, both naturally occurring and manmade, have a long history in food applications (see Section 1.1.1 at the beginning of this dissertation), microemulsions have had only limited use in the food industry during the more than six decades since Schulman's pioneering work. This underutilization is due more to difficulties in the formulation and use of appropriate microemulsions—produced with surfactants safe for human consumption and meeting other relevant criteria—than to a lack of desirable characteristics. Indeed, the defining qualities of microemulsions make them ideal for many food-industry applications: (1) small droplet size, which facilitates flavor release and perception; (2) transparency (a consequence of droplet size), which has applications in food analysis and quality control as well as in the more subjective and culture-dependent area of consumer preference (clear beverages may be seen as desirable); (3) the ability to host compounds within the dispersed-phase droplets, e.g., vitamins, flavors, and (in the case of O/W systems) non-soluble compounds; and (4) thermodynamic stability, in contrast to the susceptibility to destabilization processes (creaming, flocculation, and coalescence) that is typical of emulsions [1-5].

Despite their obvious potential for food and beverage applications, the difficulties in formulating microemulsions using edible and safe ingredients have so far often seemed insurmountable—or not worth the effort: (1) The edible oils in question—soybean, canola, etc.—are mostly triglycerides containing long-chain fatty acids, which are semipolar (in contrast to hydrocarbons, which are nonpolar) and are too bulky and too

long to allow the bending of the interface; (2) the choice of emulsifiers, and other permissible food additives, is limited; and (3) the concentration of surfactant and cosurfactant should be low enough not to impart an undesirable taste or odor to the end product. Thus, a method allowing the formulation of microemulsions with a GRAS ("generally recognized as safe") emulsifier would be a highly desirable achievement [6].

Using the titration method, described above in Section 2.2.3.2, it is possible to formulate O/W or W/O microemulsions of triglycerides or flavor oils with GRAS emulsifiers. These transparent systems, characterized by dispersed-phase droplets measuring 10-40 nm in diameter and high solubilization capacities, make excellent hosts for "guest molecules" including so-called nutraceuticals.

Presenting this formulation technique serves as a vehicle for the theoretical task of this chapter: proving that microemulsions form spontaneously when the surfactant interfacial film is equally soluble in both phases, even when surfactant and cosurfactant have completely different structures. This is a generalization of the specific case presented in Chapter 2, in which both surfactant and cosurfactant are nonylphenolethylene oxides (NP(EO)n) and thus differ only in their number of ethylene oxides (hydrophilic groups).

4.2 "FLAVORED WATER": SOFT DRINKS AND THEIR FLAVORINGS

4.2.1 BEVERAGE FLAVORS

Soft drinks—essentially, flavored water, usually sweetened, carbonated or not—are consumed in great quantities by people around the world. Although cola flavors continue to be the most popular in the United States market, globally speaking the leaders

are citrus-based: orange, followed by lemon/lime, with other citrus fruits playing a lesser but growing role [7, 8]. The citrus flavorings used in these drinks are essential oils extracted from fruit peel and are insoluble in water; the drinks themselves are essentially dilute O/W emulsions in dilute solutions of sugar (or an alternative sweetener). The diluted emulsion must remain stable for at least six months, and often undergoes intermediate storage temperatures ranging from -10 to + 40^{o} C. In general, instability in emulsions manifests itself through three mechanisms: creaming, flocculation, and coalescence. Although beverage emulsion concentrates exhibit all three, only creaming is likely to be noticed by the consumer.

Microemulsions would thus seem to be promising candidates for applications in soft-drink flavorings—particularly in citrus-flavored drinks where transparency is a desirable feature—but the extensive body of research carried out to date in this area (mostly by existing players in the soft-drink industry) has yielded few visible results on the market. Gaonkar and Bagwe [9], describing a literature search covering the years 1967-2000, note that among 6387 articles on microemulsions, only 91 referred to food applications: "It should be emphasized that even among the 91 entries for the food microemulsions, very few of them were made using food-grade, GRAS (generally recognized as safe) ingredients."

4.2.2 FLAVOR OILS

The citrus flavorings used in soft drinks are naturally occurring oils, found in balloon-like cells ("oil glands") in the colored outer peel of the fruit ("flavedo"). The oil is held in place by the so-called turgor pressure, and to liberate the oil from the gland a pressure

higher than the turgor pressure must be exerted (if an externally applied pressure drops below this threshold value, the oil is sucked back into the gland).

As Stauffer explains in his helpful summary of emulsion applications in the soft-drink industry, citrus flavor oils are composed primarily of monoterpenes (typically more than 90%) and sesquiterpenes: these are aliphatic compounds containing, respectively, 10 and 15 carbon atoms (formed by the combination of two or three molecules of isoprene) [8]. Although these hydrocarbons are by themselves nearly odorless and flavorless, they are carriers for the compounds—alcohols, aldehydes, ketones, acids, and esters—that combine in varying proportions to yield the individual aromas and flavors associated with orange, lemon, grapefruit, etc. For example, aldehyde levels are used as an objective measure of the quality of lemon oil, with values between 2 and 3.8 percent ("high aromatic oil") taken to indicate a high-quality oil [10].

It should be noted that the perceived flavor of a food or beverage is dependent on more than the measurable flavor compounds present in it. As the Van Nostrand Reinhold Encyclopedia of Chemistry puts it, "The *flavor* of a food substance is the combined sensation of *taste* and *odor* as perceived by the eater/drinker of that substance. Although the components (*flavorings)* are present in a food substance, the full aspects of flavor require intimate contact between substance and consumer… Flavor is a unique combination of nerve impulses on the brain centers as the result of actions upon receptors located on the tongue and in the lining of the nose and is thus the result of interaction between the food substance and the consumer."

4.3 MATERIALS AND METHOD

4.3.1 MATERIALS

Polyoxyethylene derivatives of sorbitan esters, Tween series (Uniqema, Wilmington, DE); polyglycerol ester of interesterified ricinoleic acid, Grinsted PGPR90 (Danisco, New Century, KS); glyceryl caprylate/caprate, Capmul MCM (Abitec Corporation, Janesville, WI); PEG-6 caprylic/capric glycerides, Acconon CC-6 (Abitec); polyoxyethylene 35 soybean glycerides, Acconon S-35 (Abitec); PEG-8 caprylic/capric glycerides, Labrasol (Gattefosse Corporation, Westwood, NJ); glyceryl oleate and propylene glycol 11%, Arlacel 186 (Uniqema); PEG-15 glyceryl oleate, TMGO-15, and PEG-5 glyceryl oleate, TMGO-5 (Barnet Products Corp., Englewood Cliffs, NJ); ethoxylated monoglycerides, Mazol 80 (BASF, Mount Olive, NJ); polyoxyethylene glycerol monoleate, Tagat O2V (Goldschmidt Chemical Corp., Hopewell, VA); ethanol and tetrahydrofuran (THF) (Spectrum, New Brunswick, NJ); glycerol monoleate, Mazol GMO (BASF); high purity ethoxylated glycerol monoleate, ESO-9920 (NOF Corp, White Plains, NY); hydroxylated lecithin (Barnet); refined vegetable oil (Jarchem Industries Inc., Newark, NJ); lemon oil California type (Symrise, Teterboro, NJ); orange oil Valencia type, mandarin oil Italian type, lime oil Indian type, and grapefruit oil Florida type (Citrus and Allied Essences LTD, Floral Park, NY); polystyrene standards, Easycal A and B (Agilent Technology, Palo Alto, CA).

4.3.2 METHOD

Although the goal of the investigation described below is a broadly theoretical one—a demonstration that microemulsions form spontaneously when the surfactant interfacial film is equally soluble in both phases, even when the surfactant and the cosurfactant have

completely different structures—the systems studied were deliberately chosen to conform to the constraints of food/beverage industry applications. Thus, the O/W and W/O microemulsions studied are all based on edible vegetable and citrus flavoring oils, and most of the surfactants used are GRAS (generally recognized as safe).

This choice of (mostly) GRAS surfactants means that my investigational protocol could not be an exact copy of that used above in Chapter 2. Typically, GRAS surfactants used in food products do not have an exact structure or molecular weight, which makes it impossible to determine the minimum amount of surfactant needed to cover the interface by the calculation method. The first step in the alternative technique used involves the determination of the optimum amount of dispersed phase for a given quantity of primary surfactant. An optically transparent micellar solution is prepared by mixing continuous phase and surfactant in a water-jacketed beaker maintained at constant temperature; continuous stirring with a magnetic stirrer throughout the procedure ensures a homogenous solution. Dispersed phase is then added dropwise from a microburette. For small aliquots of dispersed phase the system remains transparent, but it becomes opaque after a certain amount of dispersed phase is added. The minimum dispersed-phase volume that allows us to prepare a milky emulsion represents the optimum amount of dispersed phase to primary emulsifier used.

From this point on, the method described in Chapter 2 for microemulsion preparation—the so-called point method—can be used. The next step involves titrating the optically opaque emulsion to clarity with cosurfactant.

The optically opaque emulsion was produced by mixing a given initial weight of surfactant and an initial volume of the continuous phase with an experimentally

determined amount of dispersed phase. Titrating this emulsion to clarity with cosurfactant produces a microemulsion. The minimum volume of cosurfactant needed to bring the system to clarity, for the initial continuous-phase volume, is recorded. An additional volume of continuous phase is then added to the system, causing it to become optically opaque again. Once more, additional cosurfactant is added to bring the system to clarity; the total volume of cosurfactant corresponding to the newly clear system is recorded. This procedure—adding more continuous phase and titrating with additional cosurfactant—is repeated so as to generate numerous data points. Plotting these data points, and applying a linear regression formula, yields a straight line and allows its slope and intercept to be determined. Finding the cosurfactant volume at the interface, which is given by the extrapolated y-intercept (and which corresponds to an idealized zero-volume continuous phase), it is possible to determine the composition of the interface—the surfactant/cosurfactant ratio—assuming that both surfactants are adsorbed at the interface. Knowing the composition of the interface allows us to determine the surfactants' HLB at the interface. Also, for a given volume of the continuous phase, the difference between the total amount of cosurfactant and the amount of cosurfactant at the interface represents the amount of cosurfactant at equilibrium in the continuous phase.

In the case of a gel formation during the titration process, the experiment was repeated with a mixture of water and ethanol as the dispersed phase.

Tables 4.1, 4.2, 4.3, and 4.4 summarize the W/O and O/W microemulsions prepared with different types of oil, primary surfactants, and cosurfactant.

4. 5 EXPERIMENTAL

4.5.1 SIZE-EXCLUSION CHROMATOGRAPHY

Surfactants of unknown molecular weight were dissolved in THF (Tetrahydrofuran) (1mg/mL) for SEC analysis (see Section 4.8 for a brief discussion of this technique). External standards Easycal A and B (Polystyrene standards of known molecular weight) are supplied inside a 2mL vial; 1ml of THF was added to each vial to dissolve the standards. To generate a calibration curve, the standards were run before and after the set of 2mL vials containing the surfactant solutions. SEC was carried out under the following conditions:

HPLC: Waters Alliance (Agilent, courtesy of Ciba Specialty Chemicals)

Column: Plgel 5μm, M Mixed C

Mobile phase: Tetrahydrofuran (THF) Stabilized with BHT

Detection: Refractive Index (RI)

Injection: 100 μL

Temperature: Ambient

Flow rate: 1ml/min

Run time: 20min

Figures 4.1 and 4.2 show, respectively, the calibration curve plotting molecular weight used vs. retention time; and the plot of Log (molecular weight) vs. retention time. Table 4.5 shows the molecular weights of the Easycal standards used and their retention times. Using the calibration curve in 4.2, the molecular weight of each surfactant was determined. Table 4.6 shows the molecular weight and HLB (hydrophilic lipophilic balance) of each surfactant.

4.5.2 QUASI ELASTIC LIGHT SCATTERING

The droplet-size analysis of the W/O microemulsions was performed at a wavelength of 661 nm and an angle of 90^{o}. The microemulsion was filtered with a 0.1 micron PTFE syringe to ensure a low, flat baseline. After filtering, the microemulsion was placed inside the 90 plus particle-size analyzer and the size of the droplets determined. Figure 4.3 shows the amount of cosurfactant needed to yield microemulsions of varying volume of dispersed phase, and the diameter of each microemulsion produced.

4.5.3 VISCOSITY MEASUREMENTS

The frequency-sweep experiments of W/O microemulsions were carried out on an advanced Rheometrics Expansion System (Rheometric Scientific Inc., Piscataway, NJ) using the dynamic oscillatory mode with parallel plate fixture of 25 mm. The measurements were done at ambient temperature, 25^{o}C (see Tables 4.7-4.17). The results are shown in Figure 4.4.

4.5.4 TRANSMITTANCE MEASUREMENTS

Once the surfactant/cosurfactant composition of the interfacial film has been determined for the W/O and O/W microemulsions under investigation, using the titration method, transmittance measurements were carried out to determine the solubility of the surfactant film in the two phases. Separate samples of each of these surfactant/cosurfactant blends were dissolved in 5 mL of the water phase and in 5 mL of the oil phase; after mixing, the percent transmittance at 520 nm was determined. Table

4.18 shows the percent transmittance of the surfactant/cosurfactant composition in the two phases of each system tested.

4.6 RESULTS AND DISCUSSION

4.6.1 TITRATION

Table 4.1 shows six W/O microemulsions: these are all water-in-medium chain triglycerides microemulsion systems (W/MCT), formed with different types of Tween surfactant as the primary surfactant. In each system, the same cosurfactant—Capmul MCM—is used. With Tween 80, 40, or 60 as primary surfactant, the W/MCT microemulsion forms spontaneously, and the volume of cosurfactant at the interface is approximately constant over the three cases (1-3). With Tween 20, 21, or 85 as a surfactant, gel formation prevents formation of a microemulsion. The replacement of the original water dispersed phase with a water-ethanol mixture (1g, 1g) makes it possible to form a microemulsion (cases 4-6).

Tables 4.2 and 4.3 show water-in-edible vegetable oil microemulsions with different types of oil and surfactant (Tween 80, Mazol 80, and Acconon S35); in all cases, the cosurfactant is polyglycerol ester of esterified ricinoleic acid (PGPR). For each system, the slope of the titration curve and the amount of cosurfactant at the interface are also included.

Table 4.4 summarizes 16 O/W microemulsions, prepared with citrus flavor oil (cases 2-14) or vegetable oil (cases 1, 15, and 16) as the oil phase, water or water ethanol as the aqueous phase, and various surfactants and cosurfactants (some systems needed no cosurfactant). Again, for each system in which a cosurfactant was used, the slope of the

titration curve and the amount of the cosurfactant at the interface (intercept of the titration curve) are shown.

Table 4.1 demonstrates the effect of the hydrophobic chain of the surfactant on the formation of W/O microemulsions. When Tween 20 (sorbitan monolaurate$(EO)_{20}$) is used as the primary surfactant, the microemulsion does not form unless ethanol is added to the system. In contrast, no added ethanol is required to form the microemulsion with Tween 80 (sorbitan monoleate$(EO)_{20}$), Tween 40 (sorbitan monopalmitate$(EO)_{20}$), or Tween 60 (sorbitan monostearate$(EO)_{20}$) as the surfactant. Using Tween 21—sorbitan monolaurate$(EO)_4$, which has 4 ethylene oxides (EO) instead of 20—as the surfactant still requires the addition of ethanol; the same is true with Tween 85—sorbitan trioleate$(EO)_{20}$—as the surfactant (cases 5 and 6).

The systems in which the microemulsion forms spontaneously, without addition of ethanol, all include a surfactant having as a hydrophobic chain, a mono fatty acid of length C_{16} or C_{18} (oleic acid (C_{16}), palmitic acid (C_{16}), or stearic acid (C_{18}), corresponding to cases 1-3 of Table 4.1). Using instead a surfactant having as its hydrophobic chain, *either* a mono fatty acid of length C_{12} (lauric acid) (Tween 20 or 21) *or* a trioleic acid (Tween 85) impedes the formation of the microemulsion. Therefore, for these W/MCT microemulsions a Tween surfactant with a hydrophobic chain consisting of mono fatty acid with chain length higher that C_{12} is crucial for spontaneous microemulsion formation.

Tables 4.2 and 4.3 include results for identical systems titrated to clarity at different dispersed-phase volumes (1g and 0.5g, respectively). The much higher amounts of cosurfactant (at the interface) needed to clear the systems in Table 4.2 suggest that

more than a simple increase in dispersed-phase volume is involved; the high volume of cosurfactant needed is probably due to a structure change resulting from percolation of the microemulsion. In general, the amount of surfactants required to make food microemulsions is higher compared to other microemulsions due to high molecular weight of commonly used GRAS emulsifiers (PGPR, with molecular weight 3000 g/mol, is an extreme case; see Table 4.6). Amounts and structural issues aside, Tables 4.1, 4.2, and 4.3 are significant as demonstrating that W/O microemulsions of edible vegetable oils using GRAS emulsifiers are possible, despite widespread belief that the formulation of such microemulsions presents insurmountable difficulties.

4.6.2 PERCOLATION-INDUCED STRUCTURE CHANGE

Figures 4.3 and 4.4 demonstrate microemulsion percolation for triglyceride microemulsions. Figure 4.4 presents two curves, plotting various dispersed-phase volumes of water-in-soybean oil microemulsion against (a) the corresponding microemulsion diameter and (b) the volume of the cosurfactant required to form the microemulsion. As the volume of the dispersed phase increases—while remaining less than 0.7 mL—the diameter of the microemulsion droplet remains constant. Further increases in dispersed-phase volume—above 0.7 mL—cause a marked increase in diameter. (These results agree with the results of the light-scattering experiments described in Chapter 2 for the investigation into percolation phenomena; see Section 2.4.5.)

Figure 4.4 (constructed from the viscosity results shown in Tables 4.7-4.17) plots (a) microemulsion viscosity—measured at a frequency of 1 rad/sec—for a different set of

dispersed-phase volumes of the water-in-soybean oil formulation shown in Figure 4.4 and (b) the volume of cosurfactant (PGPR) needed to clear each microemulsion. As the volume of the dispersed phase increases, the viscosity of the microemulsion increases—for dispersed-phase volumes below 0.7 mL; above 0.7 mL the viscosity of the microemulsion drops dramatically.

For both figures, the sharp change—increased diameter (Figure 4.3) or decreased viscosity (Figure 4.4)—corresponds to the onset of percolation. Since the phenomenon of percolation in microemulsions involves droplet association—merging and re-forming of microemulsion droplets—it has a direct influence on internal structure and, in turn, on viscosity. Measurements of microemulsion viscosity provide information on the overall geometry of the particles of the dispersed phase. Results reported in this thesis, and in other publications as well, have revealed variable viscosity behavior in microemulsions. Moulik, presenting a typical viscosity plot in which the viscosity first increases and then decreases with increasing dispersed-phase volume, attributed the shape of the curve to the phenomenon of microemulsion percolation (structure change) [11, p.163].

The results reported above in Chapter 2 showed that, above a certain dispersed-phase volume, the threshold volume Φ, percolation of the microemulsion occurs, with droplet association; the scenario presented at that point to explain the sharp increase in microemulsion conductance involved the formation of a set of globules. If this scenario is accurate, a change in the viscosity of the microemulsion should occur at the threshold volume. Figure 4.4, which shows the predicted change in the microemulsion's viscosity at the threshold volume, thus supports the scenario proposed in Chapter 2.

4.6.3 SURFACTANT INTERFACIAL FILM SOLUBILITY AT THE INTERFACE

Table 4.18 shows percent transmittance of the surfactant interfacial film composition at the interface for various microemulsions produced with surfactant/cosurfactant pairings in which the two have different structures. These results demonstrate that microemulsions form when the surfactant interfacial film is equally soluble in the two phases even though the surfactant and the cosurfactant have different structures, a generalization of the case presented in Chapter 2 for nonylphenol ethylene oxide ($NP(EO)_n$) microemulsion systems.

4.6.4 MICROEMULSIONS AND "FLAVORED WATER" APPLICATIONS

Table 4.4 demonstrates that a wide variety of citrus oil-in-water microemulsions could be formulated, with two surfactants or with a single surfactant. These types of microemulsions could be substantially diluted and still remain stable. Such microemulsions could have wide application in the beverage industry, if the currently available GRAS emulsifiers did not have both a pronounced taste and a high molecular weight. Developing new emulsifiers based on flavor oils (citrus oils) could be a solution.

4.7 CONCLUSION

It was demonstrated in this chapter that a non-ionic microemulsion forms when the surfactant interfacial film at the water/oil interface has equal solubility in the two phases, regardless of the structure of the surfactant and cosurfactant used. This is a generalization of the case of nonylphenol ethylene oxide (NP(EO)n) surfactant systems,

presented in Chapter 2; in those systems, the surfactant and the cosurfactant have the same structure.

The results of the investigation of water-in-MCT microemulsions showed that the chain length and structure of the hydrophobic tail of the Tween surfactants used had a pronounced effect on microemulsion formation.

Since surfactants and oils are aligned at the interface, the properties of the interface—on which microemulsion formation and stability depend—are inevitably affected by the matching or mismatching of the oil and the hydrophobic chain of the surfactant**.** This finding agrees with the conclusion of Shiao et al., who found that chain length compatibility is an important factor in systems involving interfacial films [12].

Within the field of formulation chemistry, using the hydrophile-lipophile balance (HLB) and critical packing parameter (CPP) in order to predict which combination of surfactant, cosurfactant, and oil will produce a microemulsion is a widespread practice [13]. The work presented in this thesis shows that the structure of the interface is as important as the HLB and CPP for the prediction of microemulsion formation.

The viscosity measurements demonstrate that percolation of the microemulsion induces structural change, and offer further support for the experimental results presented in Chapter 2.

4.8 APPENDIX: SURFACTANT MOLECULAR WEIGHT DETERMINATION

Size-exclusion chromatography (SEC) is a standard method for determining molar mass averages and molar mass distributions (MMDs) of polymers. (Although the terms “gel permeation chromatography” (GPC) and “gel filtration chromatography”

(GFC) are also used, "size-exclusion chromatography" is preferable, since it describes the mechanism more precisely.) Polymer molecules are separated according to their hydrodynamic volumes (which can be correlated with molar mass), with the larger molecules leaving the column first, followed by the smaller ones. Molar masses are determined from a calibration or using molar mass sensitive detectors.

The separation principle in SEC is determined by the selective permeation of the polymers into and out of the mobile phase-filled pores of the column packing. The elution time of a polymer is governed by the time that it remains in the pores; hence, larger molecules, which spend less time in the pores, elute first, and smaller molecules elute later (see Figure 4.5).

The principal factor affecting the SEC of a polymer is its hydrodynamic volume and not its molecular weight. If a calibration method is used to determine molar mass, the apparent molecular weight of the polymer sample is determined by comparing its chromatogram with that of standards having known molecular weights. The relationship between molecular size and molecular weight depends on the conformation of the dissolved solute molecules; however, for any soluble conformation (such as random coil, rigid rod, or hard sphere), the molecular size increases with molecular weight. The rate at which the molecular size increases with molecular weight varies for the different possible solute conformations.

If a series of standards with known molar mass is available, the individual elution volumes must be determined. The calibration curve thus established allows the molar mass for a given elution volume (V_e) to be determined. In general, there is a "linear" relationship between Log (Molecular weight) and V_e and it depends on the particular

column used. The calibration curve—molecular weight vs. retention time—is often sigmoidal, rather than linear. In most cases, a polynomial equation provides a better fit for the experimental data of the calibration curve. If the calibration curve for the standards used has a good correlation factor, and the retention time of the sample of unknown molecular weight has been determined, the calibration curve equation will permit the determination of its molecular weight [14-17].

Exp #	Surfactant	Chemical description	HLB	Dispersed phase	Cosurfactant at the interface
1	Tween 80	POE (20) Sorbitan monoleate	15	Water (1g)	Capmul MCM (1.3 g)
2	Tween 40	POE (20) Sorbitan Monopalmitate	15.6	Water (1g)	Capmul MCM (1.29 g)
3	Tween 60	POE (20) Sorbitan monostearate	14.9	Water (1g)	Capmul MCM (1.29 g)
4	Tween 20	POE (20) Sorbitan monolaurate	16.7	Water (1g) Ethanol (1g)	Capmul MCM (2.28 g)
5	Tween 21	POE (4) Sorbitan monolaurate	13.3	Water (1g) Ethanol (1g)	Capmul MCM (1.86 g)
6	Tween 85	POE (20) Sorbitan trioleate	11	Water (1g) Ethanol (1g)	Capmul MCM (1.57 g)

Table 4.1 Water-in-MCT (medium chain triglyceride) microemulsions

Exp #	Surfactant	Continuous phase	Dispersed phase	Cosurfactant at interface	Slope
1	Tween 80 (1.6 g)	MCT-M5 oil	Water (1 g)	PGPR (2.24 g)	0.128
2	Tween 80 (1.6 g)	Soybean oil	Water (1 g)	PGPR (2.27 g)	0.175
3	Tween 80 (1.6 g)	Corn oil	Water (1 g)	PGPR (2.26 g)	0.100
4	Tween 80 (1.6 g)	Sesame oil	Water (1 g)	PGPR (2.26 g)	0.200
5	Tween 80 (1.6 g)	Nobee oil	Water (1 g)	PGPR (2.27 g)	0.154
6	Tween 80 (1.6 g)	Almond oil	Water (1 g)	PGPR (2.21 g)	0.137
7	Tween 80 (1.6 g)	Sunflower oil	Water (1 g)	PGPR (1.65 g)	0.193
8	Mazol 80 (1.6 g)	Soybean oil	Water (1 g)	PGPR (3.93 g)	0.155

Table 4.2 Water-in-vegetable oil microemulsions (Food microemulsion)

Exp #	Surfactant	Continuous phase	Dispersed phase	Cosurfactant at interface	Slope
1	Tween 80 (1.6 g)	MCT-M5	Water (0.5 g)	PGPR (0.64 g)	0.052
2	Tween 80 (1.6 g)	Soybean oil	Water (0.5 g)	PGPR (0.76 g)	0.084
3	Tween 80 (1.6 g)	Olive oil	Water (0.5 g)	PGPR (0.74 g)	0.055
4	Tween 80 (1.6 g)	Sesame oil	Water (0.5 g)	PGPR (0.79 g)	0.075
5	Tween 80 (1.6 g)	Almond oil	Water (0.5 g)	PGPR (0.74 g)	0.060
6	Tween 80 (1.6 g)	Sunflower oil	Water (0.5 g)	PGPR (0.68 g)	0.055
7	Tween 80 (1.6 g)	Corn oil	Water (0.5 g)	PGPR (0.66 g)	0.070
8	Tween 80 (1.6 g)	Safflower oil	Water (0.5 g)	PGPR (0.72 g)	0.088
9	Acconon S 35 (1.6g)	Soybean oil	Water (0.5 g)	PGPR (1.41 g)	0.075
10	Mazol 80 (1.6 g)	Soybean oil	Water (0.5 g)	PGPR (0.27 g)	0.122

Table 4.3 Water-in-vegetable oil microemulsions

Exp #	Surfactant	Continuous phase	Dispersed Phase	Cosurfactant at interface	Slope
1	Tagat O2V (1 g)	Water	MCT-M5 oil (1 g)	Capmul MCM (1.2 g)	0.16
2	Acconon-CC6 (2 g)	Water	Lemon oil (1 g)	--------	------
3	Acconon-CC6 (2 g)	Water	Lime oil (1 g)	--------	------
4	Labrasol (2 g)	Water	Mandarin oil (1 g)	--------	------
5	Labrasol (2 g)	Water	Tangerine oil (1 g)	--------	------
6	Labrasol (2 g)	Water	Grapefruit oil (1 g)	--------	------
7	Tagat O2V (1 g)	Water	Lemon oil (1 g)	Acconon-CC6 (1.48 g)	0.1
8	Tagat O2V (1 g)	Water 5 % Ethanol	Orange oil (1 g)	Capmul MCM (1.3 g)	0.15
9	ESO 9920 (1.2 g)	Water	Lemon oil (1 g)	Capmul MCM (1.2 g)	0.14
10	ESO 9920 (1.2 g)	Water	Mandarin oil (1 g)	Capmul MCM (1.2 g)	0.15
11	Acconon-CC6 (2 g)	Water	Lime oil (1 g)	--------	------
12	ESO 9920 (1.2 g)	Water	Mandarin oil (1 g)	Hydroxylated Lecithin (1.3 g)	0.14
13	ESO 9920 (1.2 g)	Water 2 % Ethanol	Grapefruit oil (1 g)	Capmul MCM (1.3 g)	0.14
14	Acconon-CC6 (2 g)	Water	Lemon oil (1 g)	--------	------
15	Acconon-CC6 (2 g)	Water	MCT-M5 oil (1 g)	--------	------
16	Arlacel 186 (1 g)	Water 40 % Ethanol	Soybean oil (0.4 g)	Tween 20 (0.35 g)	0.335

Table 4.4 Citrus oil or vegetable oil-in-water microemulsions

STDs	Molecular Weight (MW)	log (MW)	Retention time (minutes)
1	19720	9.889388628	11.086
2	9920	9.2023082	11.962
3	4490	8.409607981	13.137
4	2360	7.766416898	14.124
5	1180	7.073269717	15.212
6	580	6.363028104	16.297

Table 4.5 Easycal molecular weight standards (STD) and their retention time

Surfactant	Name	MW (g/mol)	HLB	Company
PGPR 90	Polyglycerol ricinoleic acid	3000	2	Danisco
Mazol 80	$P(OE)_{20}$ monodiglycerides	1100	13.5	BASF
Labrasol	PEG-8 caprylic/capric glyceride	670	14	Gattefosse
Acconon CC 6	PEG-6 caprylic/capric glyceride	590	12	Abetic
Acconon S 35	PEG-35 soy Glycerides	2100	15.5	Abetic
Capmul MCM	Glyceryl capryate	300	5.5	Abetic
Tween 80	$P(OE)_{20}$ sorbitan monoleate	1310	15	Uniqema
Tween 60	$P(OE)_{20}$ sorbitan stereate	1312	14.9	Uniqema
Tween 40	$P(OE)_{20}$ sorbitan monopalmitate	1284	15.6	Uniqema
Tween 85	$P(OE)_{20}$ sorbitan trioleate	1839	11	Uniqema
Tween 20	$P(OE)_{20}$ sorbitan monolaurate	1228	16.7	Uniqema
Tween 21	$P(OE)_4$ sorbitan monolaurate	563	13.3	Uniqema
GMO	Glyceryl monoleate	357	3.8	Uniqema
Arlacel 186	GMO/propylene glycol 11%	357/76	3.8	Uniqema

Table 4.6 Commercial emulsifiers, with name, molecular weight, and HLB

Frequency rad/s	G' Pa	G" Pa	Tan Delta	Eta* Pa/s
100	0.13935	4.76645	34.2039	0.04768
79.4328	0.00352	3.82567	1085.63	0.04816
63.0957	-0.0184	3.03082	-164.97	0.04804
50.1187	0.05346	2.41986	45.2665	0.04829
39.8107	0.05345	1.92945	36.1013	0.04848
31.6228	0.03215	1.52277	47.3635	0.04816
25.1189	0.02562	1.21713	47.5124	0.04847
19.9526	0.02144	0.94465	44.0539	0.04736
15.8489	0.00227	0.76876	337.975	0.04851
12.5893	-0.0042	0.61274	-145.13	0.04867
10	0.0088	0.48523	55.1199	0.04853
7.94328	0.00907	0.3904	43.0427	0.04916
6.30957	0.00243	0.31512	129.684	0.04994
5.01187	0.01505	0.24733	16.4337	0.04944
3.98107	0.0012	0.19284	160.824	0.04844
3.16228	-0.0045	0.16234	-36.386	0.05136
2.51189	-0.0013	0.12453	-94.632	0.04958
1.99526	-0.0028	0.10579	-37.194	0.05304
1.58489	1.06E-04	0.08183	768.997	0.05163
1.25892	-0.0024	0.06082	-25.492	0.04835
1	0.00445	0.05404	12.1423	0.05422

Table 4.7 Viscosity measurements for soybean oil

Frequency Rad/s	G' Pa	G" Pa	tan Delta	Eta* Pa/s
100	0.61406	15.2492	24.8333	0.15262
79.4328	0.39843	12.1051	30.3822	0.15248
63.0957	0.21386	9.62053	44.9852	0.15251
50.1187	0.17995	7.6636	42.5873	0.15295
39.8107	0.10287	6.08196	59.1234	0.15279
31.6228	0.05434	4.82988	88.8828	0.15274
25.1189	0.05529	3.81624	69.0161	0.15194
19.9526	0.03683	3.02443	82.1096	0.15159
15.8489	0.03035	2.4163	79.6274	0.15247
12.5893	0.01626	1.9119	117.618	0.15187
10	0.01409	1.52175	107.985	0.15218
7.94328	0.00319	1.20173	376.98	0.15129
6.30957	0.00883	0.95539	108.195	0.15143
5.01187	2.65E-04	0.74907	2828.61	0.14946
3.98107	0.00818	0.60104	73.509	0.15099
3.16228	-0.0044	0.47648	-108.51	0.15068
2.51189	0.00105	0.37664	358.037	0.14994
1.99526	-0.0079	0.30296	-38.459	0.15189
1.58489	0.00418	0.244	58.4018	0.15397
1.25892	0.00793	0.18141	22.8791	0.14424
1	-0.0137	0.14898	-10.861	0.14961

Table 4.8 Viscosity measurements for water-in-soybean oil microemulsion

Mass of the dispersed phase: 0.2 g

Frequency rad/s	G' Pa	G" Pa	tan Delta	Eta* Pa/s
100	2.26809	12.5215	5.5207	0.12725
79.4328	1.88486	10.215	5.41949	0.13077
63.0957	1.5204	8.24314	5.4217	0.13285
50.1187	1.31239	6.7009	5.10587	0.13624
39.8107	1.08325	5.46897	5.04868	0.14004
31.6228	0.88362	4.46953	5.05819	0.14407
25.1189	0.73461	3.63819	4.95254	0.14776
19.9526	0.60103	2.98681	4.96946	0.1527
15.8489	0.47575	2.45976	5.17029	0.15808
12.5893	0.37452	2.01007	5.36706	0.16241
10	0.2964	1.6525	5.57529	0.16789
7.94328	0.22835	1.35654	5.94076	0.17318
6.30957	0.17705	1.10653	6.24986	0.1776
5.01187	0.13461	0.90131	6.69594	0.18183
3.98107	0.10562	0.7368	6.97569	0.18697
3.16228	0.07451	0.58656	7.87252	0.18698
2.51189	0.0554	0.47721	8.6137	0.19126
1.99526	0.04057	0.3925	9.67524	0.19777
1.58489	0.02386	0.30548	12.8021	0.19333
1.25892	0.01416	0.24735	17.4732	0.1968
1	0.01498	0.20464	13.6582	0.20519

Table 4.9 Viscosity measurements for water-in-soybean oil microemulsion

Mass of the dispersed phase: 0.311 g

Frequency rad/s	G' Pa	G" Pa	tan Delta	Eta* Pa/s
100	2.25585	14.0901	6.24603	0.1427
79.4328	1.83167	11.3938	6.22041	0.14528
63.0957	1.54555	9.06179	5.86316	0.14569
50.1187	1.21151	7.37551	6.08787	0.14913
39.8107	0.99141	5.97002	6.02175	0.15201
31.6228	0.80971	4.84796	5.98725	0.15543
25.1189	0.66535	3.94192	5.92463	0.15915
19.9526	0.54716	3.2097	5.86611	0.16319
15.8489	0.44368	2.61374	5.89107	0.16727
12.5893	0.36261	2.12996	5.87399	0.17162
10	0.3056	1.73813	5.68768	0.17648
7.94328	0.24317	1.40671	5.78481	0.17972
6.30957	0.20393	1.15885	5.68272	0.18649
5.01187	0.17062	0.93836	5.49983	0.1903
3.98107	0.13763	0.77328	5.61871	0.19729
3.16228	0.11332	0.64689	5.70832	0.20768
2.51189	0.09757	0.52329	5.36338	0.21192
1.99526	0.07814	0.41624	5.32711	0.21226
1.58489	0.07268	0.35694	4.91135	0.22984
1.25892	0.06141	0.28812	4.69183	0.23401
1	0.05897	0.22894	3.88239	0.23641

Table 4.10 Viscosity measurements for water-in-soybean oil microemulsion

Mass of the dispersed phase: 0.356 g

Frequency rad/s	G' Pa	G" Pa	tan Delta	Eta* Pa/s
100	3.79755	14.193	3.73742	0.14692
79.4328	3.25665	11.6509	3.57757	0.1523
63.0957	2.70817	9.55826	3.52941	0.15745
50.1187	2.40327	7.87953	3.27867	0.16437
39.8107	2.01954	6.52585	3.23135	0.17159
31.6228	1.67069	5.45279	3.2638	0.18034
25.1189	1.37782	4.54378	3.29779	0.18902
19.9526	1.12785	3.7825	3.35371	0.19782
15.8489	0.90726	3.15788	3.48068	0.20731
12.5893	0.72395	2.64941	3.65964	0.21817
10	0.5733	2.18655	3.81397	0.22605
7.94328	0.43453	1.8032	4.14975	0.23351
6.30957	0.33771	1.49664	4.43173	0.24316
5.01187	0.25818	1.23721	4.79198	0.25217
3.98107	0.19788	1.01608	5.13479	0.26002
3.16228	0.15126	0.83264	5.50482	0.26761
2.51189	0.10997	0.67606	6.14794	0.27268
1.99526	0.09204	0.54925	5.96751	0.27911
1.58489	6.43E-02	0.43886	6.82268	0.27986
1.25892	0.04878	0.36163	7.41387	0.28985
1	3.00E-02	0.29297	9.78341	0.2945

Table 4.11 Viscosity measurements for water-in-soybean oil microemulsion

Mass of the dispersed phase: 0.412 g

Frequency rad/s	G' Pa	G" Pa	tan Delta	Eta* Pa/s
100	4.40358	15.1043	3.43001	0.15733
79.4328	3.85313	12.5132	3.24755	0.16483
63.0957	3.20696	10.345	3.22579	0.17165
50.1187	2.69959	8.61166	3.18999	0.18007
39.8107	2.32082	7.11981	3.0678	0.1881
31.6228	1.91961	5.94591	3.09746	0.19758
25.1189	1.58668	4.97459	3.13522	0.20787
19.9526	1.2742	4.16053	3.26521	0.21808
15.8489	1.03084	3.48311	3.3789	0.22919
12.5893	0.80634	2.91086	3.60995	0.23993
10	0.63504	2.41447	3.80209	0.24966
7.94328	0.48886	1.99711	4.08523	0.25884
6.30957	0.37156	1.64897	4.43793	0.2679
5.01187	0.28556	1.34969	4.72646	0.27526
3.98107	0.21391	1.10798	5.17972	0.28345
3.16228	0.14536	0.90252	6.20902	0.28908
2.51189	0.11307	0.73824	6.52926	0.29733
1.99526	0.08589	0.59701	6.95104	0.30229
1.58489	0.06634	0.4819	7.26401	0.30693
1.25892	0.04849	0.39947	8.23845	0.31964
1	0.03975	0.32461	8.16624	0.32703

Table 4.12 Viscosity measurements for water-in-soybean oil microemulsion

Mass of the dispersed phase: 0.478 g

Frequency rad/s	G' Pa	G" Pa	tan Delta	Eta* Pa/s
100	5.41122	17.5218	3.23806	0.18338
79.4328	4.62193	14.5923	3.15718	0.1927
63.0957	3.83914	11.9083	3.10182	0.1983
50.1187	3.24897	9.91224	3.05089	0.20813
39.8107	2.83892	8.16175	2.87495	0.21706
31.6228	2.36285	6.8107	2.88241	0.22797
25.1189	2.00713	5.66875	2.82431	0.23941
19.9526	1.68683	4.74384	2.81228	0.25234
15.8489	1.40715	3.984	2.83125	0.26659
12.5893	1.17151	3.3387	2.84991	0.28105
10	0.95934	2.80157	2.92032	0.29613
7.94328	0.79601	2.36296	2.96849	0.31391
6.30957	0.64644	1.98796	3.07526	0.33131
5.01187	0.52339	1.67274	3.19596	0.34971
3.98107	0.41999	1.39295	3.31665	0.36545
3.16228	0.33122	1.16562	3.51919	0.38319
2.51189	0.2602	0.96989	3.72753	0.39977
1.99526	0.18542	0.80301	4.33078	0.41305
1.58489	0.14984	0.6667	4.44932	0.43115
1.25892	0.10366	0.54192	5.22779	0.43827
1	0.08618	0.45762	5.31038	0.46567

Table 4.13 Viscosity measurements for water-in-soybean oil microemulsion

Mass of the dispersed phase: 0.518 g

Frequency rad/s	G' Pa	G" Pa	tan Delta	Eta* Pa/s
100	6.01501	19.0704	3.17047	0.19997
79.4328	5.07066	15.7941	3.1148	0.20883
63.0957	4.29679	13.0914	3.04679	0.21837
50.1187	3.67808	10.808	2.93851	0.22779
39.8107	3.17206	9.00178	2.83784	0.23974
31.6228	2.64981	7.48284	2.82391	0.25103
25.1189	2.28576	6.26085	2.73907	0.26534
19.9526	1.95776	5.25671	2.68506	0.28114
15.8489	1.64314	4.38278	2.66733	0.29533
12.5893	1.37762	3.68611	2.67571	0.31258
10	1.14577	3.1086	2.7131	0.3313
7.94328	0.94645	2.61676	2.76482	0.35032
6.30957	0.77468	2.21398	2.85794	0.37175
5.01187	0.62008	1.87306	3.02069	0.39367
3.98107	0.50007	1.56026	3.1201	0.41156
3.16228	0.38238	1.30256	3.40642	0.42929
2.51189	0.29701	1.10486	3.71992	0.45547
1.99526	0.23314	0.89919	3.85689	0.46557
1.58489	0.167	0.75627	4.52847	0.48867
1.25892	0.13872	0.62356	4.49503	0.50742
1	0.09738	0.5098	5.2351	0.51901

Table 4.14 Viscosity measurements for water-in-soybean oil microemulsion

Mass of the dispersed phase: 0.584 g

Frequency rad/s	G' Pa	G" Pa	tan Delta	Eta* Pa/s
100	6.58714	20.64	3.13338	0.21666
79.4328	5.46952	17.1311	3.13211	0.22639
63.0957	4.66373	14.1516	3.03439	0.23615
50.1187	3.97335	11.7376	2.95408	0.24725
39.8107	3.36094	9.78014	2.90994	0.25977
31.6228	2.87642	8.09889	2.81562	0.27178
25.1189	2.43949	6.75896	2.77064	0.28607
19.9526	2.01654	5.67557	2.81451	0.30187
15.8489	1.70976	4.78697	2.79979	0.32072
12.5893	1.42306	4.02813	2.83062	0.33935
10	1.17855	3.39089	2.87716	0.35899
7.94328	0.95886	2.84675	2.96891	0.37817
6.30957	0.76566	2.39317	3.12561	0.39823
5.01187	0.60996	2.00949	3.29447	0.41901
3.98107	0.47909	1.68787	3.52307	0.44072
3.16228	0.36552	1.4097	3.8567	0.46053
2.51189	0.27206	1.1677	4.29202	0.47732
1.99526	0.19824	0.97381	4.91219	0.49807
1.58489	0.1391	0.7858	5.64917	0.50351
1.25892	0.11377	0.64714	5.68792	0.52193
1	0.06956	0.53574	7.7013	0.54023

Table 4.15 Viscosity measurements for water-in-soybean oil microemulsion

Mass of the dispersed phase: 0.655 g

Frequency rad/s	G' Pa	G" Pa	tan Delta	Eta* Pa/s
100	4.61146	23.4668	5.0888	0.23916
79.4328	3.73349	19.1557	5.13077	0.24569
63.0957	2.95921	15.7058	5.30743	0.2533
50.1187	2.28334	12.8506	5.62797	0.26042
39.8107	1.78186	10.5181	5.90285	0.26797
31.6228	1.40301	8.51707	6.07057	0.27296
25.1189	1.04395	6.94208	6.64981	0.27948
19.9526	0.77299	5.6288	7.28185	0.28476
15.8489	0.54963	4.60112	8.37138	0.29238
12.5893	0.40791	3.70858	9.09171	0.29636
10	0.29673	2.97132	10.0135	0.29861
7.94328	0.21542	2.39851	11.1341	0.30317
6.30957	0.16312	1.93161	11.8416	0.30723
5.01187	0.10441	1.54513	14.7992	0.309
3.98107	0.08043	1.24152	15.4364	0.31251
3.16228	0.04876	0.98738	20.2518	0.31262
2.51189	0.03289	0.79805	24.2644	0.31798
1.99526	0.03069	0.62775	20.4578	0.315
1.58489	7.06E-03	0.50339	71.3414	0.31765
1.25892	0.01813	0.41353	22.8062	0.32879
1	2.15E-04	0.31965	1489.67	0.31965

Table 4.16 Viscosity measurements for water-in-soybean oil microemulsion

Mass of the dispersed phase: 0.808 g

Frequency rad/s	G' Pa	G" Pa	tan Delta	Eta* Pa/s
100	0.3265	34.7193	106.337	0.34721
79.4328	0.14278	27.5868	193.211	0.3473
63.0957	0.07018	21.8376	311.173	0.3461
50.1187	0.17136	17.4264	101.696	0.34772
39.8107	0.1083	13.8289	127.693	0.34738
31.6228	0.07349	10.963	149.174	0.34669
25.1189	0.0401	8.71399	217.294	0.34691
19.9526	0.01758	6.90273	392.585	0.34596
15.8489	0.02917	5.47354	187.649	0.34536
12.5893	0.02281	4.33323	189.934	0.34421
10	0.00589	3.45013	585.265	0.34501
7.94328	0.01822	2.73215	149.943	0.34397
6.30957	0.00968	2.17364	224.483	0.3445
5.01187	0.00588	1.72868	294.066	0.34492
3.98107	0.00621	1.37014	220.699	0.34417
3.16228	0.0035	1.07698	307.71	0.34057
2.51189	0.00537	0.86382	160.892	0.3439
1.99526	-0.0034	0.68351	-198.69	0.34257
1.58489	0.00664	0.55681	83.8564	0.35135
1.25892	-0.0045	0.43109	-95.717	0.34245
1	0.00302	0.33279	110.032	0.3328

Table 4.17 Viscosity measurements for water-in-soybean oil microemulsion

Mass of the dispersed phase: 1.016 g

Exp #	Continuous phase	Dispersed phase	Surfactant	Cosurfactant at interface	% T in oil	% T in water
1	MCT-M5	Water (0.5 g)	Tween 80 (1.6 g)	PGPR (0.64 g)	9	1
2	Soybean oil	Water (0.5 g)	Mazol 80 (1.6 g)	PGPR (0.3 g)	1	7
3	Soybean oil	Water (0.5 g)	Acconon S35 (1.6 g)	PGPR (1.25 g)	0	5
4	MCT-M5	Water (0.5 g)	Tween 60 (1.6 g)	Capmul MCM (1.3 g)	0	9
6	MCT-M5	Water (0.5 g)	TMGO 15 (1.6 g)	TMGO 5 (0.7 g)	0	4
7	MCT-M5	Water (0.5 g)	ESO 9920 (1.6 g)	Capmul MCM (1.28 g)	0	2
8	MCT-M5	Water (0.5 g)	Tween 40 (1.6 g)	Capmul MCM (1.3 g)	0	7
9	Corn oil	Water (0.4 g)	Acconon CC 6 (1.6 g)	Arlacel 186 (0.93 g)	51	59
10	Water	Soybean oil (0.4 g)	Arlacel 186 (1.6 g)	Acconon CC 6 (1.93 g)	49	53

Table 4.18 Surfactant/cosurfactant composition solubility in the oil and water phases

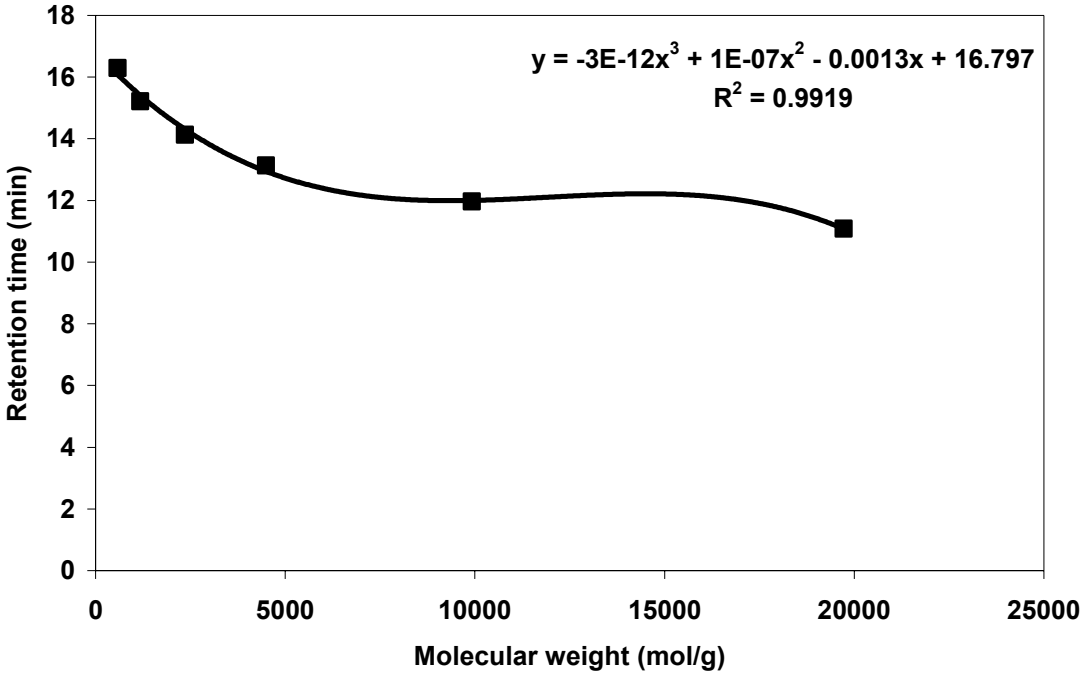

Figure 4.1 Retention time of molecular weight standards vs. molecular weight standards

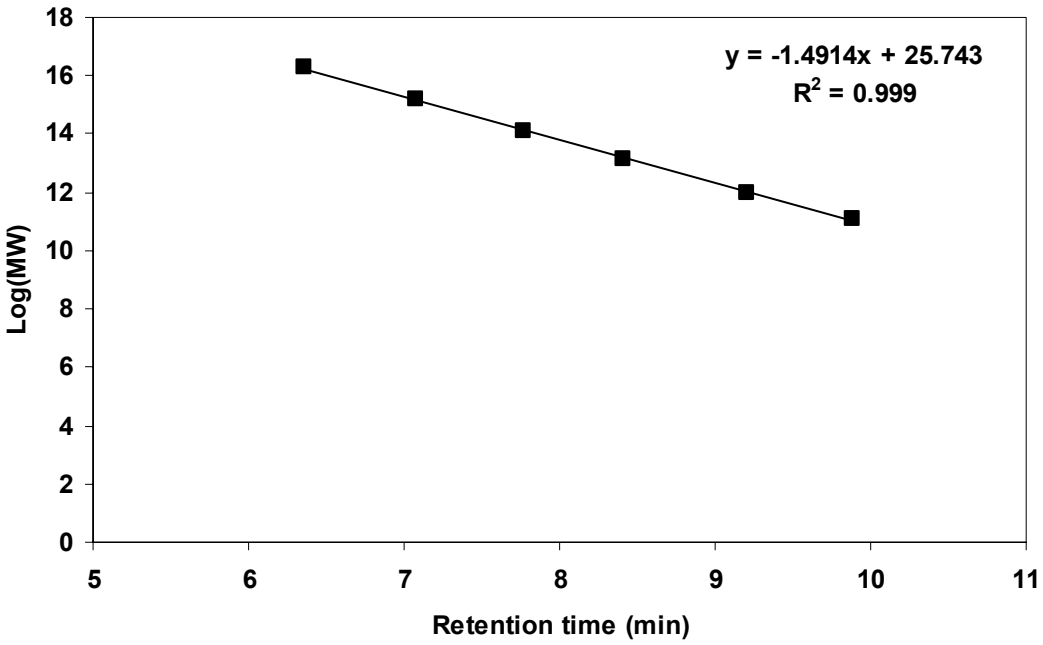

Figure 4.2 Log of molecular weight standards vs. retention time

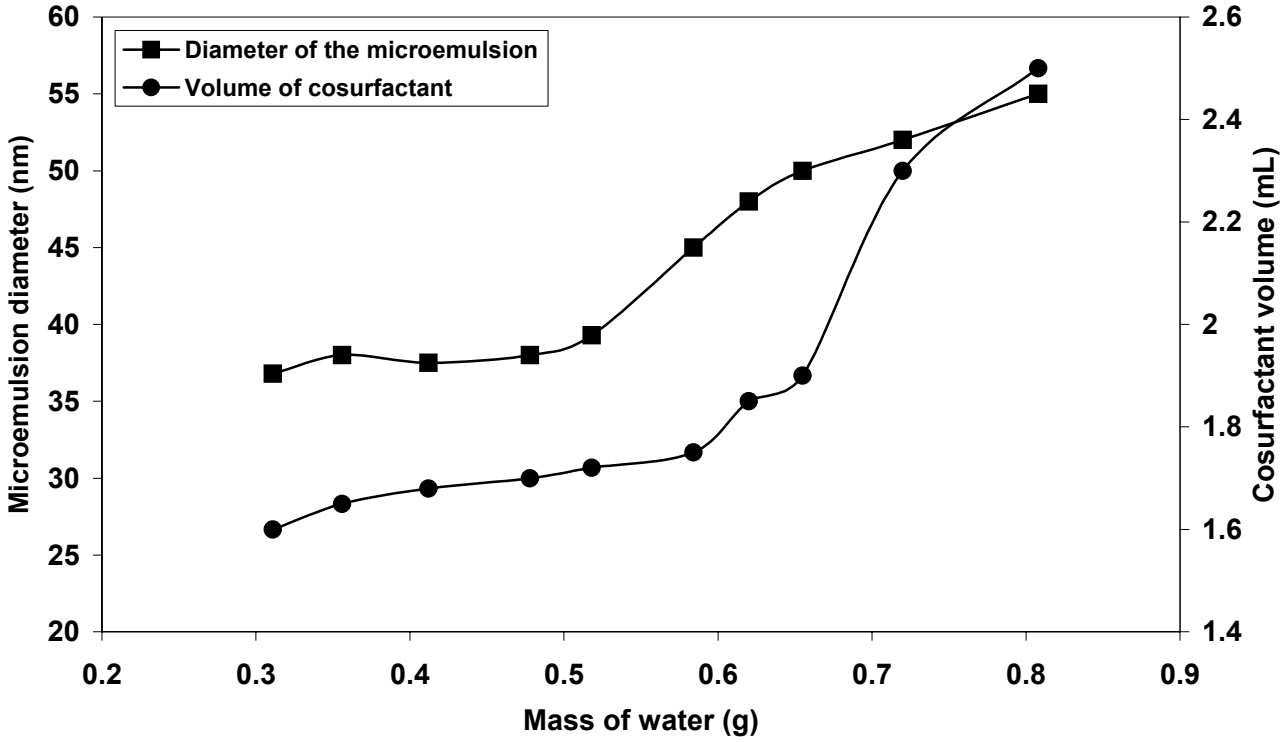

Figure 4.3 Quasi Elastic light scattering measurements for water-in-soybean oil microemulsions

Tween 80 1.6 g, Cosurfactant PGPR, Soybean oil 15 g

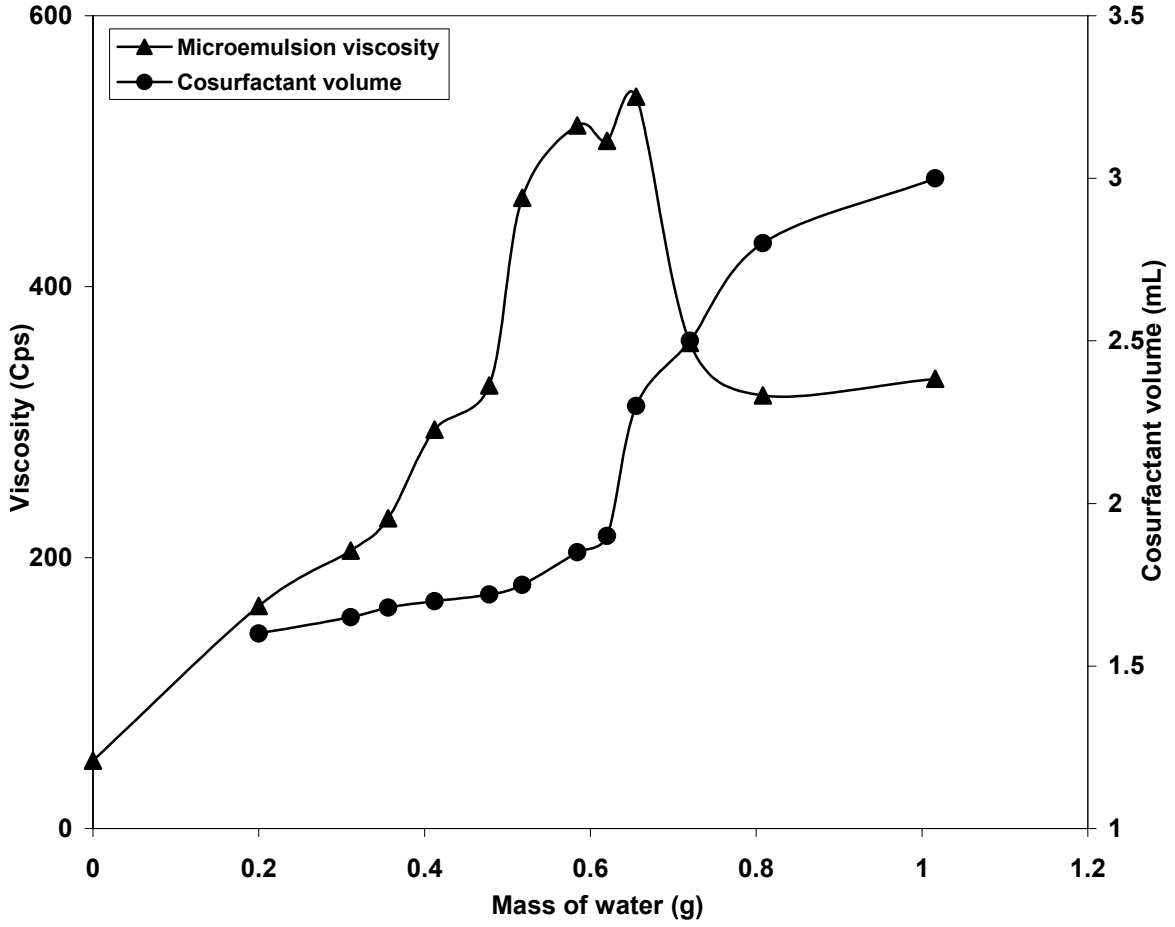

Figure 4.4 Viscosity measurements of water-in-soybean oil microemulsion at 1rad/sec

Tween 80 1.6 g, Cosurfactant PGPR, Soybean oil 15 g

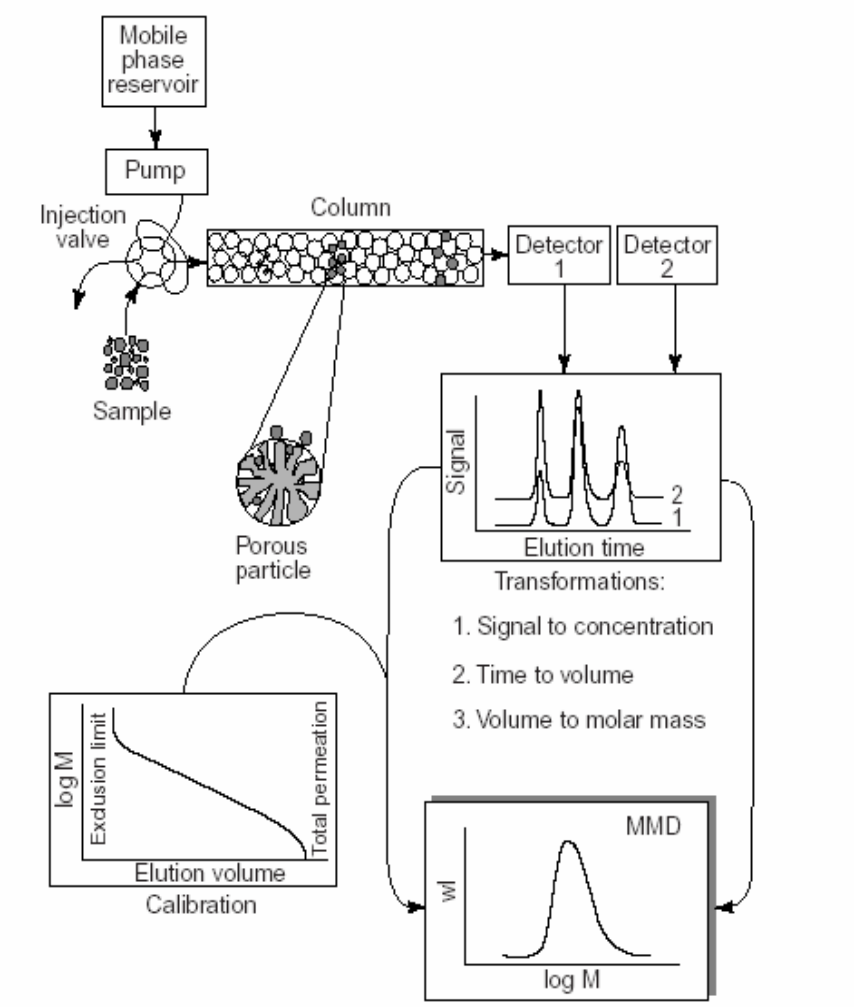

Figure 4.5 Size Exclusion Chromatography principle

CHAPTER 5

SUMMARY

As has been described in the previous chapters, microemulsions are defined as isotropic, thermodynamically stable dispersions of two immiscible liquids—generally, "oil" and "water". They are dispersions of either "water-in-oil" or "oil-in-water" stabilized by single or mixed surfactants. The individual droplets of the dispersed phase have an average diameter in the range of 6-50 nm. Microemulsions differ fundamentally from emulsion in that the former are thermodynamically stable whereas the latter are kinetically stable.

Investigation of the non-ionic surfactant microemulsion systems yielded results relevant both to formation mechanisms and to single-surfactant microemulsions. These results suggest that several conditions must be met for the formation and stability of a microemulsion.

- The amount of surfactant(s) used must be sufficient to cover the total interfacial area of the droplets and the volume of dispersed phase adequate to accommodate the hydrophilic or the hydrophobic groups of the surfactant.
- The chain length of the oil must be compatible with the hydrophobic part of the surfactants to facilitate the formation of microemulsions.
- The surfactant(s) must reduce the free energy at the O/W boundary, thus facilitating the formation of the interface; nevertheless, at equilibrium, the

interfacial tension must have a positive value, causing the curling of the interface that leads to droplet formation.

- The interfacial mixed film of non-ionic surfactant(s) must be of equal solubility in both the oil and the aqueous phase.

Using Triglycerides microemulsions, it was demonstrated that a non-ionic microemulsion forms when the surfactant interfacial film at the water/oil interface has equal solubility in the two phases, regardless of the structure of the surfactant and cosurfactant used. As was mentioned in chapter 4, this is a generalization of the case of nonylphenol ethylene oxide ($NP(EO)_n$) surfactant systems, where the surfactant and the cosurfactant have the same structure.

Determination of surfactant/cosurfactant molar compositions at the interface using the Rosano titration method permits the formulation of single surfactant microemulsions. The results presented in this thesis show that the titration method gives significant information on the surfactant molar composition at the water/oil interface.

Thermodynamics investigations of the free energy values corresponding to the adsorption of cosurfactant at the interface (free energy of formation) demonstrate that all free energies for systems under study are negative numbers, indicating that the process of microemulsion formation is spontaneous. Moreover, the small positive values of the entropy for these systems indicate that the formation of microemulsion is entropy-driven .

Concerning the dynamic behavior of microemulsion systems, two distinct regions of phase behavior occur.

- At low volumes of the dispersed-phase (below the threshold volume Φ), the individual droplets behave as isolated entities, with no interdroplet interaction taking place (stable microemulsion).
- At high volume of the dispersed-phase (above Φ), the system changes dramatically, and individual droplets begin to interact, and a dynamic equilibrium is established, with droplets merging and re-forming while the system as a whole remains a single transparent phase (percolation of the microemulsion).

A separate investigation of the effects of dispersed-phase volume on microemulsion dynamics explained the shift in droplet behavior (percolation) observed above the threshold value Φ in terms of the limited capacity of the surfactant interfacial film to hold dispersed phase droplets in a stable configuration.

Experimental validation of the mathematical model of microemulsion formation, demonstrates that the rigidity of the interface and the interfacial tension at the oil/water interface plays a key role in the formation and stability of the microemulsion.

Citrus oil microemulsions could have a wide application in the beverage industry, if the currently available GRAS emulsifiers did not have both a pronounced taste and a high molecular weight.

References

Chapter 1

1. Bourrel, M.; Shechter, S. R. *Microemulsions and Related Systems: Formulation, Solvency and Physical Properties*. New York: Marcel Dekker, 1998.
2. Eicke, H.-F. *J. Phys. Chem. B*. **2001**, *105*, 2753.
3. Kahlweit, M.; Lessner, E.; Haase, D. *J. Phys. Chem*. **1985**, *89*, 163.
4. Moulik, S. P.; Paul, B. K. *Adv. Colloid Interface Sci*. **1998**, *78*, 99.
5. De Gennes, P. G.; Taupin, C. *J. Phys. Chem.* **1982**, *86*, 2294.
6. Shinoda, K.; Kunieda, H. *J. Colloid Interface Sci*. **1973**, *42*, 381.
7. Rosano, H. L. *J. Soc. Cosmetic Chem*. **1974**, *25*, 609.
8. Hoar, T. P.; Schulman, J. H. *Nature* (*London*). **1943**, *152*, 102.
9. Schulman, J. H.; McRoberts, T. S. *Trans. Faraday Soc*. **1946**, *42B***,** 165.
10. Schulman, J. H.; Matalon, R.; Cohen, M. *Disc. Farday. Soc*. **1951**, *11*, 117.
11. Bowcott, J. E. L.; Schulman, J. H. *Z. Electrochem*. **1955**, 59, 283.
12. Schulman, J. H.; Stoeckenius, W.; Prince, L. M. *J. Phys. Chem*. **1959**, *63*, 1677.
13. Stoeckenius, W.; Schulman, J. H.; Prince, L. M. *Kolloid-Z.* **1960,** *169*, 170.
14. Schulman, J. H.; Montagne, J. B. *Ann. N. Y. Acad. Sci*. **1961**, *92*, 366.
15. Prince, L. M. *J. Colloid Interface Sci*. **1967**, *23*, 165.
16. Prince, L. M. *J. Colloid Interface Sci*. **1968**, *29*, 216.
17. Prince, L. M. *J. Soc. Cosmetic Chem*. **1970**, *21*, 193.
18. Ruckenstein, E. *Ann. N. Y. Acad. Sci*. **1983***, 404,* 224.
19. Ruckenstein, E. *Fluid Phase Equilib.* **1985**, *20*, 189.
20. Talmon, Y.; Prager, S. *J. Chem. Phys*. **1978**, *69*, 2984.

21. Shinoda, K.; Friberg, S. *Adv. Colloid Interface Sci*. **1974**, *4*, 193.

22. Shinoda, K.; Kunieda, H. *J. Colloid Interface Sci*. **1972**, *42*, 381.

23. Friberg, S.; Lapczynska, I.; Gillberg, G. J. *Colloid Interface Sci*. **1976**, *56*, 19.

24. Likhtman, V. I.; Shchukin, E. D.; Rehbinder, P. A. *Physico-Chemical Mechanics of Metals*, Izdatelstvo Akad. Nauk SSSR, Moscow; p.182. English translation by Israel Program for Scientific Translations, 1964.

25. Reiss, H. *J. Colloid Interface Sci*. **1975**, *53*, 61.

26. Rosano, H. L.; Peiser, R. C.; Eydt, A. *Rev. Fran. Corps Gras*. **1969**, *16*, 249.

27. Gerbacia, W.; Rosano, H. L. *J. Colloid Interface Sci*. **1973**, *44*, 242.

28. Helfrich, W. Z. *Naturforsch*. **1973**, *28*, 693.

29. Kellay, H.; Binks, B. P.; Hendrikx, Y.; Lee, L. T.; Meunier, J. *Adv. Colloid Interface Sci*. **1994**, *9*, 85.

30. Meunier, J.; Lee, L. T. *Langmuir*. **1991**, *46*, 1855.

31. Kegel, W. K.; Bodnar, I.; Lekkerkerker, H. N. W. *J. Phys. Chem*. **1995**, *99*, 3272.

32. Sicoli, F.; Lengevin, D.; Lee, L. T. *J. Chem. Phys.* **1993**, *99*, 4759.

33. Cavallo, J. L.; Rosano, H. L. *J. Phys. Chem*. **1986**, *90*, 6817.

34. Chan, S. Y.; Rosano, H. L. *J. Dispersion Science and Technology*. **1988**, *9*, 523.

35. Oleksiak, C. B.; Rosano, H. L. "A Model of Micro- and Fine-Emulsion Formation" in *Encyclopedia of Emulsion Technology*. Paul Becher, ed. New York: Marcel Dekker, 1996, p. 289.

36. Lindman, B.; Kamenke, N.; Kathopoulis, T. M.; Brun, B.; Nilsson, P. G. *J. Phys. Chem*. **1980**, *84*, 2485.

37. Stilbs, P.; Moseley, M. E.; Lindman, B. *J. Magn. Resonance*. **1980**, *40*, 401.

38. Stilbs, P.; Moseley, M. E. *Chem. Scr*. **1980**, *15*, 176.

39. Stilbs, P.; Moseley, M. E. *Chem. Scr*. **1980**, *15*, 215.

40. Lindman, B.; Stilbs, P.; Moseley, M. E. *J. Colloid Interface Sci*. **1981**, *83*, 569.

41. Martino, A.; Kaler, E. W. *Langmuir*. **1995**, *11*, 779.

42. Full, A. P.; Kaler, E. W. *Langmuir*. **1994**, *10*, 2929.

43. Olsson, U.; Nagai, K.; Wennerstroem, H. *J. Phys. Chem*. **1988**, *92*, 6675.

44. Winsor, P. A. *Trans. Faraday Soc*. **1948**, *44*, 376.

45. Israelachvili, J. N.; Mitchell, D. J.; Ninham, B. W. *J. Chem. Soc. Faraday Trans. 2*. **1976**, *72*, 1525.

46. Rock, P. A. *Chemical Thermodynamics*. London: MacMillan, 1969.

47. Shinoda, K. *J. Colloid Interface Sci*. **1970**, 34, 278.

48. Shinoda, K., ed. *Solvent Properties of Surfactant Solutions*. New York: Marcel Dekker, 1967.

49. Saito, H.; Shinoda, K. *J. Colloid Interface Sci*. **1967**, 24, 10.

50. Shinoda, K.; Saito, H. *J. Colloid Interface Sci*. **1967**, 26, 70.

51. Shinoda, K.; Ogawa, T. *J. Colloid Interface Sci*. **1968**, 24, 56.

52. Shinoda, K.; Takeda, H. *J. Colloid Interface Sci*. **1970**, 32, 642.

53. Shinoda, K.; Friberg, S. *Adv. Colloid Interface Sci*. **1975**, *4*, 281.

54. Kumar, P.; Mittal, L.K., eds. *Handbook of Microemulsion Science and Technology.* New York: Marcel Dekker, 1999.

55. Balusubramanian, D.; Friberg, S. E. In *Surface and Colloid Science*, Vol. 15. Matijevic, E., ed. New York: Plenum Press, 1993.

56. Darwish, I. A.; Ismail, F. A.; El-khordagui, L. K. *J. Pharm. Sci*. **1992**, *6*, 101.

57. Yu, W.; Zou, A.; Guo, R. *Colloids and Surfaces A: Physicochem. Eng. Aspects.* **2000**, *167,* 293.

58. Guo, R.; Compo, M. E.; Friberg, S.E. *J. Dispersion Sci. Tech*. **1996**, *17*, 493.

59. Friberg, S. E.; Brancewicz, C.; Morrison, S. D. *Langmuir*. **1994**, *10*, 2945.

60. Lagues, M.; Ober, R.; Taupin, C. *J. Phys. Letters*. **1974**, *39*, L-487.

61. Giustini, M.; Murgia, S.; Palazzo, G. *Langmuir*. **2004**, *20*, 7381.

Chapter 2

1. Giustini, M.; Murgia, S.; Palazzo, G. *Langmuir*. **2004**, *20*, 7381.
2. Kahlweit, M.; Lessner, E.; Haase, D. *J. Phys. Chem*. **1985**, *89*, 163.
3. Moulik, S. P.; Paul, B. K. *Adv. Colloid Interface Sci*. **1998**, *78*, 99.
4. Ruckenstein, E.; Chi, C. J. *J. Chem. Soc., Faraday Trans.* **1975***, 71,* 1960.
5. De Gennes, P. G.; Taupin, C. *J. Phys. Chem.* **1982**, *86*, 2294.
6. Safran, S. A. In *Micellar Solutions and Microemulsions*: *Structure, Dynamics and Statistical Thermodynamics*. Chen, S. H.; Rajagopalan, Rr., eds. New York: Springer-Verlag, 1990; p. 165.
7. Stoeckenius, W.; Schulman, J. H.; Prince, L. M. *Kolloid-Z.* **1960,** *169*, 170.
8. Shinoda, K.; Kunieda, H. *J. Colloid Interface Sci*. **1973**, *42*, 381.
9. Hoar, T. P.; Schulman, J. H. *Nature* (*London*). **1943**, *152*, 102.
10. Adamson, A.W. *J. Colloid Interface Sci*. **1960**, *29*, 261.
11. Robbins, M. L. In *Micellization, Solubilization and Microemulsions*. Mittal, K. L., ed. New York: Plenum Press, 1977; Vol. 2, p. 713.

12. Rosano, H. L.; Lan, T.; Weiss, A.; Whittam, J. H.; Gerbacia, W. E. F. *J. Phys. Chem.* **1981**, *85*, 468.

13. Rosano, L. H.; Lan, T.; Weiss, A.; Gerbacia, W. E. F.; Whittam, J. H. *J. Colloid Interface Sci.* **1979**, *72*, 233.

14. Rosano, H. L.; Nixon, A. L.; Cavallo, J. L. *J. Phys. Chem*. **1989**, *93*, 4536.

15. Rosano, H. L. *J. Soc. Cosmetic Chem*. **1974**, *25*, 609.

16. Kanouni, M.; Rosano, H. L.; Naouli, N. *Adv. Colloid Interface Sci*. **2002,** *99,* 229.

17. Aronson, P. M. *Colloids and surfaces*. **1991**, *58*, 195.

18. Christodoulou, A. P.; Rosano, H. L. *Advances in Chemistry Series*. **1968**, *84*, 210.

19. Pecora, R., ed. *Dynamic Light Scattering: Applications of Photo Correlation Spectroscopy*. New York: Plenum Press, 1985.

20. Berne, B. J.; Pecora, R. *Dynamic Light Scattering with Applications to Chemistry, Biology and Physics*. New York: Wiley Interscience, 1976.

21. Kittel, C.; Kroemer, H. *Thermal Physics*, Second Edition. New York: W. H. Freeman, 1980.

22. Chen, S. J.; Evans, D. F.; Ninham, B.W.; Mitchell, D. J.; Blum, F. D.; Pickup, S. *J. Phys. Chem*. **1986**, *90*, 842.

23. Chen, S. J.; Evans, D. F.; Ninham, B. W. *J. Phys. Chem.* **1984**, *88*, 1621.

24. Gerbacia, W. E. F.; Rosano, H. L. *J. Colloid Interface Sci*. **1973**, *44*, 242.

25. Hansen, F. K.; Fagerheim, H. *Colloids and Surfaces A: Physicochem. Eng. Aspects*. **1998,** *137*, 217.

26. Safran, S. A.; Grest, G. S.; Bug, A. L. R. In *Microemulsion Systems.* Rosano, H. L.; Clausse, M., eds. New York: Marcel Dekker, 1987; Ch. 14, p. 235.
27. Cavallo, J. L.; Rosano, H. L. *J. Phys. Chem*. **1986**, *90*, 6817.
28. Menger, F.; Donahue, J.; Williams, R. *J. Am. Chem. Soc*. **1973**, *95*, 286.
29. Lessner, E.; Teubner, M.; Kahlweit, M. *J. Phys. Chem*. **1981**, *85*, 3167.
30. Ruckenstein, E. *Chem. Phys. Lett*. **1978**, *57*, 3517.
31. Monduzzi, M.; Mele, S. *J. Phys. Chem. B*. **2001**, *105*, 12579.
32. Eicke, H.-F. *J. Phys. Chem. B*. **2001**, *105*, 2753.
33. Hait, S. K.; Moulik, S. P.; Palepu, R. *Langmuir*. **2002**, *18*, 2471.
34. Cazabat, A. M.; Langevin, D.; Meunier, J.; Pouchelon, A. *J. Phys. Lett*. **1982**, *43*, 89.
35. Dogra, A.; Rakshit, A. K. *J. Phys. Chem*. *B*. **2004**, *108*, 10053.
36. Mori, Y.; Shinoda, H.; Kitagawa, T.; Nakano, T. *J. Phys. Chem. B*. **2004***, 108,* 16313.

Chapter 3

1. Hoar, T. P.; Schulman, J. H. *Nature* (*London*). **1943**, *152*, 102.
2. Ekwall, P.; Mandell, L.; Fontell, K. *J. Colloid Interface Sci*. **1970**, *33*, 215.
3. Rosano, H. L.; Lan, T.; Weiss, A.; Gerbacia, W. E. F.; Whittam, J. H. *J. Colloid Interface Sci.* **1979**, *72,* 233.
4. Adamson, A. W. *J. Colloid Interface Sci*. **1969**, *29*, 261.
5. Giustini, M.; Murgia, S.; Palazzo, G. *Langmuir*. **2004**, *20*, 7381.
6. Moulik, S. P.; Paul, B. K. *Adv. Colloid Interface Sci*. **1998**, *78*, 99.

7. Kahlweit, M.; Lessner, E.; Haase, D. *J. Phys. Chem*. **1985**, *89*, 163.

8. Cavallo, J. L.; Rosano, H. L. *J. Phys. Chem*. **1986**, *90*, 6817.

9. Chan, S. Y.; Rosano, H. L. *J. Dispersion Science and Technology*. **1988**, *9*, 523.

10. Oleksiak, C. B.; Rosano, H. L. "A Model of Micro- and Fine-Emulsion Formation." In *Encyclopedia of Emulsion Technology.* Paul Becher, ed. New York: Marcel Dekker, 1996; p. 289.

11. Rosano, H. L.; Naouli, N.; Kanouni, M. "New development for a mathematical model for the formation of microemulsions." Presented at 226th ACS Conference, New York, 2003.

12. Hyde, S.; Andersson, S.; Larsson, K.; Blum, Z.; Landh, T.; Lidin, S.; Ninham, B. W. *The Language of Shape. The Role of Curvature in Condensed Matter: Physics, Chemistry and Biology.* Amsterdam: Elsevier, 1997.

13. Gradzeilski, M.; Langevin, D.; Farago, B. *Phys. Rev. E.* **1996**, *53*, 3900.

14. Safran, S. A.; Turkevich, L. A. In *Surfactant in Solution*. Mittal, K.; Lindman, B., eds. New York: Plenum Press, 1984.

15. Helfrich, W. Z. Naturforsch. **1973**, *28c*, 693.

16. Naouli, N.; Rosano, H. L. "Non-ionic Microemulsion: Mechanism of Formation and Percolation." Submitted for publication in *Adv. Colloid Interface Sci*.

17. Hait, S. K.; Sanyal, A .; Moulik, S. P. *J. Phys. Chem. B* **2002,** *106,* 12642.

18. Dogra, A.; Rakshit, A. K. *J. Phys. Chem*. *B.* **2004,** *108,* 10053.

19. Eicke, H.-F. *J. Phys. Chem. B*. **2001**, *105*, 2753.

20. Cazabat, A. M.; Langevin, D.; Meunier, J.; Pouchelon, A. *J. Phys. Lett*. **1982**, *43*, 89.

21. Hait, S. K.; Moulik, S. P.; Palepu, R. *Langmuir*. **2002**, *18*, 2471.

22. Saito, H.; Shinoda, K. *J. Colloid Interface Sci*. **1970**, *32*, 647.

23. Reed, L. R.; Healy, N. R. In *Improved Oil Recovery by Surfactant and Polymer Flooding.* Shah, O. D.; Schechter, R. S., eds. New York: Academic Press, 1977.

24. Friberg, S. E.; Solans, C. *Langmuir*. **1986**, *2*, 21.

25. De Gennes, P. G.; Taupin, C. *J. Phys. Chem.* **1982**, *86*, 2294.

Chapter 4

1. Kumar, P.; Mittal, L. K., eds. *Handbook of Microemulsion Science and Technology.* New York: Marcel Dekker, 1999, pp.789-796.

2. El-Nokaly, M.; Hiler, G. D.; McGrady, J. In *Microemulsion and Emulsion in Foods.* El-Nokaly, M.; Cornell, D., eds. Washington, DC: American Chemical Society, 1991, pp. 26-43.

3. Garti, N.; Yaghmur, A.; Leser, M. E.; Clement, V.; Watzke, H. J. *J. Agric Food Chem*. **2001**, *49*, 2552.

4. EngstrÖm, L. *J. Dispersion Sci. Technol*. **1990**, *11*, 479.

5. Jacobsson, M.; Sivik, B. *J. Dispersion Sci. Technol*. **1994**, *15*, 611.

6. Joubran, R.; Parris, N.; Lu, D.; Trevino, S. *J. Dispersion Sci. Technol.* **1994***, 15,*687.

7. Pszczola, D. E. *Food Technology.* **2005,** *59 (No.5),* 46-63.

8. Stauffer, C. E. *Emulsifiers*. St. Paul, MN: Eagan Press Handbook Series, 1999.

9. Gaonkar, A. G.; Bagwe, R. P. In *Adsorption and Aggregation of Surfactants in Solution.* Mittal, K. L.; Shah, D. O., eds. New York: Marcel Dekker, 2002; pp. 407-430.

10. Choi, H-S.; Sawamura, M. *J. Agric. Food Chem*. **2000**, *48*, 4868.

11. Moulik, S. P.; Paul, B. K. *Adv. Colloid Interface Sci*. **1998**, *78*, 99.

12. Shiao, S. Y.; Chhabra, V.; Patist, A.; Free, M. L.; Huibers, P. D. T.; Gregory, A.; Patel, S.; Shah, D. O. *Adv. Colloid Interface Sci*. **1998**, *74*, 1.

13. Warisnoicharoen, W.; Lansley, A. B.; Lawrence, M. J. *International Journal of Pharmaceutics*. **2000**, *198*, 7.

14. Taraoka, I. *Macromolecules.* **2004,** *37,* 6632.

15. Sun, T.; Chance, R. R.; Graessley, W. W.; Lohse, D. J. *Macromolecules,* **2004**, *37*, 4304.

16. Selisko, B.; Delgado, C.; Fisher, D.; Ehwald, R. *J. Chromatogr*. **1993**, *641*, 71.

17. Trathnigg, B. In *Encyclopedia of Analytical Chemistry.* Meyers, R. A., ed. Chichester, England: John Wiley & Sons Ltd., 2000, pp. 8008-8034.